TECHNISCHE UNIVERSITÄT MÜNCHEN

Lehrstuhl für Phytopathologie

Functional analysis of membrane trafficking proteins in the interaction of barley with the barley powdery mildew fungus

Maya Katharina Ostertag

Vollständiger Abdruck der von der Fakultät Wissenschaftszentrum Weihenstephan für Ernährung, Landnutzung und Umwelt der Technischen Universität München zur Erlangung des akademischen Grades eines

Doktors der Naturwissenschaften

genehmigten Dissertation.

Vorsitzender:		Univ.-Prof. Dr. K. Schneitz
Prüfer der Dissertation:	1.	Univ.-Prof. Dr. R. Hückelhoven
	2.	Univ.-Prof. Dr. J. Durner

Die Dissertation wurde am 13.02.2012 bei der Technischen Universität München eingereicht und durch die Fakultät Wissenschaftszentrum Weihenstephan für Ernährung, Landnutzung und Umwelt am 02.05.2012 angenommen.

Index of contents

Index of contents

Figures:

Tables:

Index of abbreviations

Abbreviations:

PVC	Prevacuolar compartment
TRAPP	Transport protein particle
Dsl1	Dependence on SLY 1
ER	Endoplasmic reticulum
LE	Late endosome
EE	Early endosome
MVB	Multi vesicular bodies
COPII	Coat protein complex II
COPI	Coat protein complex I
MTI	MAMP triggered immunity
NO	Nitric oxide
RLP	Receptor-like proteins
CaMV	cauliflower mosaic virus
ARF	ADP ribosylation factor
At	*Arabidopsis thaliana*
Bgh	*Blumeria graminis* f.sp. *hordei*
CATCHR	complexes associated with tethering containing helical rods
COG	conserved oligomeric Golgi
CORVET	class C core vacuole/endosome tethering
dab	days after bombardment
dai	days after inoculation
DAMPs	damage associated molecular patterns
ERES	ER export sites
EST	expressed sequence tag
ETI	effector triggered immunity
f.sp.	formae specialis
GAP	GTPase activating protein
GARP	Golgi associated retrograde protein
GDI	GDP dissociation inhibitor
GDP	guanosindiphosphate
GEF	guanine exchange factor
GP	Golden Promise
GTP	guanosintriphosphate
hai	hours after infection
HOPS	homotypic fusion and protein sorting
HR	hypersensitive response
LRR-RLK	leucine-rich repeat receptor-like kinases
LRR-RLP	LRR receptor-like proteins

MAMPs	microbe associated molecular patterns
MAPKs	mitogen activated protein kinases
MTC	multi-subunit tethering complexes
NB	nucleotide binding
Nt	*Nicotiana tabacum*
PAMPs	Pathogen-associated molecular pattern
PE	penetration efficiency
PR-protein	Pathogenesis related protein
PRR	pattern recognition receptors
PTI	PAMP triggered immunity
ROS	reactive oxygen species
R-protein	Resistance-protein
SA	salicylic acid
SI	Susceptibility index
SM	Sec1/Munc18
SNARE	soluble N-ethylmaleimide sensitive fusion protein attachment protein receptors
T3SS	type three secretion system
TGN	trans-Golgi-network
TRAP	transport protein particle
VAMP	vesicle-associated membrane protein

1 Introduction

1.1 The plant immune system

Unlike mammals, plants lack specialized immune cells, such as macrophages and do not possess an adaptive immune system. Nevertheless, plants have evolved a highly effective defence system, which enables them to avoid colonization by most potentially pathogenic microorganisms. It is organized in two layers and is based on the recognition of non-self molecules or their action.

1.1.1 Basal immunity – MAMP-recognition

The first layer of host immunity recognizes general microbe associated molecular patterns (MAMPs), which are common to a large group of microbes. Most MAMPs are essential for the viability of microbes and hence evolve slowly. Well known MAMPs of pathogens are lipopolysaccharides from the outer membrane of bacteria, the elongation factor Tu and flagellin, which derives from the bacterial flagella. Fungal MAMPs are e.g. ergosterol, β-glucan and most importantly chitin from the fungal cell wall (Zipfel and Felix, 2005). Pattern-recognition receptors (PRRs) localized to the plasma membrane are responsible for the detection of MAMPs. PRRs often represent leucine-rich repeat receptor-like kinases (LRR-RLK) consisting of LRRs, a transmembrane domain and an intracellular serine/threonine kinase domain. Besides the LRR-RLKs, PRRs with an extracellular LysM motif or LRR-receptor-like proteins (RLP), which lack the intracellular signalling domain, recognize MAMPs (Bittel and Robatzek, 2007). Consistent with the slow evolution of MAMPs, plant genes encoding PRRs are also relatively stable and inherited form generation to generation (Bent and Mackey, 2007). So far, PRRs are only known to be transmembrane or secreted proteins (Zipfel, 2008) and there is no example for intracellular MAMP-perception in plants (Nürnberger *et al.,* 2004). Detection of MAMPs by PRRs at the cell surface results in signalling cascades that involve influx of Ca^{2+} into the cells and the activation of mitogen activated protein kinases (MAPKs). This leads in turn to defence reactions like the formation of papillae, generation of reactive oxygen species (ROS) and changes in defence gene expression patterns (Nürnberger *et al.,* 2004; Göhre and Robatzek, 2008). The first plant reactions after MAMP-recognition typically lead to the production of ROS, nitric oxide (NO) and ethylene, followed by

cell wall strengthening, callose deposition and secretion of antimicrobial compounds, as well as the activation of MAPK cascades, which in turn lead to transcriptional changes (Bittel and Robatzek, 2007; see below). The perception of MAMPs by PRRs and the following plant defence reactions are called MTI for MAMP triggered immunity (Jones and Dangl, 2006; He *et al.,* 2007).

1.1.1.1 MAMP-triggered defence responses

The perception of MAMPs by the plant needs to be translated into a defence response against the pathogen. Signal transduction from the activated receptor to downstream elements is in many cases mediated by MAPK cascades. These lead to physiological changes like stomata closure or activate transcription factors, which induce reactions like cell wall modifications or expression of a large number of genes (Pitzschke *et al.,* 2009). Some of them encode PATHOGENESIS-RELATED PROTEINS (PR) and are induced in a huge variety of plant families. PR-proteins are divided into 17 main groups, for example β-1,3-glucanases, chitinases and peroxidases (Sels *et al.,* 2008). They accumulate in the apoplast (and vacuole) and can contribute to plant defence through their antimicrobial activity (Van Loon and Van Strien, 1999). Characteristic for plant-pathogen interactions is further the rapid production of ROS, called oxidative burst. ROS are produced in the apoplast via amine oxidases and peroxidases and in the plasma membrane by NADPH oxidases (Apel and Hirt, 2004; Nanda *et al.,* 2010). As a part of plant defence, ROS may have different functions. One may be their direct antimicrobial activity. Peng and Kuc (1992) showed that H_2O_2 inhibits the germination of spores of a variety of fungal pathogens. In addition, ROS function in defence signalling, as they were shown to activate MAPKs, thereby controlling transcription factors, and they are involved in the hypersensitive response (HR), a locally restricted cell suicide (for HR see 1.1.2.1; Apel and Hirt, 2004; Torres, 2010; Nanda *et al.,* 2010). Oxidative cross-linking of cell wall component is another important process in plant defence involving ROS. This causes a physical reinforcement of the cell wall, which may create an advance for activating further defence mechanisms by slowing down the speed of penetration (Lamb and Dixon, 1997). A very common defence reaction of plants against attacking fungi is the formation of cell wall appositions called papillae. They form underneath the site of attempted penetration, upon local physical pressure as applied by fungal appressoria and/or chemical stimulation e.g. by fungal toxins (Aist *et al.,* 1976). Papilla formation is accompanied by cytoplasmic aggregation, which leads to the

concentration of the main components of the secretory machinery at the site of attack, indicating that papillae are build by local secretion (Aist, 1976). The finding of An *et al.* (2006) that vesicles accumulate around the site of attempted penetration by powdery mildew fungi in barley cells supports this. Papillae contain phenolic compounds, antimicrobial molecules and H_2O_2 in addition to general cell wall components like callose or other polysaccharides. It is thought that these antimicrobial and toxic components together with the strengthened physical barrier of the cell wall are responsible for the restriction of pathogen invasion (Zeyen *et al.,* 2002). It is also interesting that papillae of cells successfully penetrated by powdery mildew, in contrast to non-penetrated papillae, do not contain H_2O_2, indicating an important role of H_2O_2 in penetration resistance (Hückelhoven *et al.,* 1999).

1.1.1.2 Examples of MAMP-recognition systems

The most prominent MAMP-PRR pair is the bacterial flagellin and the corresponding LRR-RLK FLAGELLIN-SENSING 2 (FLS2; Gómez-Gómez and Boller, 2000). Section 1.3.3.2 describes the interplay of these two molecules is in more detail. Only recently, Danna *et al.,* 2011 showed that FLS2 is, in addition to flagellin perception, responsible for the detection of a secreted protein from *Xantomonas oryzae* (Ax21) in *Arabidopsis*. Another example is the bacterial elongation factor Tu (EF-Tu), which is the most abundant protein in the bacterial cytoplasm and detected as a MAMP in *Arabidopsis thaliana* and other Brassicaceae (Kunze *et al.,* 2004). Responsible for the recognition of EF-Tu is EFR (EF-Tu receptor), which is a LRR-RLK from the same subfamily as FLS2 (Zipfel *et al.,* 2006). Interestingly, the downstream signalling of both receptors, FLS2 and EFR, requires another kinase named BAK1 (BRI-ASSOCIATED KINASE 1). BAK1 interacts with several other RLKs and participates in oomycete defence. This indicates that the perception of different MAMPs shares subsequent downstream components for signal transduction (Heese *et al.,* 2007; Chinchilla *et al.,* 2007; Zipfel, 2008; Roux *et al.,* 2011). Besides these LRR-RLKs, which recognize bacterial MAMPs, there are also receptors known for chitin, which is present in the fungal cell wall (Kombrink *et al.,* 2011). The chitin elicitor binding protein (CEBiP) of rice cells binds chitin and is a LRR (receptor-like protein), which, in contrast to RLKs, has no intracellular signalling domain. Knock down of CEBiP inhibited typical plant defence responses like the production of ROS and the expression of defence-related genes indicating its importance for chitin-detection and signalling. CEBiP localizes to the plasma membrane and contains two LysM motifs

thought to be responsible for the chitin-binding ability (Kaku *et al.,* 2006). Recently, Shimizu *et al.* (2010) identified another LysM-containing RLK CERK1 (chitin elicitor receptor kinase 1) to be required for chitin signalling together with CEBiP in rice. After chitin treatment, CEBiP and CERK1 form a complex thereby initiating downstream defence signalling. Interestingly, *Arabidopsis* also possesses a CERK1 protein, which is important for chitin-induced defence signalling but no CEBiP-like protein has been identified. This leads to the speculation that the chitin perception systems of rice and *Arabidopsis* could be different to some extent (Miya *et al.,* 2007; Wan *et al*., 2008; Petusching *et al*., 2010). In contrast to the dicot *Arabidopsis*, CEBiP has been reported in the monocot model plant barley, where it seems to be involved in basal resistance against *Magnaporte oryzae* (Tanaka *et al.,* 2010). Another important fungal MAMP is xylanase, which induces ethylene biosynthesis, PR-gene expression and HR. In tomato, LeEIX2 (ethylene inducing xylanase) is the receptor responsible for xylanase-perception (Ron and Avni, 2004). Beside MAMPs, plants also detect DAMPs (damage-associated molecular patterns), released if plant cells are damaged. Similar to MAMP-recognition, PRRs mediate the perception of the resulting molecules. In *Arabidopsis* the PEP1 (perpetual flowering 1) protein serves as a DAMP and its detection by the cognate receptor protein PEPR1 (PEP1 receptor 1) and PEPR2 (PEP1 receptor 2), LRR-RLKs, leads to defence signalling (Tör *et al.,* 2009; Yamaguchi *et al*., 2010).

1.1.2 Effector-triggered defence

Pathogens aim to overcome plant MTI and therefore evolved effectors to suppress MAMP-triggered defence. This suppression may either happen by directly preventing perception, through interfering with defence signalling pathways or by inhibiting defence function (Grant *et al.,* 2006). The effectors are dispensable for the pathogens viability, evolve more rapidly and clearly contribute to its virulence if the plant does not detect them (Bent and Mackey, 2007). There are different definitions concerning the term “effector”. Some researchers prefer a more strict definition of effectors as “proteins secreted by pathogens and translocated into plant cells, where they exert specific functions”, while others favour the more inclusive definition as “all pathogen proteins and small molecules that alter host cell structure and function” (Alfano, 2009). To defend itself against these pathogen-derived effectors, the plant developed specific receptor-like RESISTANCE (R) proteins, as a second layer of defence. R proteins recognize effectors either by direct effector binding or indirectly

by monitoring effector targets. The simplest model for effector recognition is the direct interaction between an effector and a plant R protein. Flor first described this so-called gene-for-gene relationship in 1942. An example for this gene-for-gene relationship is the rice R protein Pi-ta, which recognizes the *M. grisea* metalloprotease AvrPita by direct interaction, thereby conferring resistance against the rice blast fungus (Jia *et al.,* 2000). Directly detected effectors can evade recognition through mutations, and the R proteins also adapt easily (Bent and Mackey, 2007). Besides direct recognition there have been indirect recognition hypothesis described. The guard hypothesis states that the R protein is monitoring an effector target and that it detects effector action on this target protein. Modification of a guarded effector target (guardee) is recognized by the R protein and this induces defence responses (Van der Biezen and Jones, 1998; Lahaye and Bonas, 2001). A number of effectors are known to encode enzymes that alter host protein function (Mudget *et al.,* 2005). A prominent example for the guard hypothesis is RIN4 (RPM1-INTERACTING PROTEIN 4) from *Arabidopsis*. Several effector proteins from *Pseudomonas syringae* interfere with RIN4 to inhibit MAMP-induced defence. The R proteins RPM1 (*R*ESISTANCE TO *P. SYRINGAE* PV. *MACULICOLA* 1) and RPS2 (RESISTANT TO *P. SYRINGAE* 2) recognize these modifications leading to defence responses against *Pseudomonas* strains expressing the respective effectors (Kim *et al.,* 2005; Day *et al.,* 2005). Besides the guard hypothesis, the decoy model arose. In the decoy model, the guarded protein has some kind of a double which is called decoy, without any function in the absence of the cognate R protein, but the modification of the decoy leads to defence induction if the R protein is present (van der Hoorn and Kamoun, 2008). An example for this is given with the R protein PRF (PSEUDOMONAS RESISTANCE AND FENTHION SENSITIVITY), which interacts with the PTO (RESISTANCE TO *P. SYRINGAE* PATHOVAR *TOMATO*) kinase from tomato. PTO recognizes PRF-targeting effectors, which in turn induces defence (Gutierrez *et al.,* 2010). In addition, RIN4 could also be a decoy, given that the fungus does not directly benefit from RIN4 modification (van der Hoorn and Kamoun, 2008). To prevent indirect perception, the pathogen would have to stop its action on the plant protein and this would mean los of virulence in most cases. This is in agreement with the fact that indirectly percepting R proteins evolve more slowly (Bent and Mackey, 2007). According to their domain structure, R proteins are divided into two main classes. Most of them possess a nucleotide binding site (NB) and a LRR

domain and are localized to the cytoplasm of the host cell (Jones and Dangl, 2006; Chisholm *et al.,* 2006). The second class are RLPs with extracellular LRR domains (Dangl and Jones, 2001; Chisholm *et al.,* 2006). This type of defence-related pathogen detection, pathogen-derived effectors recognized by plant R proteins, is called effector-triggered immunity (ETI; Jones and Dangl, 2006). Effectors need to be transported to the host cytoplasm as the recognition of effectors by R proteins takes place there in most cases. For this purpose, gram-negative bacteria like *Pseudomonas syringae* employ the so-called type-three-secretion system (T3SS). It enables them to inject effectors directly via a pilus that connects the bacterium with the host cytoplasm (Büttner and He, 2007). Effectors from oomycete and powdery mildews also interact with intracellular R proteins (Ridout *et al.,* 2006; Whisson *et al.,* 2007; Dou *et al.,* 2008). How they reach the host cytoplasm is not clear in detail but they are introduced into the host cell from specialised structures called haustoria. In case of the oomycete effectors, an RXLR motif is responsible for the translocation, which might to involve host-mediated endocytosis (Whisson *et al.,* 2007; Dou *et al.,* 2008).

1.1.2.1 Defence reactions following effector perception

This second layer of plant defence frequently results in an HR and the expression of PR-proteins as well as callose deposition (Thordal-Christensen, 2003; Bent and Mackey, 2007; De Wit, 2007). A rapid localized death of cells surrounding the site of attack is the main characteristic of an HR (Heath, 2000). The recognition of effectors by *R*-gene products and their activation elicit the HR (Ingle *et al.,* 2006). For example, interaction of the effector-R-protein systems AvrPTOB-PTO-PRF as well as AvrRPM1-RIN4-RPM1/RPS2 triggers an HR (Mur *et al.,* 2008). Early evidences for the beginning of an HR are Ca^{2+} influx into the cytoplasm, the accumulation of ROS, which might be translated into a MAPK signalling cascade, and the activation of defence gene expression (Heath, 2000). ROS might be produced not only by NADPH oxidases in the apoplast but also through mitochondria and chloroplast dysfunction leading to the accumulation of ROS inside the cell (Mur *et al.,* 2008). Another important factor for the initiation of HR is salicylic acid (SA). NahG plants, unable to accumulate SA, fail to conduct a HR. Moreover, dead cells accumulate SA at high levels, while living, neighbouring cells have only slightly enhanced SA inside (Alvarez, 2000). The third important molecule involved in HR initiation is NO (Wendehenne *et al.,* 2004). Without NO accumulation, *Arabidopsis* cells respond with

a reduced HR (Zeier *et al.,* 2004). The execution of the HR is characterized by several cellular rearrangements like nucleus movement, reorganisation of the actin cytoskeleton, cessation of cytoplasmic streaming, DNA cleavage and finally the loss of plasma membrane function and protoplast shrinkage. Due to the accumulation of phenolic compounds, the cells become brown and autofluorescent (Heath, 2000). Although many aspects of the HR are well studied, a detailed model of the molecular mechanisms is still incomplete (Mur *et al.,* 2008). For biotrophic pathogens, which need a living host cell, cell death might be an effective defence mechanism itself but it seems as if the effects of the hypersensitive cell death exceed this direct function. HR has been implicated in the systemic acquired resistance by priming neighbouring cells for defence and HR goes along with many induced defence responses (Heath, 2000). But the HR initiating molecules ROS, SA and NO trigger defence in the absence of HR, suggesting that HR might be a consequence of defence rather than the actual defence mechanism (Mur *et al.,* 2008).

1.1.2.2 Examples for the interference of effectors with plant defence

How pathogen-derived effectors manipulate host defence is best studied for effectors of the type III secretion system of bacteria. They mainly target three host processes, which represent essential parts of host defence (Block *et al.,* 2008). First, they interfere with protein abundance either by using the host ubiquitination machinery or by direct cleavage. This was shown e.g. for effectors of *Ralstonia solanacearum* called GALA, which interact with components involved in ubiquitination in *Arabidopsis* (Angot *et al.,* 2006). Second, some effectors modulate host transcription. The *Xanthomonas campestris* effector AvrBs3 e.g. binds to the promoter of *upa20* and induces its expression. Upa20 is a transcription factor, which is presumably responsible for cell enlargement of which the pathogen benefits (Kay *et al.,* 2007). Thirdly, they alter the phosphorylation status of signalling kinases. The *Pseudomonas syringae* effector AvrHopAI1 directly interacts with MAPKs acting in FLS2 downstream signalling, thereby preventing flg22 (22 amino acids of the conserved part of flagellin)-triggered PTI immune responses (Pitzschke *et al.,* 2009). Pathogens often posses a set of effectors with overlapping functions, which most likely target important plant defence processes. This is the case e.g. for AvrPTO and AvrPTOB, both interfering with the flagellin-induced defence. The same is true for the already mentioned effector target protein RIN4, which is addressed by at least three different effectors, AvrB, AvrRPM1 and AvrRPT2, indicating that RIN4 marks an important

point of plant defence. The effector set AvrE, HopR1 and HopM1 interferes with vesicle trafficking by influencing the function of MIN7 (HopM1 INTERACTOR 7), an ARF (ADP-RIBOSYLATION FACTOR)- GEF (GUANIN EXCHANGE FACTOR), in *Arabidopsis* (Pritchard and Birch, 2011; see also section 1.3.3.5). Other effectors target the function of plant hormones like the *P. syringae* effector HopAM1. It increases abscisic acid signalling, leading to stomata closure and thereby to the protection of the plant and the bacterial colony from water stress (Goel *et al.,* 2008). Concerning fungal and oomycete effectors there is not as much information available. However, prominent example for fungal effector function is Avr4 from *Cladosporium fulvum*, which is thought to protect the fungus from plant chitinases thereby circumventing chitin perception by the plant (Stergiopoulos and de Wit, 2009).

1.2 The barley – powdery mildew model system

Powdery mildew fungi are Ascomycete fungi that belong to the order of *Erysiphales* and herein to the family of *Erysiphaceae,* which consists of 16 genera and 650 species worldwide. Altogether this family infects more than 9000 dicot- and over 600 monocot plant species. Most monocot host species such as barley and wheat belong to the *Poaceae* family (Inuma *et al.,* 2007). The majority of powdery mildew fungi only infect a strongly restricted range of host plants, often only one single host species. *Blumeria graminis*, which contains highly specialized *formae speciales* infects cereal plants. Barley only is colonized by the barley powdery mildew fungus (*Blumeria graminis* f.sp. *hordei*, *Bgh*), while it is for example resistant to infection by the wheat powdery mildew fungus (*B. graminis* f.sp. *tritici*; Saenz *et al.,* 1999; Wyand and Brown, 2003). All powdery mildew fungi are obligate biotrophic parasites and characterized by their epiphytic growth on host plants. Macroscopically visible symptoms are typical white velvety pustules or plane and even covering mycelium that can develop on the aerial parts of infected plants.

Bélanger *et al.* (2002) have reviewed the lifecycle of (cereal) powdery mildew fungi in detail. Cereal powdery mildew fungi produce asexual conidiospores that germinate 0.5-1 h after leaf contact with a primary germ tube, which is the first emerging structure (Kunoh, 2002). It functions in sensing and adhering the fungus to the leaf surface as well as in water uptake (Carver and Bushnell, 1983; Carver and Ingerson, 1987). Subsequently, about 3-4 hours after infection (hai), a hook-shaped appressorial germ tube emerges (Kunoh, 2002). It releases liquid material containing esterases such as cutinases, which together with local turgor pressure enables the

infection peg to penetrate the plant cell wall and papillae (Francis *et al.,* 1996; Pryce-Jones *et al.,* 1999). The penetration takes place about 12-15 hai. To gain access to nutrients, powdery mildew fungi form a special feeding structure, the haustorium, which invaginates the host plasma membrane without disrupting it. The so-called haustorial complex consists of an inner haustorial cytoplasm that is surrounded by the haustorial plasma membrane, the haustorial cell wall, the so-called extrahaustorial matrix and the extrahaustorial membrane (Gil and Gay, 1977). The haustorial plasma membrane and the haustorial cell wall derive from the fungus, whereas the extrahaustorial membrane is in continuum with the host plasma membrane. However, the extrahaustorial membrane differs from the normal plant plasma membrane in structure and function. For example, it is thicker and contains a different set of proteins than the normal plant plasma membrane (Gil and Gay, 1977; Koh *et al.,* 2005). Since it represents the site of most intimate contact, the haustorial complex may be responsible for nutrient transfer between host and pathogen (Eichmann and Hückelhoven, 2008).

1.3 The cellular transport machinery in eukaryotes

Life and functionality of a eukaryotic cell depends on the correct organization of different organelles, structures and membrane systems. It is becoming more and more clear that plant defence also relies on a functional transport and secretion machinery (see e.g. Hückelhoven, 2007b; Robatzek, 2007; Frei dit Frey and Robatzek, 2009; Bednarek *et al.,* 2010). Each cellular compartment is composed of specific proteins that maintain its function and integrity. Therefore, a highly specific transport system is necessary that is able to connect the different compartments and to ensure the delivery of the respective proteins to their destination at the right point in time. Fully functional cells depend on the correct synthesis, sorting and delivery of many different kinds of proteins. Proteins produced and sorted in the secretory pathway are either secreted proteins, proteins and enzymes that belong to the different cell compartments, or plasma membrane-resident proteins. Targeting domains that direct the nascent protein through its maturation process ensure the correct processing of proteins. Proteins that are destined for the secretory pathway are generally labelled with a signal peptide at their N-terminus. This signal peptide leads to the attachment of the ribosome together with the nascent protein to the endoplasmic reticulum (ER) membrane. During translation, soluble proteins are

released into the lumen of the ER, while membrane-localized proteins are inserted into the ER membrane (Lodish *et al.,* 2000; Buchanan *et al*., 2002).

Following translation, the proteins are folded and modified before they are shipped to the cis-Golgi compartment via COPII (*c*oat protein complex II) vesicles that mediate the transport from the ER to the early Golgi. The formation of vesicles involves ER-resident proteins, a small GTPase (guanosintriphosphate) called SAR1 (secretion-associated RAS-related protein 1) and cytosolic coat proteins. After budding, the COPII vesicle travels to and fuses with the cis-Golgi membrane. Tethering factors and the formation of specific SNARE (soluble N-ethylmaleimide sensitive fusion protein attachment protein receptors) complexes for vesicle fusion assist this process. Upon arrival at the cis-Golgi membrane, the proteins are further modified, while migrating through the Golgi compartment from the cis to the trans-side, ending up in the trans-Golgi-network (TGN). To maintain the integrity of the different compartments COPI (coat protein complex I) vesicles carry escaped proteins backwards form trans to cis-Golgi and from the cis-Golgi to the ER. The formation of COPI vesicles involves the small GTPase ARFI. The TGN functions as a sorting station sending proteins to their respective compartment either by continuous secretion or via secretory vesicles that deliver their cargo after a stimuli. Clathrin-coated vesicles mediate transport from the TGN or the plasma membrane. The classical secretory pathway from the ER via Golgi and further on along to the destination compartments is called anterograde transport. Similar to the transport of proteins out of the cell there is also an uptake of proteins from the exterior of the cell by endocytosis. This mechanism allows the cell to sense environmental changes, which for example is important for the detection of pathogens. Internalization of material form the cell surface also involves clathrin-coated vesicles. The fist compartment that is reached by endocytosed vesicles is the early endosome/TGN. Here the proteins are sorted either into the late endosome/MVB (multi-vesicular bodies) pathway for degradation (default endocytosis) in the vacuole or into a recycling endosome. Internalized proteins are either destined for degradation in the lytic compartments or recycled back to the plasma membrane. In addition, there are signal-mediated pathways like the retrograde transport, which is responsible for the recycling of escaped proteins (Lodish *et al.,* 2000; Buchanan *et al*., 2002; Bassham *et al.,* 2008; Viotti, 2010). Figure 1 shows a simplified scheme of the basic transport processes described above.

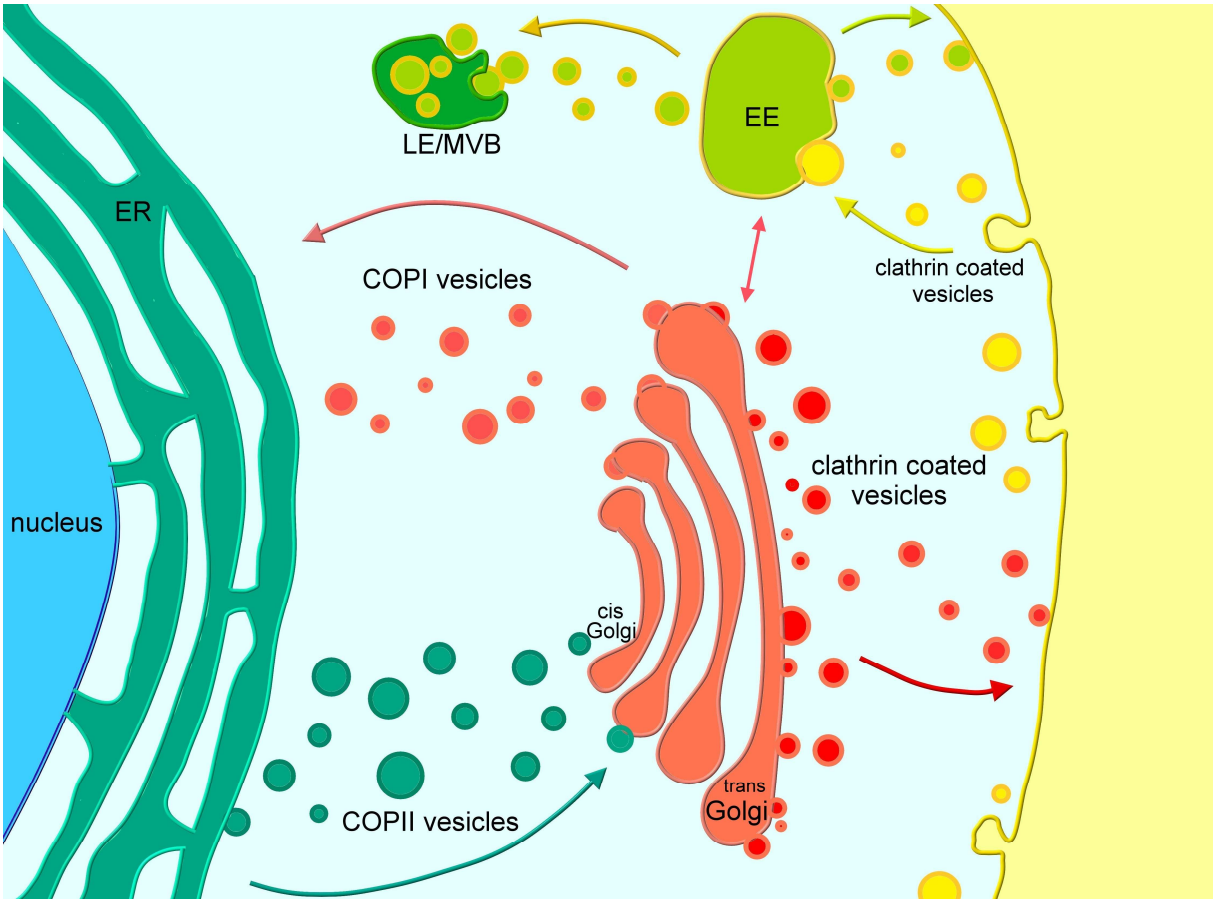

Figure 1: Simplified scheme of transport processes in eukaryotic cells

The secretory default pathway is responsible for the transport of proteins from the ER to the Golgi via COPII vesicles and further on to the plasma membrane in clathrin-coated vesicles. The endocytic default pathway carries material form outside the cell in clathrin-coated vesicles to the vacuole via EE (early endosome) and LE (late endosome)/MVB (multi-vesicular bodies). In addition, retrograde transport mediates recycling of escaped proteins using COPI vesicles.

1.3.1 Peculiarities of transport in plant cells

This rough general model (Figure 1) is manly based on information from yeast an animal cells but many important traffic proteins have homologues in plants. In a phylogenetic analysis of different transport proteins Dacks *et al.* (2008) showed that despite the existence of many conserved proteins, others evolved after the last common eukaryotic ancestor independently in the different kingdoms. This might explain the in many cases large protein families found in plants. For example the SNARE protein family is highly expanded in plants with at least 54 members in *Arabidopsis*, while only 21 and 35 exist in *Saccharomyces cerevisiae* and *Homo sapiens*, respectively (Uemura *et al.,* 2004; Moreau *et al.,* 2007). The same is true for the Rab-GTPase family with 11 members in *Saccharomyces cerevisiae* and 57 in

Arabidopsis (Rutherford and Moore, 2002). Important is also that in contrast to the yeast and mammalian Golgi the plant Golgi bodies are highly mobile. They move through the cell along the ER/actin network driven by myosin motors or actin depolymerisation/polymerisation (Hawes *et al.,* 2008). Another main difference between the general model and transport in plant cells is that all attempts to proof the existence of COPII vesicles failed. However, COPII proteins are highly conserved and there are more isoforms existing in plants compared to yeast and mammals (Robinson *et al.,* 2007). Nevertheless, they influence the transport between ER and Golgi. The question how cargo from the ER reaches the Golgi still needs to be elucidated in detail but two models arose: one considers the two compartments as a mobile unit and the other as a kiss and run association. According to the one unit model, cargo is exported during a synchronous movement of the Golgi along the ER at specialized ER export sites (ERES), while in the kiss and run model, cargo is exported during temporary association of the Golgi at the ERES. The transfer of proteins might be carried out by tubular connections that form between the Golgi and the ERES and this process might be COPII dependent (Hanton *et al.,* 2006; Marti *et al.,* 2010).

1.3.2 Specificity of transport processes

The basic processes of the eukaryotic trafficking system seem to be highly conserved and ancient although there has been functional diversification (Koumandou *et al.,* 2007). Vesicles mediate the transfer of material between distinct membrane compartments. An ingenious transport system has evolved to ensure the correct loading, budding, transport and fusion of these vesicles. Specificity is achieved by the interplay of many different proteins and protein complexes that ensure the correct localization of the distinct proteins.

1.3.2.1 Initiation and budding: Genesis of vesicles

The three main vesicle classes, clathrin, COPI and COPII vesicles, share structural and functional features. Each vesicle coat is composed of two sub-complexes, one representing the inner and one the outer layer of the vesicle. The inner layer serves as adaptor for the outer cage. The coat components interact with cargo molecules either directly or indirectly (via adaptor proteins) and thus play an important role in cargo recruitment. In addition, they interact with multiple accessory proteins, which assist diverse steps of vesicle cycling, e.g. by supporting cargo recruitment,

promoting vesicle movement, coat polymerisation or coat disassembly (McMahon and Mills, 2004). According to Springer *et al.* (1999), the assembly of a "priming complex" initiates the formation of a transport vesicle. For this purpose a GEF recruits its small GTPase (from the ARF or SAR family for COPI and clathrin or COPII vesicles, respectively) to the donor membrane where it is converted to its active state. The active GTPase interacts with a primer protein, e.g. the appropriate v-SNARE. A coat component carrying a GAP protein (GTPase activating protein) binds this dimer, thereby completing the priming complex (consisting of a GTPase, a primer and a coat protein). In the following, additional priming complexes and cargo proteins accumulate (coat polymerisation) and deform the donor membrane, initiating budding. Therefore, priming complexes contribute to transport accuracy by the defined localization of the GEFs and by cargo selection (Springer *et al.,* 1999). More recently, it has become clear that cargo proteins themselves play an important role in the formation of vesicles. This was shown for the cargo protein p24, which facilitates the formation of COPI vesicles by stabilizing the priming complexes (Aguilera-Romero *et al.,* 2008). In addition to ARF and SAR-GTPases, some Rab-GTPases are important for cargo selection. For example, Rab9 is involved in the recycling of a TGN-derived receptor from the endosome back to the TGN (Aguilera-Romero *et al.,* 2009). Many of these key proteins of the vesicle budding machinery are present in plants (Hawes *et al.,* 2008; Hwang and Robinson, 2009; Marti *et al.,* 2010) but there are also some differences. For example Donohoe *et al.* (2007) identified two different types of COPI vesicles in *Arabidopsis* and named them COPIa and COPIb. The main difference seems to be in their coat architecture and the zone of action. COPIa vesicles are responsible for the transport from the cis-Golgi back to the ER and bud from cis-Golgi cisternae, while COPIb vesicles seem to mediate intra-Golgi retrograde transport, budding from medial and trans-cisternae.

1.3.2.2 Movement: direction of the vesicle to its destination

After fission of a vesicle, it reaches its destination either by diffusion or by motor-mediated transport along the cytoskeleton. Most motor proteins belong to the kinesin, dynein or myosin protein family. Rab proteins, which may serve as receptors for the motor proteins mediate their recruitment to the vesicle (Hammer and Wu, 2002). Interestingly, for Rab7, which is important for the transport of late endosomes to the lysosome in animal cells, it was shown that the motor recruitment by Rab7 is captured by pathogens (*Salmonella* SifA and *Heliobacter pylori).* They use this

pathway to enable the generation of a bacterium-containing compartment (Hutagalung and Novick, 2011).

1.3.2.3 Coat release: preparation for fusion

It was thought for a long time that a vesicle has to get rid of its coat before it can fuse with its target membrane. The uncoating classically occurs immediately after budding. Recent investigations soften the necessity of vesicle uncoating prior to fusion into a possibility (Angers and Merz, 2011). There are hints for vesicle coats also involved in tethering and in fusion processes. Interactions between various vesicle components ensure coat stability and it may be that the interference of Rab-GTPases with these interactions facilitates uncoating (Angers and Merz, 2011). In addition, tethering complexes have been considered to trigger coat release, after they have identified the vesicle type, to allow SNARE pairing (Sztul and Lupashin, 2009).

1.3.2.4 Vesicle targeting and fusion

The final step of vesicle transport is the merge of the vesicle with its target membrane. This process results in the delivery of vesicle cargo to the respective destination compartment. Several proteins or protein complexes, which ensure the correct cargo delivery, organize this highly specialized process. This final phase of vesicle transport can be divided into three steps: tethering, docking and finally fusion of the two membranes. The first contact of the vesicle with its target membrane is referred to as tethering. Tethering processes are thought to initially bridge the two membranes in a first loose interaction leaving a distance between the vesicle and the destination membrane (Whyte and Munro, 2002; Sztul and Lupashin, 2006). The currently known tethering factors can be classified into long coiled coil tethers and multi-subunit tethering complexes (MTC). Long coiled coil tethers can cover distances of more than 200 nm, while MTCs bridge distances up to 30 nm. The long coiled coil tethers are further divided into Golgins, mainly found at the Golgi membrane, and endosomal tethering factors. The MTC class comprises the HOPS (homotypic fusion and protein sorting), CORVET (class C core vacuole/endosome tethering), Dsl1 (dependence on SLY1), COG (conserved oligomeric Golgi), Exocyst, TRAPPI, II, III (transport protein particle) and GARP (Golgi associated retrograde protein) complexes (reviewed in Cai *et al.,* 2007; Bröcker *et al.,* 2010). Tethering factors seem to be important for the specificity of membrane trafficking processes,

because they interact with several critical components of the transport machinery. An overview over the different MTCs and their known interaction partners is available in the TableS1. The first group of interesting proteins identified as interaction partners of all known tethering complexes (except Dsl1) are Rab-GTPases. Most tethering complexes are effectors of Rabs, which are responsible for the recruitment of the complexes to the respective membrane. The TRAPP complexes are not effectors of Rabs but function as Rab-GEFs thereby enabling the Rab to interact with its effectors (reviewed in Sztul and Lupashin, 2009; Bröcker *et al.,* 2010; Hutagalung and Novick, 2011). The second proteins found to interact with many tethering complexes are SNARE proteins. These proteins are, together with their interaction partners, responsible for the final process of vesicle fusion.

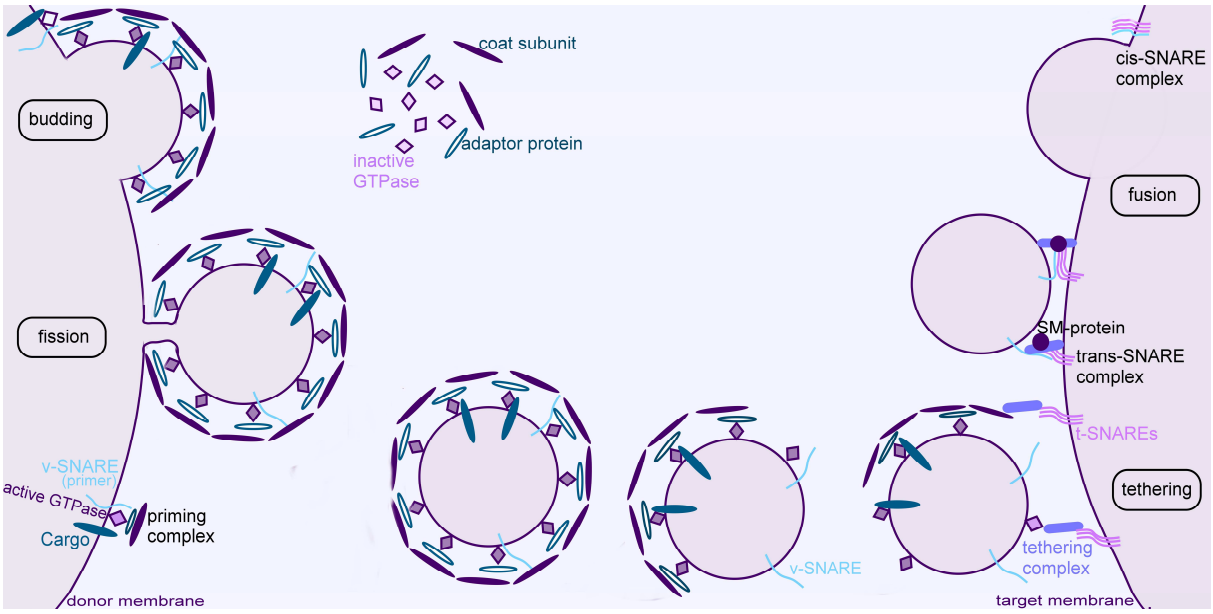

Figure 2: The life cycle of a vesicle

Formation of a vesicle at the donor membrane starts with the assembly of a priming complex composed of a v-SNARE, an active GTPase, cargo and coat proteins. Accumulation of additional priming complexes and cargo initiates budding and subsequently the vesicle fissures from the donor membrane. Prior to the first contact with the target membrane (partial) coat release is initiated. Tethering complexes may bridge the distance between vesicle and target membrane by the interaction with Rabs, SNAREs and coat proteins. Finally, the interaction of a v-SNARE with the t-SNAREs and the following conformational changes from a cis-SNARE to a trans-SNARE complex leads to fusion. SM [Sec1 (yeast) / Munc18 (mammals) -related-]-proteins assist the final SNARE protein based fusion.

The interaction between SNAREs and tethering complexes might regulate the stability of the complex or proofread SNARE assembly and it could be part of the

fusion process itself as the tethering complex might interact with a GTPase on one membrane and a SNARE on the other membrane. In addition, tethers interact with coat proteins. This interaction should occur prior to shedding of the coat raising the possibility of an involvement of tethers in vesicle uncoating (reviewed in Sztul and Lupashin, 2009; Bröcker *et al.,* 2010). For plants, there is not as much information available but some tethering complexes or subunits of them have been identified and studied to some extend. The most prominent plant-tethering complex is the exocyst. In *Arabidopsis,* multiple genes encode most subunits of the exocyst, while in yeast each subunit is encoded by a single gene. This probably points to a more diverse exocyst function in plants besides polarized secretion (Elias *et al.,* 2003; Zhang *et al.,* 2010). In addition, subunits of the HOPS/VPS complex are present in *Arabidopsis* and seem to function in membrane fusion at the prevacuolar compartment (PVC) and vacuole (Rojo *et al.,* 2003). Similarly, Guermonprez *et al.* (2008) suggested the existence of a GARP complex in *Arabidopsis* and a role for this complex in retrograde transport to the Golgi, and Thellmann *et al.* (2010) identified subunits of the TRAPP complexes in *Arabidopsis* and linked them to cell plate formation. Long coil-coiled tethers are also present in *Arabidopsis*, as for example shown for the family of Golgins (Latijnhouwers *et al.,* 2005 and 2007). After tethering, SNARE proteins mediate further specificity. These proteins can be classified either according to their localization or according to their structure. SNARE proteins that localize to the vesicle are commonly designated as v-SNAREs, while the ones, which reside on the target membrane, are called t-SNAREs (Söllner *et al.,* 1993). The structural classification distinguishes between Q and R-SNARE proteins according to the presence of the amino acid arginine or glutamine at a specific sequence position. A functional SNARE complex is composed of one R- and three Q-SNAREs (Fasshauer *et al.,* 1998) or one v- and three t-SNAREs, which form a four-helix bundle (Sutton *et al.,* 1998), the SNAREpin, also called trans-SNARE complex. This trans-SNARE complex pulls the two membranes together, thereby providing enough energy to overcome the repulsive nature of two opposing lipid bilayers (Malsam *et al.,* 2008; Südhof and Rothman, 2009). After fusion of the two membranes, the trans-SNARE complex becomes a cis-SNARE complex with all four SNAREs on the same membrane (Bonifacino and Glick, 2004; Südhof and Rothman, 2009). Finally, the cis-SNARE complex is dissolved again and the SNARE proteins can be reused (Malsam *et al.,* 2008). The most prominent SNARE complex is involved in exocytosis in

mammals and is composed of the v-SNARE synaptobrevin (=VAMP, vesicle-associated membrane protein) and the t-SNAREs syntaxin and SNAP25 (providing two α-helices). All SNARE complexes seem to be composed of proteins similar to these well-studied complex components (Bonifacino and Glick, 2004). An additional function of SNARE proteins in the regulation of membrane fusion is that non-matching SNAREs (iSNAREs for inhibitorySNARE) were shown to bind or substitute matching SNAREs thereby inhibiting the formation of a functional SNARE complex (Varlamov *et al.,* 2003). SNARE proteins confer a high degree of specificity to the membranes designated to fuse through their protein combination and localization (Bonifacino and Glick, 2004) but they cannot be responsible for the specificity of fusion processes exclusively. There are examples where SNARE proteins can be used in multiple pathways (Pelham, 2001; Malsam *et al.,* 2008), and the fact that SNARE proteins are recycled implicates that they are present not only at their site of function (Bonifacino and Glick, 2004). In *Arabidopsis* Uemura *et al.* (2004) identified 54 different SNARE proteins, much more than in the yeast or mammalian genome. They examined their cellular localization and found six at the ER, nine at the Golgi, four at the TGN, two in endosomes, 17 at the plasma membrane, seven in PVC and the vacuole, two in the TGN, the PCV and the vacuole and one in the TGN, PVC and at the plasma membrane. An interesting protein family associated with the mediation of additional specificity to fusion processes are SM [Sec1 (yeast) / Munc18 (mammals) -related-] proteins. These proteins seem to have a proofreading and regulatory function on SNAREs or SNARE complexes, respectively. On the one hand, they have a function as negative regulators of fusion when they are bound to the t-SNARE syntaxin1. This interaction keeps the respective t-SNARE in a closed confirmation, which prevents SNARE complex formation. On the other hand, SM-proteins also interact with the trans-SNARE complexes and this interaction promotes fusion (SM proteins as positive regulators of fusion; Malsam *et al.,* 2008). The mammalian SM-protein Munc18-1 was shown to be important for the delivery (probably by influencing the actin network), tethering and docking (by binding to monomeric syntaxin1) and fusion (by clasping the trans-SNARE complex) of transport vesicles (Toonen and Verhage, 2007). Another example for additional regulating components are again Rab-GTPases. Endosomal SNARE proteins and proteins of the Sec1 family interact with Rab effectors or directly with Rab-GTPases. The interaction of Rab-GTPases with well-known components of the fusion

machinery confers an additional layer of accuracy to the fusion process (Stenmark, 2009; Hutagalung and Novick, 2011). Six Sec1 related proteins exist in the genome of *Arabidopsis* but only one (KEULE) has been characterized and shown to play a role in cytokinesis (Assaad *et al.,* 2001; Lipka *et al.,* 2007).

1.3.2.5 Rab-GTPases

Many of the vesicle trafficking steps involve the action of Rab-GTPases. Stenmark (2009) and Hutagalung and Novick (2011) have described the multiple roles of Rab-GTPases in transport processes in detail. Rab-GTPases are the hugest subgroup of the super family of small Ras-like-GTPases. In yeast 11 different Rab-GTPases have been identified, while there are more than 60 Rabs in mammals (and about 60 in *Arabidopsis*; Pinheiro *et al.,* 2009). Rab-GTPases cycle between the cytosol and their respective membrane, depending on their GDP/GTP status (guanosindiphosphate/guanosintriphosphate). The inactive, GDP-bound form is inserted into the membrane via geranylgeranyl modification. GDP dissociation inhibitors (GDIs) assist this process. The inactive membrane bound Rab is activated by GEFs, which facilitate GDP release, and high cytosolic GTP levels ensure the binding of GTP instead. Activated Rab-GTPases interact with a broad range of effector proteins, which in turn facilitate the transport pathway they act in. A GTPase-activating protein (GAP) stimulates the intrinsic GTPase activity of the Rab and it is converted into is inactive, GDP-bound form again. GDI aids the release of the inactive form from the membrane and the Rab is available for the next GTPase cycle. Rab effector proteins are defined as proteins that interact predominantly with the activated Rab form. These effectors represent a wide range of proteins, including proteins for cargo recruitment, vesicle movement, vesicle uncoating, tethering and fusion, as already outlined in the sections above. In addition, Rab-GTPases play an important role in membrane identity because their insertion into a specific membrane recruits a certain set of effectors selectively to this membrane sections. Interestingly, the disease strategy of several microorganisms targets Rabs. *Salmonella* and *Clamydia* for example, both release proteins that prevent the Rab-dependent transport of their resident vacuoles to the lysosome (Hutagalung and Novick, 2011). Viruses also manipulate Rab-dependent pathways for their internalisation (Stenmark, 2009). The *Arabidopsis* genome encodes 93 small GTPases, which are divided into four subgroups: Rho, Rab, Arf and Ran (but no Ras-GTPases). The Rab family contains 57 members, representing the largest group and functions in intracellular

transport processes. It is further divided into eight subfamilies named AtRabA-F (Vernoud *et al.,* 2003).

1.3.3 Trafficking and transport in plant-pathogen interactions

Membrane trafficking and secretion are important processes for plant immune responses. Pathogens are recognized by plants via specialized receptors and the subsequent signal transduction induces various defence reactions of which many involve endo- or exocytic transport processes. The precise execution of defence-related transport processes by the plant and on the other hand the disruption of the same by pathogen-derived effectors is critical for the outcome of the plant-pathogen interaction (reviewed in Robatzek, 2007; Hückelhoven, 2007a; Hückelhoven, 2007b; Kwon *et al.,* 2008a; Frei dit Frey and Robatzek, 2009; Bednarek *et al.,* 2010).

1.3.3.1 Global changes in attacked cells

In plant cells attacked by pathogens, massive reorganization events take place on the cellular level. Remodelling of the cytoskeleton leads to the aggregation of the cytoplasm, nucleus, ER and Golgi bodies underneath the site of attempted penetration. The focal arrangement of the cytoskeleton depends on actin polymerisation. Inhibition of actin polymerisation prevents papilla formation and leads to enhanced susceptibility (Kobayashi *et al.,* 1997). These cell responses have been observed for several plant-pathogen interactions (Takemoto *et al.,* 2003; Koh *et al.,* 2005). The reorganization of many cellular organelles concentrates the main components of the secretory machinery to the site of attack.

1.3.3.2 Plasma membrane reactions

An interesting trafficking process upon pathogen detection is the reorganization of plasma membrane proteins. The plasma membrane is no homogenous layer but likely comprises domains with a specific composition of lipids and proteins. These specific domains are called lipid (or membrane) rafts and have been defined as “small (10 -200 nm), heterogeneous, highly dynamic, sterol- and sphingolipid-enriched domains that compartmentalize cellular processes” (Pike, 2006). Membrane rafts might function as centers of signalling events because the amount of signalling molecules like leucine-rich repeat receptor like kinases and G-proteins is high in these fractions (Shahollari *et al.,* 2004). For example, the composition of membrane

rafts changes in *Arabidopsis* cells upon flg22 treatment leading to a concentration of e.g. RLKs like FLS2 (Keinath *et al.,* 2010). Similarly, the treatment of tobacco cells with an elicitor of defence reactions (cryptogein) revealed changes in the composition of the microdomains. This indicates that lipid rafts could play a role in defence associated signalling, as it is known from rafts in animal cells (Stanislas *et al.,* 2009). The finding that a tobacco NADPH oxidase, NtRBOHD (Nt = *Nicotiana tabacum*) accumulates in lipid rafts and is speculated to be involved in defence signalling (Lherminier *et al.,* 2009) also points towards this hypothesis. Interestingly, many plasma membrane-localized proteins associated with defence concentrate at the site of attempted attack or in papillae like for example PEN1/ROR2 and PEN3, see below, or the prominent susceptibility factor MLO (MILDEW LOCUS O) from barley (Bhat *et al.,* 2005). Beside these microdomains, there are further examples for the redistribution of plasma membrane-localized proteins. One of them is the MAMP-perception receptor FLS2. FLS2 is a leucine-rich repeat receptor-like kinase, which resides in the plasma membrane and detects the bacterial MAMP flagellin (Gómez-Gómez and Boller, 2000). Mutant plants impaired in FLS2-mediated flagellin perception are more susceptible to gram negative bacteria (Zipfel *et al.,* 2004). Flagellin-sensing induces plant defence as characterized by the rapid production of ROS (Felix *et al.,* 1999), the activation of a MAPK cascade (Asai *et al.,* 2002) and enhanced expression of defence-related genes (Zipfel *et al.,* 2004). The receptor FLS2 is rapidly internalized after elicitor treatment. It disappears from the plasma membrane and localizes to small vesicles inside the cell instead (Robatzek *et al.,* 2006). This specific ligand-induced endocytosis is followed by the polyubiquitination of FLS2, leading to its degradation (Lu *et al.,* 2011). Similarly, the tomato MAMP receptor LeEIX1/2 was predicted to be an extracellular receptor containing a motif for endocytosis. This endocytosis signal is necessary for the elicitation of the defence response (Ron and Avni, 2004). Moreover, an uptake of putative ligands into the cell has also been shown. In tobacco cells for example, the bacterial-derived MAMP lipopolysaccharide binds to the plasma membrane before it is internalized (Gross *et al.,* 2005). Moreover, the plasma membrane is in continuum with the extrahaustorial membrane, which separates the haustorium from the host cytoplasm. This specialized membrane is either the invaginated and differentiated plasma membrane or synthesized de novo by targeted vesicle transport (Koh *et al.,* 2005). The latter hypothesis is supported by the finding that a resistance protein from *Arabidopsis*,

RPW8.2, is integrated into the extrahaustorial membrane of *Arabidopsis* powdery mildew fungi and found in vesicles surrounding the haustorial complex (Wang *et al.,* 2009; Micali *et al.,* 2010). Furthermore, the composition of the extrahaustorial membrane varies during haustorium development by the incorporation of plant material (Micali *et al.,* 2010). Both hypotheses necessitate the rapid provision of the required components for the generation of the extrahaustorial membrane. Therefore, secretion or recycling plays an important role for haustorium establishment.

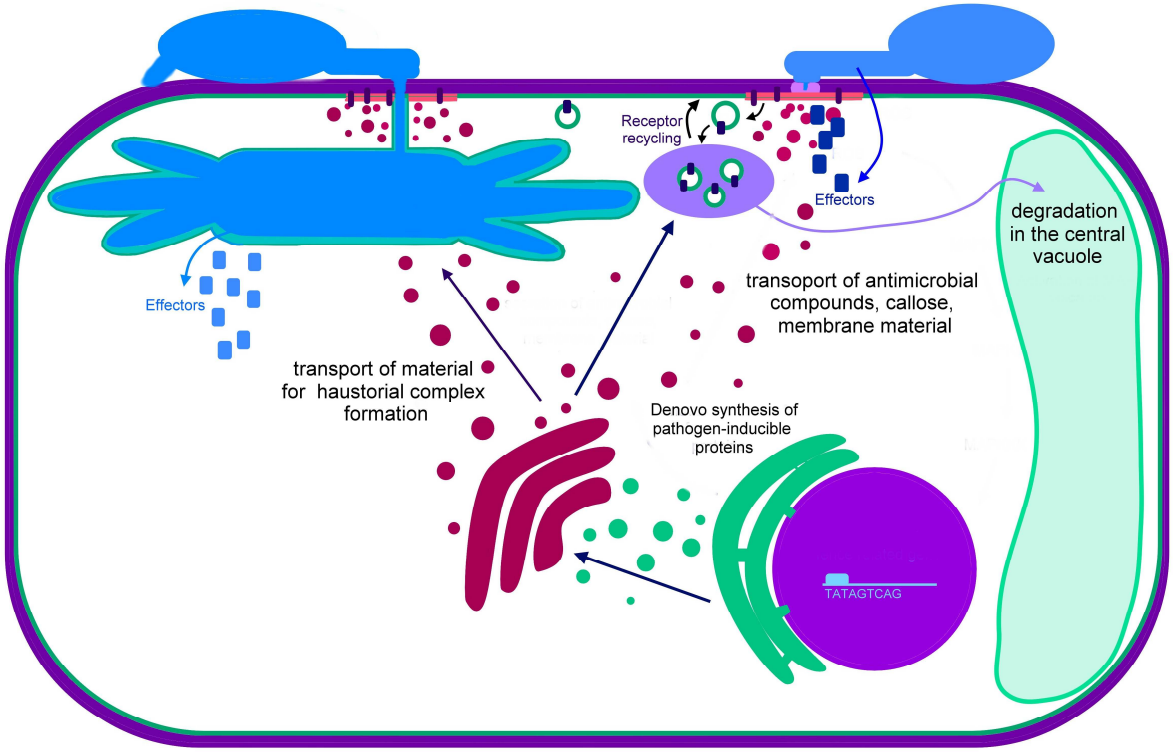

Figure 3: Examples of transport processes in plant–pathogen interactions

Pathogen recognition of plants leads to various defence reactions that involve transport processes. Signals like ROS and NO production as well as MAPK cascades end up in gene expression of defence-related genes. As a result, antimicrobial compounds, callose, and other materials are transported to the site of attack, where cell wall strengthening and papilla formation take place. This involves components of the secretory machinery and vesicle-mediated transport. At the plasma membrane, massive reorganization events occur including receptor endocytosis, degradation or recycling as well as the formation of lipid rafts (pink membrane areas). Successful biotrophic fungi establish a haustorium, which is in close contact with its host cell. Pathogen-derived effecters try to interfere with or co-opt plant defence processes at many stages.

1.3.3.3 Vesicle trafficking in plant defence

The most prominent example for the importance of vesicle trafficking in plant-pathogen interactions is a SNARE complex at the plasma membrane. It is build up by the syntaxin SYP121 (SYNTAXIN OF PLANTS 121; =PEN1, required for *Arabidopsis* penetration resistance), SNAP33 and the v-SNARE VAMP721/722 (Collins *et al.,* 2003; Kwon *et al.,* 2008b). PEN1 was discovered in a screen for *Arabidopsis* mutants with altered penetration (*Arabidopsis pen*-mutants) resistance to the non-adapted barley powdery mildew fungus (Collins *et al.,* 2003). The enhanced susceptibility to *Bgh* is accompanied by a delayed papilla formation and a reduction in callose deposition around the penetration peg (Assaad *et al.,* 2004; Kwon *et al.,* 2008b). Similar observations were made for VAMP721/722. *Arabidopsis* mutants impaired in VMAP721/722 function show not only delayed callose deposition and enhanced penetration rates after infection with the non-adapted powdery mildew *E. pisi*, but also enhanced susceptibility to the adapted *Golovinomyces orontii* and the oomycete *Hyaloperonospora arabidopsidis* (Assaad *et al.,* 2004; Kwon *et al.,* 2008b). The closest homolog of PEN1, SYP122 is rapidly phosphorylated upon treatment with flg22, indicating a pathogen-induced activation of the secretory machinery (Nühse *et al.,* 2003). PEN1 and SNAP33 localize to the plasma membrane and accumulate underneath the penetration peg upon inoculation, while VAMP721/722 is found in endomembrane compartments that relocate towards the site of attack after fungal treatment. The plasma membrane-localized SNARE complex composed of PEN1 and SNAP33 might enable targeted fusion of VAMP721/722-containing vesicles (Collins *et al.,* 2003; Assaad *et al.,* 2004; Kwon *et al.,* 2008b). *Arabidopsis* mutants of both, PEN1/SYP122 (dwarfism) and VAMP721/722 (lethal), show growth phenotypes indicating that they act in a default secretion pathway necessary for plant development. It was speculated that this pre-existing secretory pathway was co-opted for immune responses (Assaad *et al.,* 2004; Kwon *et al.,* 2008b). As callose deposition and papilla formation are delayed in the mutants, molecules necessary for cell wall strengthening might be candidates for VAMP721/722-vesicle cargo (Kwon *et al.,* 2008b). In addition it was shown that a powdery mildew attack specifically induces the accumulation of fluorophore tagged PEN1 and SNAP33 in papillae and haustorial encasements. Since the fluorescence of proteins is normally very low in the apoplast, the release of exosomes from multivesicular bodies after fusion with the plasma membrane was suggested as

transport mechanism (Meyer *et al.,* 2008). Multivesicular bodies are thought to be the plants sorting platform for recycling e.g. to the plasma membrane or vacuolar degradation (An *et al.,* 2006; An *et al.,* 2006a; Hückelhoven, 2007b). Interestingly, the barley homolog of PEN1, ROR2 (required for mlo-specific resistance) is important for basal resistance of barley to *Bgh* (Freialdenhoven *et al.,* 1996) and, like PEN1, accumulates underneath fungal appressoria. In addition, it was shown that the barley homolog of SNAP25, named HvSNAP34, interacts with ROR2 and that this protein is also involved in basal resistance of barley to *Bgh* (Collins *et al.,* 2003) like the homologs in *Arabidopsis* (see above). Another example for SNARE proteins involved in resistance comes from tobacco. Mutant plants of SYP132, a plasma membrane-localized syntaxin, show enhanced susceptibility to *P. syringae* and failed to accumulate PR proteins at the cell wall. These observations led to the hypothesis that SYP132 is responsible for the secretion of PR proteins for race-specific bacterial defence (Klade *et al.,* 2007). To defend themselves, plants produce various secondary metabolites with toxic effects on the attacking pathogen. Some of these antimicrobial molecules have been shown to be specifically transported to the site of attempted penetration (Field *et al.,* 2006). Another example for the directed vesicle transport and accumulation of toxic compounds at the site of attempted pathogen attack comes from the barley-*Bgh* interaction. Here, H_2O_2-containing vesicles are found in close proximity of papillae, and effective papillae that prevent penetration, stain positive for H_2O_2 (Hückelhoven *et al.,* 1999).

1.3.3.4 ABC-transporters

Besides vesicle trafficking and membrane fusion, an additional transport pathway for secretion of antimicrobials was observed in plants. There are several ABC (ATP-binding cassette)-transporters linked to the export of toxic compounds for defence. For example, the NpPDR1 ABC transporter from *Nicotiana plumbaginifolia* is upregulated after treatment with fungal or bacterial pathogens and seems to mediate the transport of sclareol, an antimicrobial diterpene, through the plasma membrane (Stukkens *et al.,* 2005). Another prominent ABC-transporter associated with defence is the *Arabidopsis* PEN3 protein, which localizes to the plasma membrane and accumulates underneath the penetration peg. Mutants impaired in PEN3 function show enhanced susceptibility to non-adapted powdery mildew fungi and the necreotrophic fungus *Plectosphaerella cucumerina* (Stein *et al.,* 2006). PEN3 is thought to function together with PEN2, a glycosyl hydrolase (Stein *et al.,* 2006).

PEN2 localizes to peroxisomes and was shown to accumulate at pathogen entry sites. It restricts growth of a broad spectrum of adapted and non-adapted pathogens, which is thought to be due to its catalytic activity (Lipka *et al.,* 2005). Stein *et al.* (2006) generated the hypothesis that PEN2 converts a substrate from its non-toxic into its toxic form, which is then transported out of the cell via the PEN3-ABC-transporter. In the apoplast, it then unfolds its toxicity to the invader. Indeed PEN2 cleaves indol glucosinolates, which are synthesized, by CPY81F2 and MYB51 after MAMP-perception (flg22). Glucosinolates or their hydrolytic products are prominent candidates for antifungal compounds (Clay *et al.,* 2009; Bednarek *et al.,* 2009). In addition to this antimicrobial activity, cleavage of indol glucosinolates by PEN2 is required for callose synthesis and accumulation at the cell wall upon MAMP-perception. PEN3 is also involved in the callose response and may be responsible for the transport of indol glucosinolate cleavage products to the cell wall resident callose synthase POWDERY MILDEW RESISTANT 4 (PMR4; Clay *et al.,* 2009).

1.3.3.5 Secretory machinery as target for pathogen manipulation

Because several components of the trafficking machinery have functions in plant defence reactions these pathways are appropriate targets for pathogens to interfere with. There are several examples for pathogen-derived effectors that employ molecules of the plant secretory system for the pathogen's own benefit. As already mentioned, HopM1, an effector protein from *P. syringae*, is transferred into the host cell via the T3SS and found in plant endomembrane fractions. It promotes bacterial infection by the interaction with AtMIN7, an ARF-GEF protein (Nomura *et al.,* 2006). ARFs play an important role in vesicle trafficking because they are involved in vesicle coat formation (Bassham *et al.,* 2008). The interaction of HopM1 with AtMIN7 leads to the ubiquitination and following degradation of AtMIN7. Polarized vesicle trafficking is thereby inhibited as demonstrated by the reduction of callose deposition (Nomura *et al.,* 2006). Interestingly, treatment of wild type *Arabidopsis* plants with the fungal toxin brefeldin A enabeld *P. syringae* strains lacking HopM1 to infect again (Nomura et al., 2006). This toxin also inhibits an ARF-GEF (GNOM, Geldner *et al.,* 2003), which is involved in polarized secretion. Another *P. syringae* effector called AvrPto seems to interact with the small GTPase RabE of tomato and *Arabidopsis* as indicated by yeast two hybrid screens (Bogdanove and Martin, 2000; Speth *et al.,* 2009). The *Arabidopsis* GTPase was shown to localize to the Golgi and the plasma

membrane consistent with the well-characterized role of RabE form yeast and mammals in Golgi-plasma membrane transport (Speth *et al.,* 2009). The oomycete effectors Avr1b (*Phytophtora soyae*) and Avr3a (*Phytophtora infestans*) are recognized by intracellular receptors of the plant cell. They are secreted from haustoria into the extrahaustorial matrix. The RXLR-EER motif at the N-terminus of the effectors has been identified to be responsible for the translocation of the effectors into the plant cytoplasm. The mechanism is unclear but it is speculated that the translocation process involves plant cell-mediated endocytosis of the effectors. At least for Avr1b the translocation was observed in particle bombardment experiments without any contribution of the fungus (Whisson *et al.,* 2007; Dou *et al.,* 2008). Similar results were obtained in experiments with powdery mildew-derived Avr proteins (Avra10, Avrk1), which are predicted to be in the cytoplasm, where they interact with the corresponding R-genes (MLA10 (mildew resistance locus A) and MLK (mildew resistance locus K), respectively) of the plant but here no translocation signal has been identified yet (Ridout *et al.,* 2006).

1.4 Objectives

Ensuring adequate food supply for the world population is one of the greatest challenges in theses days. The protection of crops against diseases can make a valuable contribution to achieve this. An effective way to reduce yield losses due to diseases is engineering crops, which show durable resistances against pathogens. For this purpose, understanding of plant resistance mechanisms but also mechanisms that underlie compatible plant-pathogen interactions is very important. Several proteins important for transport processes have been shown to influence the susceptibility of plants to pathogens as outlined in the introduction. To gain a deeper insight into the role of such processes in the interaction of barley with its powdery mildew fungus *Bgh*, proteins with predicted functions in membrane trafficking and secretion were analyzed here for a possible involvement in this plant-pathogen interaction. 161 candidate genes were selected for a transient knock down screening to possibly identify genes, which cause significant differences in the penetration success of *Bgh*. The knock down screening resulted in three genes, which enhanced the susceptibility of barley to *Bgh* when they are knocked down. These candidates were subject to further investigations. During the course of this work, I focused especially on HvCOG3, a subunit of a Golgi resident tethering complex, which is

important for secretion in yeast and mammals (Ungar *et al.,* 2006). In further cell biological investigations, I examined possible effects of *HvCOG3* knock down in more detail. In addition, other subunit homologs of the complex as well as potential interaction partners of COG3 in yeast were isolated and investigated in functional characterization experiments concerning a possible involvement in the interaction between barley and *Bgh*. Putative HvCOG3 interaction partners exhibiting knock down or over-expression effects on the barley-*Bgh* interaction were analyzed for their subcellular localization with and without *Bgh* treatment to visualize possible *Bgh*-induced relocalizaiton events.

2 Methods and material

2.1 Plant material, growth conditions and pathogens

For transient transformation assays the barley (*Hordeum vulgare* L.) cultivar 'Golden Promise' was used. Kernels were directly sown into soil (Typ ED 73, Einheitserde- und Humuswerke, Gebr. Patzer GmbH & Co. KG, Sinntal-Jossa, Germany) and grown in a growth chamber (Conviron, Winnipeg, Canada) at 18°C, with a relative humidity of 65% and a photoperiod of 16 h light at 150 µmol $s^{-1}m^{-2}$ photon flux density. Gene expression analyses were performed with the barley cultivar 'Ingrid' and its backcross line 'Ingrid-*mlo5*' (without a functional MLO protein), which exhibits full penetration resistance to powdery mildew. Both 'Ingrid' cultivars were provided by L. Munk (Royal Veterinary and Agricultural University, Copenhagen, Denmark). Kernels were pre-germinated over night on wet filter paper to ensure equal development before they were transferred into soil. The plants were cultivated in a growth chamber (Sanyo, München, Germany) under the same conditions as described above. Barley leaves were infected with the powdery mildew fungus *Blumeria graminis* f.sp. *hordei* (*Bgh*) race A6, which was provided by J. Pons-Kühnemann (Justus-Liebig Universität, Giessen, Germany). The fungus was maintained on the barley cultivar 'Golden Promise' in a Sanyo (München, Germany) growth chamber at the above described conditions. The inoculation took place by blowing spores from infected plants into an inoculation hood. For functional analysis, detached leaf segments were fixed on water agar in Petri dishes and inoculated with a density of up to 200 conidia per mm^2. The plants used for gene expression analysis were horizontally laid down within their pot. The inoculation density for gene expression studies ranged between 80 and 100 conidia per mm^2. *Arabidopsis thaliana* T-DNA insertion lines were purchased at the Nottingham *Arabidopsis* Stock Centre (NASC, Longhborough, UK) for four different *AtRabD*-GTPases (Table 1). As the T-DNAs were inserted into Columbia-0 (Col-0; Lehle Seeds, Round Rock, USA), Col-0 plants were used as wild type control in the functional characterization experiments.

Table 1: *Arabidopsis* T-DNA insertion lines for *AtRabD*-GTPases

Name	Locus name	NASC Stock number	T-DNA insertion
RabD1	At3g11730	Salk033433	**intron**
RabD2a	At1g02130	Salk099495	**intron**
RabD2b	At5g47200	SAIL_151_C11	**intron**
RabD2c	At4g17530	Salk034873	**intron**

The cultivation of *Arabidopsis thaliana* plants was performed in a soil sand mixture at a ratio of 2:1 (Fruhstorfer Erde, Typ P, Vechta, Germany; Quarzsand, granulation: 0.1-0.5 mm Sakret® Trockenbaustoffe Europa GmbH & Co. KG, Wiesbaden, Germany). Seeds were suspended in water containing tween20 and transferred directly on the soil sand mixture with a pipette. After a two-day incubation period at 4℃ for stratification they were grown in a growth camber (Conviron, Winnipeg, Canada) at 22℃, 64% relative humidity and a photoperiod of 10 h light for vegetative growth. The *Arabidopsis* powdery mildew *Erysiphe cruciferarum* was provided by E. Stein (Justus-Liebig Universität, Giessen, Germany) and maintained on Col-0 and the susceptible mutant *pad4* (*phytoalexin deficient 4*) under the above described conditions. For inoculation, spores from *pad4* mutant plants were used due to enhanced conidia production. *Arabidopsis* plants were put under an inoculation box, whose top was covered with a close-meshed net (0.2 mm; Eckert GmbH, Waldkirchen, Germany). The spores were wiped off from infected leaves by a smooth brush and then assigned by gently scrubbing across the net. The inoculation density ranged between three to five conidia per mm^2.

2.2 Isolation of barley RNA and generation of cDNA

Seven to nine day old barley leaves were harvested and homogenized in liquid nitrogen for RNA extraction. RNA was isolated form about 300 mg of the plant material according to a RNA extraction method (Chomicznski *et al.,* 1986) optimized for plants. The plant material was vortexed thoroughly with 1 ml RNA extraction buffer before 200 ml chloroform were added. After vortexing again, a 10 min incubation period on a shaker followed prior to centrifugation at 13.500 rpm for 15 min at 4℃. The RNA-containing supernatant was transferred into a fresh tube containing 1 ml chloroform. After an additional vortexing step, the supernatant was

mixed with iso-propanol for precipitation and incubated over night at -20℃. Centrifugation at 4℃ and 13.500 rpm for 20 min res ulted in a whitish pellet, which was washed twice with 70% ethanol, dried on ice and resolved in H_2O_{DEPC}. The concentration of total RNA was determined by measuring the optical density at 260 nm using the NanoDrop® (Peqlab Biotechnologie, Erlangen, Germany) spectrophotometer and the RNA integrity was assessed via rRNA bands using denaturating gel electrophoresis (1.2% agarose and 5% formaldehyde (w/v)).

RNA extraction solution:

Compound	Final concentration	100 ml
Phenol	38%	38 ml
Guanidin thiocyanate	0.8 M	11.82 g
Ammonium thiocyanate	0.4 M	7.6 g
3 M Sodium acetate pH 5	0.1 M	3.34 ml 3 M NaAc
Glycerol	5%	5 ml
Autoclaved H_2O_{DEPC}		add 100 ml

The obtained barley mRNA was rewrote into first strand cDNA via two step reverse transcription (RT)-PCR. For two step RT-PCR oligo (dT) primers and the M-MuLV Reverse Transcriptatse (Fermentas GmbH, St. Leon-Rot, Germany) were used to transcribe 5 µg of the total RNA. In some cases, the One-step RT-PCR kit (Qiagen, Hilden, Germany) was conducted to isolate the desired sequences directly out of RNA according to the manufacturer's instructions.

2.3 Semi quantitative gene expression analysis

To examine the gene expression levels of *HvCOG* subunits and potential *HvCOG3* interaction partners a time course experiment was conducted with 'Ingrid WT' and 'Ingrid-*mlo5*' plants. Therefore, the first leaves were inoculated with *Bgh* spores or mock-inoculated (treated alike without delivering spores) and harvested at 0, 12, 24 and 48 h after inoculation. The respective RNAs and cDNAs were generated as described above and 0.5 µl of the resulting cDNA were used for subsequent gene expression analyses using SupraTherm™ DNA polymerase (Genecraft, Münster, Germany). Between 28 and 31 cycles were used. For primer sequences see Table 2.

Table 2: PCR information for genes analyzed in semi-quantitative RT-PCR

	Gene ID	forward primer (5'→3') / reverse primer (5'→3')	annealing temperatur	product size
HvUBC2	M60175	ACCCTCGCCGACTACAACAT CAGTAGTGGCGGTCGAAGTG	60℃	263 bp
HvPDI	L33252	GAGCCAAGGGGCTTTCCAGT TGCTCAGAGCTCATCCTTCA	57℃	604 bp
HvCOG2	AK370312	ATGACCTGGAGGATGAC CGACAGGGCTAATTGTG	57℃	401 bp
HvCOG3	AK249208	TCTAGAGCCCACGCGTAGGATAT CATCTGATGCGGATGC	54℃	1200 bp
HvCOG6	AK354922	TGATCGAAACGCACAC AAACTGCAACCTCAGTC	57℃	509 bp
HvCOG7	AK363189	CAACCATTCGACTCACC ATACTCGATGTCCGCC	57℃	493 bp
HvCOG8	AK248490	TCAGCCCTACGTCTC GTCCTGTGGCAAGTC	53℃	701 bp
HvGOS1-like	TA36193_4513	CTTCTAGAAGCTCCATGAGGGAGCA GACTGCAGTTTCCAACAACGCACCGA	60℃	380 bp
HvSEC22-like	TA49055_4513	AATCTAGATGCTAGTTTGTGTCTGGTC TACTGCAGGGATGTCGAGCTTCACC	57℃	706 bp
HvVTI1-like	TA38030_4513	TATCTAGAAGCGACCATGAGCGATGTC ATGCATGCGGCACATGCTGCATTTGGA	60℃	716 bp
HvYKT6-like	TA38338_4513	CTTCTAGATCTAGCCTTGCCGGA TGGCATGCCTGGAGCCTTCCAAGAG	60℃	697 bp
HvYPT1-like	TA34665_4513	AATCTAGAGATCCCGCCATGAATCC AACTGCAGGGAGCATCATCAAGTTTGC	60℃	647 bp

2.4 Generation of constructs for transient transformation of barley

2.4.1 Origin and isolation of sequences used for cloning procedures

The candidate genes for the RNAi screening, which are involved in membrane trafficking and secretion were selected via a key word based search in the EST-database (http://harvest.ucr.edu/) of the Leibniz-Institut für Pflanzengenetik und Kulturpflanzenforschung (IPK, Gatersleben, Germany; Zhang *et al.,* 2004) by Ralph Hückelhoven (TUM, Phytopathology, Freising, Germany). They were provided in one of the following vectors: pCRblunt, pBluescript SK+, pSORT or pLambdaZAP. Screening candidates that derived from the Y2H screen were obtained from C. Höfle (TUM, Phytopathology, Freising, Germany) in the pGADT7-Rec vector. Genes differentially regulated in the BI-1 / RacB array (performed by C. Weiss, Freising, Germany) were isolated out of a cDNA pool comprising inoculated and non-inoculated leaves of the barley cultivar 'Ingrid', harvested at different time points. The 'Ingrid' RNA or cDNA pool was also used for the isolation of the *HvCOGs* and

potential *HvCOG3* interaction partners. *HvCOG3* itself was isolated out of a cDNA pool comprising leaves harvested at different time points after infection from the cultivar 'Golden Promise'. For all sequence isolation PCRs, proof reading polymerases were used. Candidate genes obtained in vectors were amplified using vector specific primers and the proof reading polymerase Pfu (Promega, Madison, WI, USA). Failures were repeated with the other proof reading polymerases Herculase (Agilent Technologies, Santa Clara, CA, USA) and Phusion (New England Biolabs, Ipswich, MA, USA). Primers and PCR conditions for the isolation of sequences for subsequent cloning into transient expression vectors are described in Table 3, Table 4 and Table 5. All primers used in this work were purchased from Eurofins MWG Operon (Ebersberg, Germany).

Table 3: Isolation of vector-provided sequences for RNAi constructs generation

	forward primer (5'→3') / reverse primer (5'→3')	**annealing temperatur**	**Polymerase**	**Product size**
pbluescript	TAGGGCGAATTGGGTA CCGCTCTAGAACTAGTGGA	53℃	Pfu	TableS2
pCRblunt	CCGCCAGTGTGCTG CGAATTGGGCCCTCTA	53℃	Pfu	TableS2
pSORT	TACGTAAGCTTGGATCCTCT GGGAAAGCTGGTACGC	54℃	Pfu	TableS2
pLambdaZAP	CGGCCGCTCTAGAAGT AGGGAACAAAAGCTGGA	53℃	Pfu	TableS2
pGADT7-Rec	TATCAACGCAGAGTGGCC CCGTATCGATGCCCACC	56℃	Pfu	TableS3

Table 4: Isolation of cDNA sequences for RNAi construct generation

	Gene/EST ID	forward primer (5'→3') / reverse primer (5'→3')	isolation	annealing temperatur	product size
HvCOG1	AK370785	GATACTGTGGCACGAACCT TGTCCTTCATCCGTTGCAC	Two step (Phusion)	59°C	312 bp
HvCOG2	AK370312	ATGACCTGGAGGATGAC CGACAGGGCTAATTGTG	Two step (Phusion)	57°C	401 bp
HvCOG3	AK249208	TAGGGCGAATTGGGTA CCGCTCTAGAACTAGTGGA	pBluescript (Pfu)	53°C	~ 1000 bp
HvCOG4	AK356539	ACGCCATCATCGAGCTG TTGCGGACCGAGTTCAG	Two step (Phusion)	57°C	301 bp
HvCOG5	AK252011	TCCTCTCCGTTCCGT TCTTGAACTGATCGAGCC	Two step (Phusion)	53°C	421 bp
HvCOG6	AK354922	TGATCGAAACGCACAC AAACTGCAACCTCAGTC	Two step (Phusion)	57°C	509 bp
HvCOG7	AK363189	CAACCATTCGACTCACC ATACTCGATGTCCGCC	Two step (Phusion)	57°C	493 bp
HvCOG8	AK248490	TCAGCCCTACGTCTC GTCCTGTGGCAAGTC	Two step (Phusion)	53°C	701 bp
HvGOS1	TA36193_4513	CTTCTAGAAGCTCCATGAGGGAGCA GACTGCAGTTTCCAACAACGCACCGA	OneStep RT-PCR kit	60°C	380 bp
HvSEC22-like	TA49055_4513	AATCTAGATGCTAGTTTGTGTCTGGTC TACTGCAGGGATGTCGAGCTTCACC	OneStep RT-PCR kit	58°C	706 bp
HvVTI1-like	TA38030_4513	TATCTAGAAGCGACCATGAGCGATGTC ATGCATGCGGCACATGCTGCATTTGGA	OneStep RT-PCR kit	60°C	716 bp
HvYKT6-like	TA38338_4513	CTTCTAGATCTAGCCTTGCCGGA TGGCATGCCTGGAGCCTTCCAAGAG	OneStep RT-PCR kit	58°C	697 bp
HvYPT1-like	TA34665_4513	AATCTAGAGATCCCGCCATGAATCC AACTGCAGGGAGCATCATCAAGTTTGC	OneStep RT-PCR kit	60°C	647 bp
Putative dynamin family protein	P_35_26912	TATGGAAGATTTGGAGAGC ACCTTAGGCATGTTGTC	OneStep RT-PCR kit	55°C	630 bp
Putative EXO70 protein	P_35_29410	TGCTGACGGTGAAGG AAATGCTACTCCGATCCC	Two step (Phusion)	55°C	394 bp
Putative Ras-like protein	P_35_21781	CGCAACGAAACGATCC CGTTGCACATGAAGATCTC	OneStep RT-PCR kit	55°C	590 bp
Putative Rac3-like protein	P_35_19046	CTCTACTTCTCTGCCCTC GCGTAATGCTGAAGCTC	Two step (Phusion)	57°C	523 bp
Putative EXPANSIN11	P_35_1070	CTTGCTGAGGATACAAGGA AGTTGCGGGACATGG	OneStep RT-PCR kit	55°C	648 bp
Putative Exosome component	P_35_12925	CACAAACAGAGTGCGG TGTGGCAGCTCAAGG	Two step (Phusion)	57°C	619 bp

Table 5: Isolation of full-length cDNA sequences for over-expression constructs

	Gene/EST ID	forward primer (5'→3') / reverse primer (5'→3')	isolation	annealing temperatur	product size
HvCOG3	AK249208	TCTAGAGCCCACGCGTAGGATAT CTGCAGCTCAGACTCAGCATCATAAC	Two step (Phusion)	53°C	2377 bp
HvCOG3ohne Stop	AK249208	TCTAGAGCCCACGCGTAGGATAT CCATGGACAGAAGACTGTCGAGCTGAG	pGY-1-HvCOG3 (Phusion)	54°C	2333 bp
HvCOG3put.GAP	AK249208	GGATCCGGCGGCGATGCTTGCGGACGTTCTTGAGCGTCTG CTGCAGCTCAGACTCAGCATCATAAC	Two step (Phusion)	55°C	1060 bp
HvGOS1-like (not full length)	TA36193_4513	CTTCTAGAAGCTCCATGAGGGAGCA GACTGCAGTTTCCAACAACGCACCGA	OneStep RT-PCR kit	60°C	380 bp
HvSEC22-like	TA49055_4513	AATCTAGATGCTAGTTTGTGTCTGGTC TACTGCAGGGATGTCGAGCTTCACC	OneStep RT-PCR kit	58°C	706 bp
HvVTI1-like	TA38030_4513	TATCTAGAAGCGACCATGAGCGATGTC ATGCATGCGGCACATGCTGCATTTGGA	OneStep RT-PCR kit	60°C	716 bp
HvYKT6-like	TA38338_4513	CTTCTAGATCTAGCCTTGCCGGA TGGCATGCCTGGAGCCTTCCAAGAG	OneStep RT-PCR kit	58°C	697 bp
HvYPT1-like	TA34665_4513	AATCTAGAGATCCCGCCATGAATCC AACTGCAGGGAGCATCATCAAGTTTGC	OneStep RT-PCR kit	60°C	647 bp
HvARFA1D-like	TA29797_4513	TCTAGAGGTGGAGGAGAAGTTTGG CTGCAGGTCGACGCTAGTTGCTTCTGCCT	OneStep RT-PCR ki	55°C	591 bp
HvARFA1B/C-like	AK252168	TCTAGAAGATCAGGCGGAGCA CTGCAGTTCCTCGAAGCAGTCCT	Two step (Phusion)	58°C	636 bp
GFP+0	-	ATGGTGAGCAAGGGCGAG GGATCCTTGTACAGCTCGTCCAT	From pGY-1-GFP (Phusion)	58°C	722 bp
HvCOG3BKT	AK249208	CCCGGGGCCCACGCGTAGGATAT CTGCAGCTCAGACTCAGCATCATAAC	Two step (KD Phusion)	59-55°C	2377 bp
HvCOPIγ-like ADT	BAJ99125.1	CCCGGGACAGCAGGGGCCATG TCTAGAATCGAAATCCCTTGTGCT	Two step (KD Phusion)	58-54°C	2768 bp
HvYPT1-like ADT	TA34665_4513	AACCCGGGGATCCCGCCATGAATCC AACTCGAGGGAGCATCATCAAGTTTGC	Two step (Phusion)	60°C	664 bp

2.4.2 Generation of RNAi constructs

RNAi constructs were generated using the Gateway® cloning system (Invitrogen, Karlsruhe, Germany), which is based on the site-specific recombination ability known from the bacteriophage λ. The Gateway® cloning system delivers the gene of interest form an entry vector with specific attachment-sites (*att*-sites) to a destination vector with *att*-sites, catalyzed by the LR-Clonase™ enzyme mix (Invitrogen, Karlsruhe, Germany). The appropriate plant vector system, the entry vector pIPKTA38 and the destination vector pIPKTA30N, as well as a cloning protocol were provided by P. Schweizer (Leibnitz-Institut für Pflanzengenetik und Kulturpflanzenforschung (IPK), Gatersleben, Germany; Douchkov *et al.,* 2005). Bacteria containing the RNAi cloning vectors were propagated in LB medium with Kanamycin (50 µg/ml; pIPKTA38 in TOP10 cells) or Ampicillin (100 µg/ml; pIPKTA30N in ccdB resistant DB3.1 cells (Invitrogen, Karlsruhe, Germany)), respectively and the plasmid DNA was isolated using the Midi plasmid isolation kit NucleoBond® Xtra (Machery und Nagel, Düren, Germany). The insert sequences were isolated as described in section 2.4.1. For the screening 5 µl of the insert-PCR products were checked on a agarose gel and the remaining 20 µl from candidates showing defined gel bands were purified using the QIAquick® PCR purification kit (QIAGEN, Hilden, Germany). The inserts isolated with specific primers were checked by loading the whole PCR reaction on an agarose gel and purified via the QIAquick® gel extraction kit (QIAGEN, Hilden, Germany). For cloning of the insert sequences into pIPKTA38 4 µl of the purified PCR product and 1 µl pPKTA38 (150 ng/µl) were mixed with 1 µl of H_2O, T4 DNA Ligase buffer, 50% PEG and NaCl (0,5M) each, 0.5 µl of *Swa*I (10 u/µl) and 0.5 µl T4 DNA Ligase (5 u/µl). The reaction mix was incubated in a PCR cycler for one to two hours at 25℃ and another 15 min at 65℃ to inactivate the ligase activity. This cloning strategy leads to the insertion of the candidate PCR product between the *att* sites of the entry vector pIPKTA38. Subsequently 3.5 µl H_2O and 0.5 µl of *Swa*I buffer, 0.5 µl *Swa*I restriction enzyme and 0.5 µl NaCl (0.5 M) were added and the mixture was incubated for additional one to two hours at 25℃ to reduce false positive clones containing uncut or re-ligated empty pIPKTA38. Subsequently the mixture was transformed into either the XL1-blue (Agilent Technologies, Santa Clara, CA, USA) or TOP10 (Invitrogen, Karlsruhe, Germany) *E. coli* cells. The obtained colonies were first checked with pIPKTA38 vector specific primers (see Table 4), before two of the PCR positive colonies were propagated and isolated via quick and dirty plasmid

isolation using the buffers of the NucleoBond® Xtra Midi kit (Machery und Nagel, Düren, Germany) as follows: 1.5 ml of the *E. coli* culture were spined down and the resulting pellet was resolved in 180 µl of the S1 buffer. After addition of 180 µl S2 buffer, the mixture was incubated at room temperature for three to five minutes before 180 µl S3 were added. After centrifugation at 4℃ and 14 .000 rpm for 10 – 20 min the supernatant was mixed with 1 ml 100% ethanol and centrifuged again for 15 - 30 min. The pellet was cleaned with 70% ethanol and centrifuged for 5 min. The resulting pellet was dried and dissolved in 30 µl distilled H_2O. A first digestion check with *Eco*RI (cuts out the cloned PCR product) identified positive colonies, which were propagated again and isolated with the NucleoSpin® Plasmid Mini kit (Machery und Nagel, Düren, Germany) to obtain pure plasmid DNA for the further subcloning procedure. For pIPKTA38 vectors containing specific PCR products and pIPKTA38 vectors containing significant screening candidates, sequence confirmation was performed by Agowa (Berlin, Germany) or GATC (Konstanz, Germany) sequencing services. The sequences of all screening candidates without significant effects were not re-checked. For the recombination reaction about 300 ng of the insert-containing pIPKTA38 were mixed with 100 ng of the destination vector pIPKTA30N, 1.6 µl Clonase buffer, 2 µl LR-Clonase™ enzyme mix (Invitrogen, Karlsruhe, Germany) and filled up to 8 µl with 1x PE buffer and incubated over night at 25°C in a PCR cycler. The LR reaction mixture was transformed into either the XL1-blue or TOP10 *E. coli* strains. Cultivation of pIPKTA30N containing bacteria was shifted from 37℃ at the beginning of the screening to 30℃ to avoid cultiva tion-associated plasmid changes. The obtained colonies were checked for insertions via colony-PCR using primers located in the intron and either in the promoter/terminator region or in the insert (see Table 4 for primer sequences). Two positive tested colonies were propagated and the plasmids were isolated using NucleoSpin® Plasmid Mini kit (Machery und Nagel, Düren, Germany) and checked for the correct insertion of the PCR product by *Eco*RV digestion (fragment sizes: PCR product + 150 bp and PCR product + 300 bp).

Table 4: Vector specific primers used for cloning and sequence confirmation:

Vector	forward primer (5'→3') / reverse primer (5'→3')	annealing temperature
pGEM-T	GTTTTCCCAGTCACGAC AACAGCTATGACCATGA	53℃
pGY-1	TGACGCACAATCCCACTAT AGAGAGACTGGTGATTTCAGC	54℃
pIPKTA38	AGCAGGCTTTAAAGGAACC TGTACAAGAAAGCTGGGTCT	53℃
pIPKTA30N 1st insert	GATGACGCACAATCCCACTATCCT TCAAATTAAACAAATGCAGTATGAAGA	53℃
pIPKTA30N 2nd insert	ATGAGCGAAACCCTATAAGAACCCTA GGATAGCCCTCATAGATAGAGTACTAACTAA	53℃
pGADT-7	CGTTCCCTTTCTTCCTTG TGGCGAAGAAGTCCAAA	53℃

2.4.3 Generation of over-expression constructs

The standard cloning procedure for the generation of over-expression constructs was conducted as follows: The basic sequences used for over-expression construct generation were obtained as described in Table 5. The blund-ended PCR products obtained by proof reading DNA polymerases were A-tailed using the SupraTherm™ DNA polymerase (by adding 1 µl SupraTherm and 1 µl dATP (2mM) to the PCR products and incubation of the mixture for 10 – 15 min at 72℃). Subsequently, the PCR products were ligated into the pGEM®-T vector (Promega, Madison, WI, USA) according to the manufacturer's constructions. The pGEM®-T vector is suitable for cloning PCR products with adenine overhang, because the vector possesses a thymine overhang and it is capable for blue/white selection. After ligation, the constructs were transformed into 100 µl or 50 µl of the *E. coli* strains XL1-blue or TOP10, respectively. The obtained colonies were usually checked by vector specific colony-PCR before propagation in the appropriate medium, plasmid isolation (NucleoSpin® Mini kit; Machery und Nagel, Düren, Germany) and control digestion. See Table 4 for vector specific primers used. The sequences of plasmids with positive digestion results were confirmed by the sequencing services of Agowa or GATC prior to further subcloning steps. For subcloning, donor and target vector were digested with appropriate restriction enzymes. The bands were separated on an agarose gel and purified using QIAquick® gel extraction kit (QIAGEN, Hilden, Germany). Subsequently, the fragment to be inserted and the open target vector were mixed in the ratio 3:1 together with ligase buffer and 1 µl T4 DNA Ligase (Fermentas GmbH, St. Leon-Rot, Germany) in a reaction volume of 20 µl, incubated over-night at 8℃ and transformed into XL1-blue or TOP10 cells. For detailed

information on subcloning, see Table 5. All enzymes used for the cloning procedures were obtained form Fermentas GmbH (St. Leon-Rot, Germany) if not described differently.

Table 5: Enzymes used for subclonig into plant expression vectors

Construct	Donor vector	Enzymes for subcloning	Plant expression vector
All RNAi constructs	pIPKTA38-X	LR-Clonase™	pIPKTA30N
HvCOG3 OEx	pGEM-T-*HvCOG3*	*Xba*I / *Pst*I	pGY-1-*HvCOG3*
HvCOG3ohneStop OEx	pGEM-T-*HvCOG3ohneStop*	*Xba*I / *Nco*I	pGY-1-*HvCOG3ohne Stop*
HvCOG3ohneStop-GFP OEx	pGY-1-GFP	Phusion, blunt	pGY-1-*HvCOG3ohneStop-GFP*
GFP-HvCOG3 OEx	pGEM-T-*HvCOG3*	*Xba*I / *Pst*I	pGY-1-*GFP-HvCOG3*
HvCOG3put.GAP	pGEM-T-*HvCOG3put.GAP*	*Nco*I / *Pst*I blunt / *Sma*I	pGY-1-*HvCOG3put.GAP*
HvGOS1-like (c-term) OEx	pGEM-T-*HvGOS1-like*	*Xba*I / *Pst*I	pGY-1-*HvGOS1-like*
HvSEC22-like OEx	pGEM-T-*HvSEC22-like*	*Xba*I / *Pst*I	pGY-1-*HvSEC22-like*
HvVTI1-like OEx	pGEM-T-*HvVTI1-like*	*Xba*I / *Pae*I	pGY-1-*HvVTI1-like*
GFP-HvVTI1-like OEx	pGY-1-*HvVTI1-like*	*BamHI*	pGY-1-*GFP+0-HvVTI1-like*
HvYKT6-like OEx	pGEM-T-*HvYKT6-like*	*Xba*I / *Pae*I	pGY-1-*HvYKT6-like*
HvYPT1-like OEx	pGEM-T-*HvYPT1-like*	*Xba*I / *Pst*I	pGY-1-*HvYPT1-like*
GFP-HvYPT1-like OEx	pGEM-T-*HvYPT1-like*	*BamHI*	pGY-1-*GFP+1-HvYPT1-like*
HvARFA1D-like OEx	pGEM-T-*HvARFA1D-like*	*Xba*I / *Pst*I	pGY-1-*HvARFA1D-like*
HvARFA1B/C-like OEx	pGEM-T-*HvARFA1B/C-like*	*Xba*I / *Pst*I	pGY-1-*HvARFA1B/C-like*
HvCOG3 dsRNA	pGEM-T-*HvCOG3-like*	*SalI*	pGEM-T-*HvCOG3dsRNA*
HvMLO dsRNA	pGEM-T-*HvMLO*	*AatII*	pGEM-T-*HvMLOdsRNA*

2.4.4 Constructs for targeted yeast two hybrid

The potential interaction partners of HvCOG3 were selected due to sequence homology to the published interaction partners of COG3 in yeast. To investigate a possible interaction of the barley proteins, a targeted yeast two hybrid assay was performed (see section 2.7). For this purpose, cDNAs from *HvCOG3, HvCOPIγ-like* and *HvYPT1-like* (see section 2.4.1) were cloned into pGEM-T. After sequence confirmation, the cDNAs were subcloned into pGBKT7 containing the DNA-binding domain (BD) or pGADT-7-Rec containing the activation domain (AD; Yeast Protocol

Handbook, Matchmaker Two-Hybrid Library Construction and Screening Kit, Clontech-Takara Bio Europe, Saint-Germain-en-Laye, France). *HvCOG3* was subloned into the yeast vector pGBKT7 in frame with the DNA-BD using the *Xma*I and *Pst*I restriction sites. The putative interaction partners *HvCOPIγ-like* and *HvYPT1-like* were cloned into the yeast vector pGADT-7-Rec in frame with its activation domain using *Xma*I / *Xba*I and *Xho*I / *Sma*I restriction sites, respectively.

2.4.5 Generation of a *dnHvYPT1-like* construct

The yeast *YPT1* gene is represented by a gene family with four members in *Arabidopsis*, which are thought to be redundant (Pinheiro *et al.,* 2009). This might be the case also in barley and therefore, we wanted to analyze the specificity of the RNAi result through the generation of dominant-negative (dn) version of the *HvYPT1-like* gene used for over-expression and RNAi experiments in this work. We used the Transformer^{TM} Site-Directed Mutagenesis protocoll (Clontech, Heidelberg, Germany) for the exchange of the 121st amino acid asparagin with isoleucine, which is described by Pinheiro *et al.* (2009) to produce a dominant-negative HvYPT1-like protein in *Arabidopsis*. The mutagenesis procedure is based on the use of mutagenic primers, one specific for the exchange of the respective nucleotide (CTTCTCGTGGGGATCAAATGTGATCT), and one selection primer (AAATGCTTCAATGATATCGAAAAAGGAAG), which changes the restriction site *Ssp*I of the pGY-1 vector into an *Eco*RV site. All enzymes used were purchased from Fermentas (St. Leon-Rot, Germany). In a first step, a 20 µl mixture containing 6 µl of T4 Polymerase buffer, 0.5 µg pGY-1-*HvYPT1-like*, 0.15 µg of the phosphorylated selection primer and 0.15 µg of the phosphorylated mutagenesis primer were incubate for 5 min in a water bath at 100°C. Afterwards, the mixture was transferred immediately on ice before 1 µl T4 DNA polymerase, 2 µl T4 DNA Ligase, 1.5 µl dNTPs (10mM) and 2 µl ATP (10mM) were added and filled up to 30 µl. The reaction mixture was incubated for 2 h at 37°C for DNA elongation and ligation before an incubation step at 70°C terminated the reaction. In a first selection step, the restriction enzyme *Ssp*I was used to eliminate unmutated plasmids by incubation for 2 h at 37°C and stopped at 70°C for 5 min. Mutated plasmids do not contain the *Ssp*I recognition sequence anymore and stay intact. The digested plasmid mixture was transformed into BMH71-80 *mutS E. coli* cells and propagated. For the subsequent plasmid isolation, the quick and dirty method (described in generation of RNAi

constructs) was used. The digestion with *Ssp*I was repeated with 1 µl of the isolated plasmid DNA at 37°C and after 2 h digestion, another µl *Ssp*I was added and the mixture was incubated for one more hour. This resulted in the linearization of unmutated plasmids, which are less efficiently transformed into *E. coli*, and thus the probability of the selection of positive clones is enhanced. The *Ssp*I treated plasmid mixture was transfered into TOP10 cells.

2.5 Generation of double stranded RNA (dsRNA)

Due to difficulties in the reproducibility of the *HvCOG3* RNAi result obtained during the screening, double stranded RNA was generated and introduced into barley epidermal cells as described in section 2.8 to verify the screening result. The pGEM-T vectors used as templates were generated as described in Table 5. To linearize the plasmids, 10 µg each were cut in two reactions behind the insert (with regard to the respective RNA-polymerase promoters T7 or Sp6) as follows: pGEM-T-*HvMLOdsRNA* was cut using *Pst*I (T7) and *Aat*II (Sp6), pGEM-T-*HvCOG3dsRNA* using *Sal*I (T7) and *Xba*I (Sp6) and pGEM-T-*RFP* using *Sal*I (T7) and *Aat*II (Sp6). The mixture was incubated for two hours at 37°C before it was transferred into a new reaction tube containing 170 µl $H_2O_{DEPC.}$ To remove the restriction enzymes 200 µl phenol/chloroform/isoamylacohol (pH 8) were added before the mixture was centrifuged for 5 min at 20.800 rcf and 4°C. Afterwards, 200 µl of the supernatant were mixed with 420 µl ethanol (100%) and precipitated for 20 min on ice before an additional 30 min centrifugation step followed. Then, the supernatant was removed and after drying, the pellet was dissolved in 10 µl $H_2O_{DEPC.}$ To generate the RNA-single strands (sense and antisense), the RNA polymerases T7 and Sp6 from Fermentas (St. Leon-Rot, Germany) were used. Two µg of the linearized plasmid were mixed with 2 µl of the respective RNA polymerase, 8 µl buffer, 1 µl RNase-inhibitor, 5 µl NTPs (10mM) and filled up to 50 µl with $H_2O_{DEPC.}$ The mixture was incubated for two hours at 37°C before the two reactions were combined, denatured for 5 min at 95°C and cooled down within the thermo block at -20°C. The mixtures were checked on an agarose gel before and after the synthesis of the double stranded RNA. To determine the dsRNA concentration, 6 µl $H_2O_{DEPC,}$ 1 µl sodium acetate (3M) and 25 µl ethanol were added to 4 µl of the reaction mixture. After centrifugation at 4°C and 20.800 rcf for 10 min, the supernatant was removed before

the pellet was washed with 70% ethanol and resolved in 400 µl H_2O_{DEPC} by heat treatment. Finally, the concentration was determined at the wavelength of 260 nm.

2.6 Constructs for stable transformation of barley

Two constructs for the generation of stable transgenic barley plants lacking *HvCOG3* were generated. The *HvCOG3* sequence, which was already used for the transient RNAi construct generation, was introduced into the stable RNAi vectors pIPKb007 and pIPKb010 (Himmelbach *et al.,* 2007). In pIPKb007, the *HvCOG3* RNAi cassette is expressed under the control of the ZmUbi promoter and thus it is silenced in the whole plant, while in pIPKb010 the construct is controlled by the epidermis specific promoter TaGst1A1 (of the wheat glutathione S-transferase), which results in silencing in epidermal cells only. As this vector set for stable construct expression in barley is gateway compatible, I generated the constructs using the LR-Clonase™ enzyme mix (Invitrogen, Karlsruhe, Germany) as described in section 2.4.2 for transient RNAi constructs. As entry vector, the *HvCOG3*-containing pIPKTA38 from the screening was used. The constructs were checked for proper intron orientation by several restriction enzymes and sequencing. The transgenic plants were generated at the IPK (Gatersleben, Germany) by Götz Hänsel in the barley cultivar 'Golden Promise' background.

2.7 Yeast transformation

A targeted yeast two hybrid experiment was conducted to investigate possible interactions between the barley *HvCOG3* and *HvCOPIγ-like* or *HvYPT1-like* according to the lithium acetate (LiAc) method for small-scale yeast transformation (Yeast Protocol Handbook, Clontech-Takara Bio Europe, Saint-Germain-en-Laye, France). Chemically competent cells of the *Saccharomyces cerevisiae* strain AH109 were transformed according to the Yeast Protocol Handbook with pGBKT-7-*HvCOG3* and pGADT-7-*HvCOPIγ-like* or pGADT-7-*HvYPT1-like*, respectively. The AH109 strain was pre-cultured in YPDA medium at 30℃ to a n optical density (OD) of OD_{600} > 1.5 and then used to inoculate the main-culture, which was cultivated until the OD_{600} reached 0.4 to 0.6. After centrifugation the yeast cells were rinsed with sterile water and re-suspended in 1x TE (0.1 M Tris-HCl, 10 mM EDTA in H_2O_{dest}, pH 7.5) / 1x LiAc (1 M lithium acetate in H_2O_{dest}, pH 7.5) solution (ratio 1:1). 0.2 µg of each plasmid and 0.1 mg of ultra sonicated (20 min) salmon testes carrier DNA (Sigma-

Aldrich Chemie GmbH, München, Germany) were mixed and incubated on ice for 30 min. The mixture was added to 100 µl of competent yeast cells. Then 600 µl PEG/LiAC, (40% polyethylene glycol in 1x TE / 1x LiAc solution) were added and after an incubation period of 30 min at 30℃, 70 µl of 100% DMSO (dimethyl sulfoxide) were added, followed by an incubation step at 42℃ in a water bath. Before the suspension was centrifuged and re-suspended in sterile 1x TE buffer it was chilled on ice for 5 min. The transformed cells were cultivated on a selective synthetic dropout medium, which lacks the amino acids tryptophan (tryp) and leucine (leu) as a transformation control. To test for interactions, cells were plated on the interaction selective medium QDO (quarto drop out), which lacks the amino acids tryptophan, leucine, histidin (his) and adenine (ade). After several days, colony development was examined.

YPDA medium		
Peptone	2 %	20 g
Yeast extract	1 %	10 g
Adenine	0.03 %	30 mg
Glucose	2 %	20 g
Agar-agar (for plates only)	1.5 %	15 g
adjust pH to 6.5 and autoclave		ad H_2O_{dest} 1l

Dropout media				
	Double dropout (-tryp, -leu)		**Quadruple dropout (-tryp, -leu, -ade, -his)**	
Yeast nitrogen base without amino acids	0.17 %	1.7 g	0.17 %	1.7 g
Ammonium sulphate	0.5 %	5 g	0.5 %	5 g
Appropriate 10x amino acid mix	0.059 %	590 mg	0.055 %	550 mg
Glucose	2 %	20 g	2 %	20 g
Agar-agar (for plates only)	1.5 %	15 g	1.5 %	15 g
adjust pH to 5.8 and autoclave	ad H_2O_{dest} 1l		ad H_2O_{dest} 1l	

50% polyethylene glycol (PEG)	
PEG mol. Wt. 3300	50 g
autoclave	ad H_2O_{dest} 100 ml

10x dropout stock (mg/l)	
L-adenine hemisulfate salt	200 mg
L-arginine HCl	200 mg
L-histidine HCl monohydrate	200 mg
L-isoleucine	300 mg
L-leucine	1000 mg
L-lysine HCl	300 mg
L-methionine	200 mg
L-phenylalanine	500 mg
L-threonine	2000 mg
L-tryptophan	200 mg
L-tyrosine	300 mg
L-uracil	200 mg
L-valine	1500 mg

2.8 Transient transformation of barley epidermal cells

The first leaves of seven day old barley plants were transiently transformed via gold particle delivery into barley epidermal cells. For the gold particle stock solution, 27.5 mg of 1.0 Micron gold (Biorad, München, Germany) were suspended in 1 ml H_2O_{bidest} and incubated in the ultra sonic bath for 30 sec before a centrifugation step for 30 sec at 14.000 rpm. The supernatant was discarded and the gold particles were cleaned with another ml of water and two times with 100% ethanol before the gold pellet was dried in a thermo block at 50℃ and resu spended in 1 ml of 50% glycerol. The gold stock solution was stored at -20℃. The ba llistic transformation of barley epidermal cells was done using the Particle Inflow Gun system PDS-1000/HeBiolistic Particle Delivery, offered by Biorad (München, Germany). The shooting procedure was adapted from P. Schweizer (IPK, Gatersleben, Germany) with some modifications and applied as follows: The first leaves of barley plants were cut and

laid with the abaxial side up on Petri dishes containing 0.5% (w/v) water agar with 0.01 mg/ml benzimidazol (stock solution: 40 mg/ml in 96% ethanol), which is a senescence inhibitor, to keep the leaves alive for at least five days. The gold particles were coated with the desired plasmids as follows: The gold stock solution was incubated for at least 15 min in an ultra sonic bath, to destroy possible particle clusters. For functional analysis, the hepta-adapter system was used. Therefore, 7 µg of the plasmid containing the gene of interest and 7 µg of the plasmid carrying the reporter gene were mixed in a 1.5 ml tube before adding 60 µl of the gold stock solution. To adhere the plasmids to the gold particles, the mixture was vortexed vigorously, while slowly adding the calcium nitrate (1M, pH10) in a drop wise manner. The volume of calcium nitrate was calculated for each shot as the volume of total plasmid DNA plus the volume of the gold particle solution. For localization studies, the single shot system was applied. Here, 1 µg of the plasmid containing the gene of interest, 1 µg of the plasmid carrying the reporter gene and 10 µl of the gold stock solution were used. As a control, the empty vector was included in each experiment and for RNAi experiments pIPKTA36 (MLO-RNAi; Douchkov *et al.,* 2006) was used in addition as a positive control. The gold-plasmid mixture was incubated for 30 min at room temperature and inverted from time to time. Afterwards the coated particles were spun down and the supernatant was discarded. The gold pellet was washed with 1 ml 70% ethanol and centrifuged at 14.000 rpm for 30 sec. This step was repeated with 1 ml 100% ethanol before the supernatant was carefully removed. The pellet was dissolved in 30 µl 100% ethanol for shooting with the hepta-adapter and in 8 µl for single shots in a ultra sonic bath. The dissolved gold-plasmid solution was evenly distributed on the macro-carriers (Biorad, München, Germany) and these as well as the Petri dish containing the leaves, were placed into the Particle Inflow Gun. For ballistic transformation of the barley leaves, 26 Hg (quicksilver) vacuum were applied and the gas pressure was regulated by rupture discs of 900 psi (pounds per square inch; Biorad München, Germany).

2.9 Microscopic evaluation of transformed barley epidermal cells

2.9.1 Evaluation of RNAi and over-expression experiments

For functional characterization, the gene of interest, cloned into either the RNAi vector pIPKTA30N or the over-expression vector pGY-1, was introduced into barley epidermal cells (cv. 'Golden Promise') via particle bombardment using the hepta-adapter (see section 2.8). Barley leaves were inoculated 48 h after bombardment with *Bgh* as described in section 2.1. The evaluation took place 48 h after inoculation by fluorescence microscopy using a Leica DM 1000 microscope (Leica Microsystems, Wetzlar, Germay). In RNAi experiments, the transformed cells were analyzed by calculating the susceptibility index (SI) as the ratio between all transformed cells and cells containing a fungal haustorium. In over-expression experiments, the penetration efficiency (PE) was calculated as the ratio between all cells that have been attacked by the fungus and the cells where the fungus has successfully established a haustorium. Statistical evaluation was done using a two-sided unpaired Students t-test.

2.9.2 Evaluation of subcellular localization

The subcellular localization of GFP fusion proteins was examined *in planta* using the confocal laser-scanning microscope Leica TSC SP5 (Leica Microsystems, Wetzlar, Germany). Epidermal cells of the barley cultivar 'Golden Promise' were transiently transformed via the particle delivery system described above using single shots. To determine the subcellular localization, the GFP-fusion proteins were co-transformed together with genes encoding the marker proteins mCherry, CFP, GmMAN:1 or sGFPHDEL and analyzed two days after bombardment. Probes for the assessment of possible fungal-induced localization changes were inoculated 4 h after bombardment and analyzed two days later. For information on spectral excitation and detection, settings see Table 6. Generally, experiments were scanned bidirectional and with a line average of 2-3. If appropriate, cells were scanned sequentially.

Table 6: Wavelengths used for excitation and detection of fluorescent proteins

Fluorescent protein	Excitation	Detection
pGY-1-GFP (Schultheiss *et al.,* 1999) pGY-1-*sGFPHDEL* (Eichmann, 2005)	488 nm	495 – 530 nm
pGY-1-*mCherry* (D. Liu & G. Langen, Justus Liebig Univ. Giessen) / *GmMAN*:*1* (Yang *et al.*, 2005)	561 nm	570 – 625 nm
pGY-1-*CFP* (R. Eichmann, TUM, Phytopathology, Freising)	458 nm	465 – 500 nm

2.10 Microscopic evaluation of *Arabidopsis* T-DNA insertion lines

To determine differences in the proliferation of the *Arabidopsis* powdery mildew *E. cruciferarum* on different T-DNA insertion lines (Table 1), fungal structures were stained with wheat germ agglutinin-tetramethylrhodamin (WGA-TMR; Invitrogen, Karlsruhe, Germany) or with acetic ink (10% blue ink and 25% acetic acid in water). For the WGA-TMR staining solution 0.01 µg/µl WGA-TMR, 0.01 µg/µl bovine serum albumin were solved in 1x PBS buffer (8% NaCl, 0.2% KCl, 0.765% Na_2HPO_4 x H_2O, 0.2% KH_2PO_4 in H_2O_{bidest}). WGA-TMR binds to extra- and intracellular chitin structures of fungi, while the acetic ink stains only extra cellular structures. The *Arabidopsis* leaves were harvested five days after inoculation and discoloured (ethanol : chloroform : trichloracetate; 8 : 2 : 1.5%) before staining. For ink staining, the leaves were incubated for two minutes in the acetic ink solution. For WGA-TMR staining, the leaves were rinsed with water and incubated in 1x PBS buffer for a few minutes. Then the leaves were transferred into the staining solution and vacuum infiltration was applied two times. After incubation in the dark over night, the probes were examined. By using fluorescence or bright-field microscopy, the amount of conidia-chains developed per colony was examined.

3 Results

3.1 Screening for candidates using transient gene silencing

As pointed out in the introduction membrane trafficking and secretion may play a key role in the interaction of plants with pathogens. This work aimed in the identification and analysis of genes that are involved in these processes and influence the barley defence reaction after *Bgh* infection. Therefore, R. Hückelhoven (TUM, Phytopathology, Freising, Germany) selected candidate genes with a transport/secretion-associated annotation via a keyword-based research in the HarvEST-database (http://harvest.ucr.edu/) and ordered correspoding ESTs from the Leibniz-Institut für Pflanzengenetik und Kulturpflanzenforschung (IPK, Gatersleben, Germany). If possible, ESTs were selected that derive from barley epidermis inoculatied with *Bgh* (HO library; Zhang *et al.,* 2004). In addition to these membrane trafficking candidates, interesting genes from a previous yeast two-hybrid screen with a constitutively activated mutant of the barley *Rac1*-GTPase performed by C. Höfle (TUM, Phytopathology, Freising, Germany) were included. Furthermore some genes differentially expressed in an array experiment with stable transgenic plants over-expressing the known susceptibility factors *HvRacB* and *HvBI-1* (*Bax Inhibitor1*), performed by C. Weis (TUM, Phytopathology, Freising, Germany) were also analyzed. Over-expression of the constitutively activated form of the small GTPase *HvRac1* was found to be involved in susceptibility of barley to *Bgh* (Pathuri *et al.* 2008), as it was shown for *HvRacB* (Schultheiss *et al.,* 2002; Schultheiss *et al.,* 2003) and for *HvBI-1* (Eichmann *et al.,* 2010). Therefore, potential interaction partners of *HvRac1*, and differentially regulated genes in *HvRacB* and *HvBI-1* over-expressers were of special interest. In summary, the project started with a candidate gene set comprising 135 membrane trafficking/secretion-related genes, 20 from the previous *HvRac1*-Y2H screen and six genes differentially expressed in the micro-array. Most membrane trafficking/secretion-related EST-sequences were annotated as “putatively expressed protein” or “predicted protein” when the corresponding nucleotide sequence translated into the protein sequence was blasted against the NCBI protein database. Therefore, the best-hit protein sequence was analyzed for conserved domains by NCBI protein blast. Based on the predicted domains, I classified them

into 16 groups, shown in Figure 4. Each group and the Y2H/array-candidates are represented with their percentage of the initial set of the 161 candidate genes.

For the identification of candidates involved in the interaction of barley with *Bgh* the TIGS (transient induced gene silencing) system described in Douchkov *et al.* (2005) was established. I adopted the procedure in general with some modifications. The main differences between the original protocol and the execution in this work are that I used *GFP* as a reporter gene instead of *GUS* and that I evaluated the experiments by manual microscopy instead of using an automated robot evaluation system. In addition, the amount of gold used per shot was reduced, to reduce leaf damage. In sum, 146 (91%) from the initial 161 candidates were apmlified. Out of them, 137 (94%) were cloned into the entry vector pIPKTA38 and thereof 107 (78%; 87 membrane trafficking candidates, 16 Y2H candidates and 4 array candidates) were successfully subcloned into the plant RNAi-vector pIPKTA30N under the control of the cauliflower mosaic virus (CaMV) 35s promoter (vectors: Douchkov *et al.,* 2005).

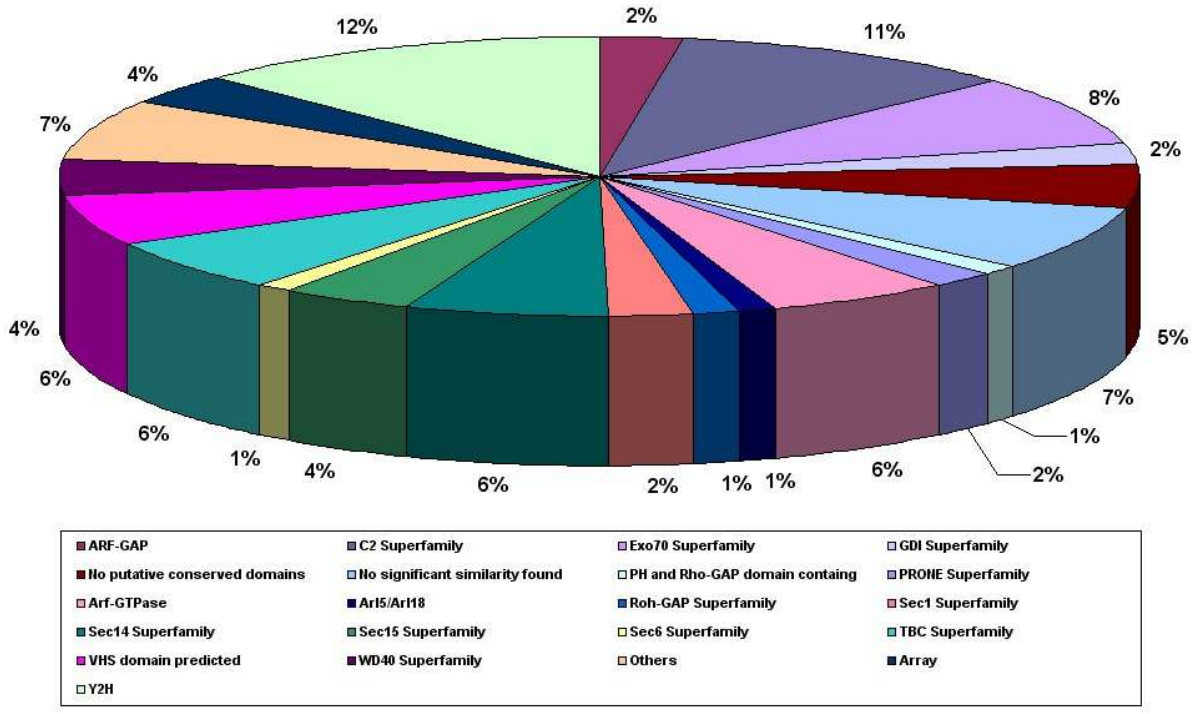

Figure 4: Classification and protein domains predicted for the initial set of genes

EST-sequences of the candidate genes were blasted against the NCBI nucleotide database, the best hit was translated into the corresponding protein sequence and this protein sequence was blasted against the NCBI protein database. The obtained putative conserved domains were used to create the diagram.

Results

Detached leaves of the barley cultivar ‘Golden Promise’ were transiently transformed via particle gun-mediated transformation. The leaves were inoculated with the powdery mildew fungus *Bgh* two days after bombardment and analyzed microscopically two days after inoculation for differences in the outcome of the barley-*Bgh* interaction. The susceptibility index of epidermal cells was calculated as the ratio between the amount of all transformed cells and the amount of transformed cells containing haustoria. Each TIGS experiment included the empty-vector as well as a *MLO*-RNAi construct (pIPKTA36, Douchkov *et al.,* 2005) as controls. MLO is a susceptibility factor conserved in barley and *Arabidopsis*. Mutations in the *MLO* gene in barley confer complete and race-unspecific penetration resistance to barley powdery mildew isolates (Eichmann and Hückelhoven, 2008), making it a good positive control.

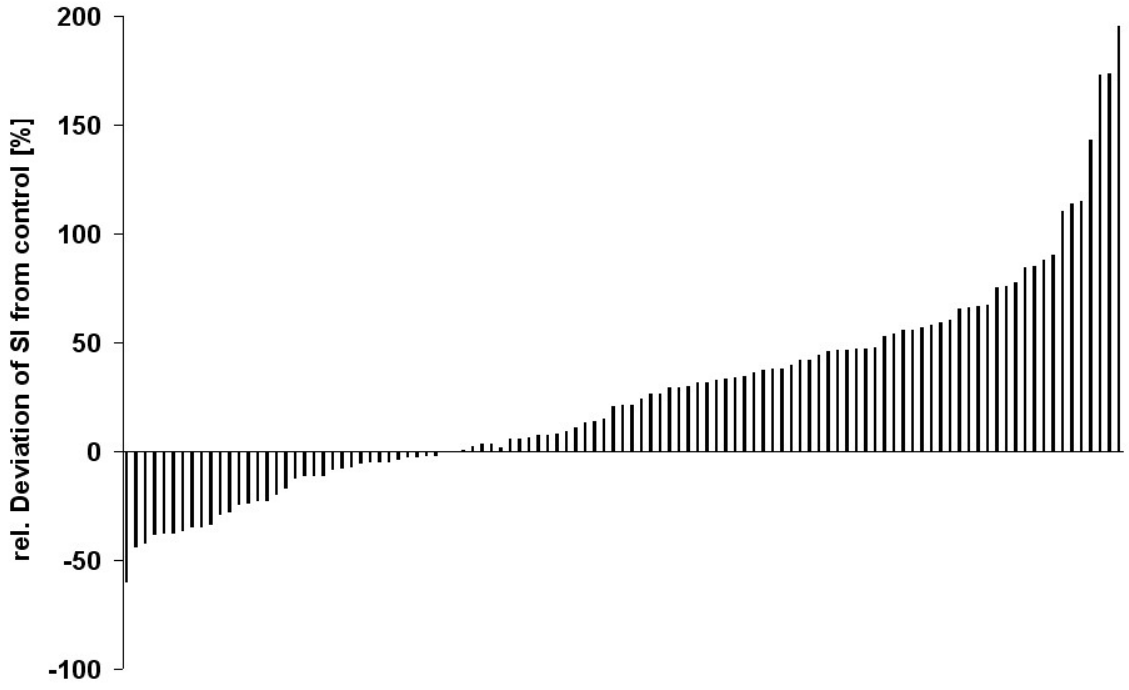

Figure 5: Summary of the TIGS screening

Candidate genes were transiently knocked down via ballistic transformation in barley epidermal cells of the cv. ‘Golden Promise’ and analyzed microscopically for an influence on the barley-*Bgh* interaction (see TableS2, S3, S4 for candidate IDs and screening result). The detached leaf segments were co-bombarded with a pGY-1-*GFP* construct, used as transformation marker, and the respective pIPKTA30N-candidate RNAi-construct. Leaf segments were inoculated with the powdery mildew fungus *Bgh* two days after bombardment (dab) and examined microscopically two days after inoculation (dai). Columns represent the mean values of all conducted independent experiments of each candidate.

After the first TIGS experiments, I repeated all candidates, which induced susceptibility by more than 100% (21 candidates) or reduced susceptibility by more than 50% (9 candidates) in comparison to the empty vector control at least three times. In addition, candidates with interesting annotations (28 canditates) were repeated irrespective of those thresholds. This let to 305 TIGS experiments for the 107 candidates. In Figure 5 all screened candidates are shown, ordered by the relative deviation of the susceptibility index from the control. Each column represents the mean value of all conducted TIGS experiments of the respective candidate. Interestingly, the majority (67%) of the candidates showed a tendency towards more susceptibility although not significantly. Knock down of 33% of the tested candidates reduced the susceptibility of barley epidermal cells. Although the TIGS screening system has been described as a powerful screening method (Douchkov *et al.,* 2005; Ihlow *et al.,* 2008) the variation of the susceptibility indices between different TIGS experiments on one candidate was high during the screening. This made it difficult to obtain consistent effects but at the end of the screening three candidates turned out to alter the susceptibility of barley to its powdery mildew fungus significantly. They were subject to further investigations as described in the following sections.

3.2 Candidates significantly influencing the interaction of barley with *Bgh*

3.2.1 A predicted protein putatively containing an EXO70 domain

Transient silencing of a gene annotated as a predicted protein (EST-accession no.: HD14N02r; internal screen no.: 19) resulted in 84% enhanced susceptibility of barley epidermal cells to *Bgh* (Figure 6A). This was statistically significant at $p < 0.01$ according to Student's *t* test applied on seven independent TIGS experiments. The susceptibility index of the individual experiments varied from 23 to 151% increased susceptibility relative to the control. The first *in silico* analysis of the EST-sequence HD14N02r (in the middle of 2010; nucleotide blast against the NCBI and TIGR nucleotide databases) did not reveal a full length sequence as the comparison with the most closely related *Arabidopsis* and rice sequences indicated. NCBI analysis of the corresponding truncated protein sequence of HD14N02r revealed a conserved EXO70 domain at the c-terminal part of the protein.

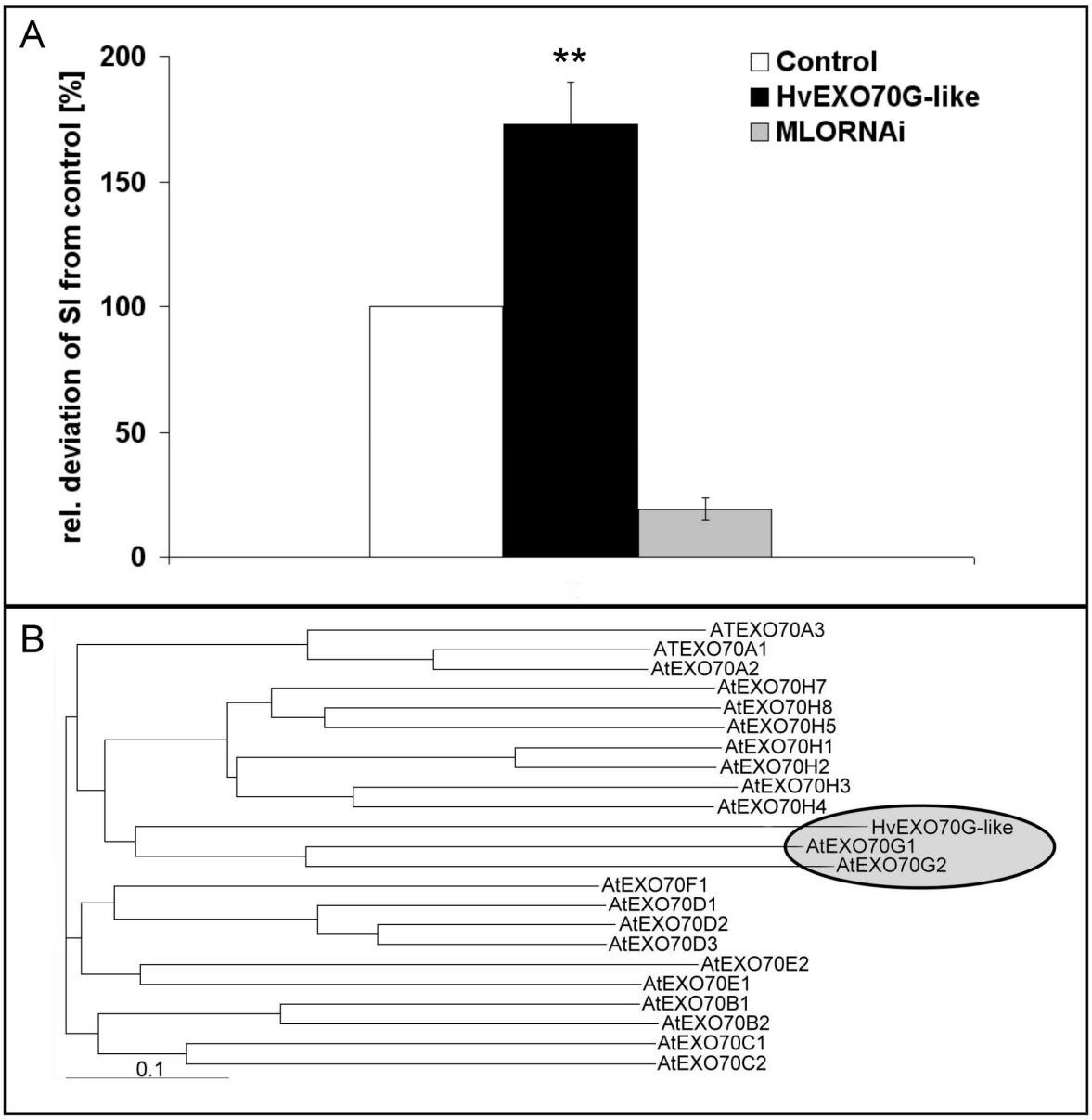

Figure 6: Knock down and phylogenetic analysis of the putative *EXO70G-like* gene

A: Relative deviation of the SI of *HvEXO70G-like*-RNAi from the empty vector control. Transient silencing of *HvEXO70G-like* resulted in a significant induction of the susceptibility of barley cv. 'Golden Promise' to *Bgh* (+ 84%, Student's *t* test $p < 0.01$). The detached leaf segments were co-bombarded with the transformation marker *GFP* (in pGY-1) and the *HvEXO70G-like* RNAi-construct (in pIPKTA30N) or the empty vector, respectively. Inoculation took place two dab and the microscopic analysis was conducted two dai. The SI of the control was set to 100%, while candidate and *MLO*-RNAi control are given as mean values of seven independent TIGS experiments rel. to the empty vector control. The bars represent standard errors. **B:** Phylogenetic analysis of AK362856. Protein sequences of the EXO70 family from *Arabidopsis* (Synek *et al.,* 2006) were used to phylogenetically classify AK362856, which branches together with the AtEXO70G-group. The protein sequences were aligned using the program ClustalW (http://www.ebi.ac.uk/Tools/msa/clustalw2/) and the phylogenetic tree was generated using TreeView.

EXO70 is a protein that belongs to a tethering complex, which is involved in the docking of vesicles to the plasma membrane (Zhang *et al.,* 2010). The initial candidate set contained 13 EST-sequences for which NCBI predicted an EXO70 domain in the corresponding protein sequence. I subcloned seven of them successfully into the pIPKTA30N RNAi-vector but TIGS experiments revealed only for HD14N02r knock down an effect on the barley-*Bgh* interaction. Later sequence analysis (in 2011) using the NCBI nucleotide blast identified the EST-sequence HD14N02r to match with the nucleotide sequence of *AK362856,* a potential full length mRNA. Synek *et al.* (2006) described 22 EXO70 genes in *Arabidopsis*. I used the protein sequences corresponding to these genes to classify the putative EXO70 domain-containing protein from the screening. The phylogenetic analysis showed that the protein, corresponding to *AK362856*, groups in a branch together with the EXO70G proteins from *Arabidopsis* (Figure 6B). Therefore, it was termed *HvEXO70G-like*. Due to the lack of full-length sequence information at the end of the screening, I did not analyze this candidate in more detail although a putative EXO70 domain made it an interesting candidate.

3.2.2 Two ADP ribosylation factor

Two ADP ribosylation factor proteins (ARF) seemed to interfere with the defence response of barley to *Bgh* in the knock down screening experiments (Figure 7A+B). One (EST-accession no.: HO30E03S = internal screen no.: 86) enhances the susceptibility of barley to *Bgh* significantly (Student's *t* test $p < 0.05$), while the other (EST-accession no.: HO02D01S; internal screen no.: 36) shows a clear tendency towards more susceptibility ($p = 0{,}059$) in comparison to the control. ARF-GTPases are responsible for the recruitment of coat proteins for COPI and clathrin coated vesicles to the donor membranes (Bassham *et al.,* 2008). The initial set of candidate genes contained 11 EST-sequences of putative GTPases (9 ARF-GTPases and 2 ARF-like-GTPases), which all have been analyzed in the screening. Beside the two above-mentioned constructs, none conferred a consistent effect. Nucleotide blast of the two EST-sequences, with significant effects in the screening (HO02D01S and HO30E03S), against the TIGR database identified *TA29797_4513* (HO02D01S) and *TA29770_4513* (HO30E03S) to code for the full-length sequences of the corresponding ARF proteins. Vernoud *et al.* (2003) and Böhlenius *et al.* (2010) described the ARF-GTPase protein families of *Arabidopsis* and barley respectively.

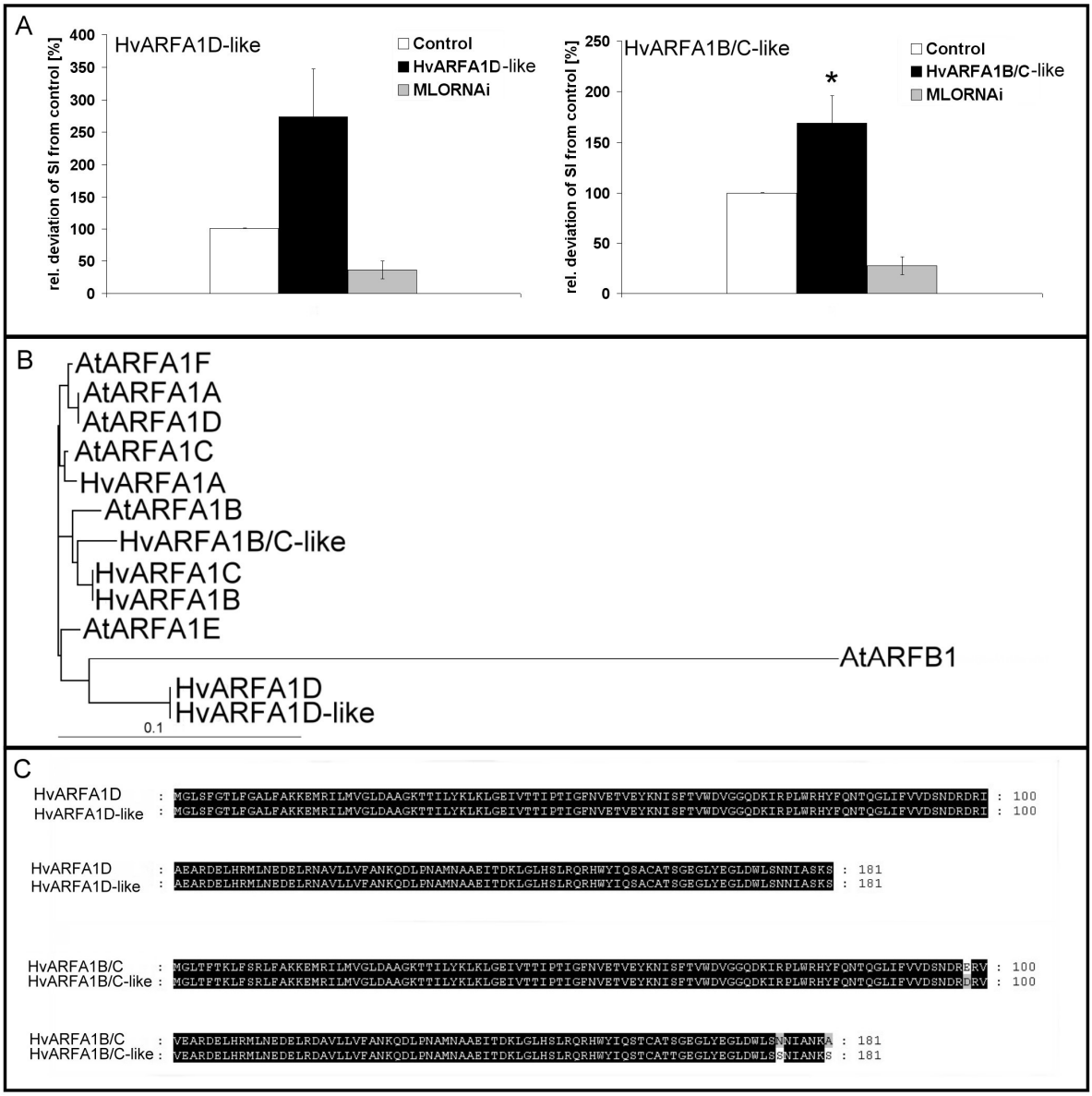

Figure 7: Two ADP-ribosylation factors influence the barley-*Bgh* interaction

A: Relative deviation of the SI from the empty vector control. Transient knock down of both, *HvARFA1D-like* (*HO02D01S*) and *HvARFA1B/C-like* (*HO30E03S*), resulted in increased susceptibility of barley cv. 'Golden Promise' to *Bgh* (*HvARFA1D-like*: + 173%, Student's *t* test p = 0.059; *HvARFA1B/C-like*: + 69%, Student's *t* test p < 0.05). The detached leaf segments were co-bombarded with the transformation marker *GFP* (in pGY-1) and the RNAi-constructs of *HvARFA1D-like* or *HvARFA1B/C-like* (in pIPKTA30N) or the empty vector, respectively. They were inoculated two dab and analyzed two dai microscopically. The SI of the control was set to 100%. *HvARFA1D-like*/*HvARFA1B/C-like* and the *MLO*-RNAi control are given as mean values of nine independent TIGS experiments for each candidate rel. to the empty vector control. The bars represent standard errors. **B:** Phylogenetic tree of the protein sequences of ARF A-family members from *Arabidopsis* (Vernoud *et al.,* 2003) and barley (Böhlenius *et al.,* 2010) and the screening ARF-candidates HvARFA1D-like and HvARFA1B/C-like. Protein sequences were aligned using the program ClustalW (http://www.ebi.ac.uk/Tools/msa/clustalw2/) and the phylogenetic tree was generated using TreeView. **C:** Alignments of the protein sequences of HvARFA1D-like and HvARFA1 are shown as well as of HvARFA1B/C-like and HvARFA1B/C.

Comparison of the protein sequences from the screening HvARFs with the described sequences of *Arabidopsis* and barley revealed that both of them belong to the ARF A family. The protein sequence of HvARFA1D-like is identical to HvARFA1D and HvARFA1B/C-like is most closely related to HvARFA1C with 97% identical amino acids (Figure 7C). Phylogenetic analysis also showed that they cluster together with the respective proteins from barley (Figure 7B). The sequences of the four barley ARFA-GTPases are very similar and the RNAi-constructs are quite long. It seems likely, that both constructs knock down the whole ARFA family because they contain more than 20 contiguous homolog nucleotides. Therefore, it is not yet possible to relate the screening results to one individual GTPase due to co-silencing of various other ARF-GTPases. To analyze the potential involvement of ARFA-GTPases in more detail, I isolated the full-length sequences of *HvARFA1D-like* and *HvARFA1B/C-like* out of RNA for over-expression experiments. They were inserted into the plant over-expression vector pGY-1 under the control of the CaMV35s promoter (Schweizer *et al.,* 1999) and transiently over-expressed in barley epidermal cells using particle bombardment.

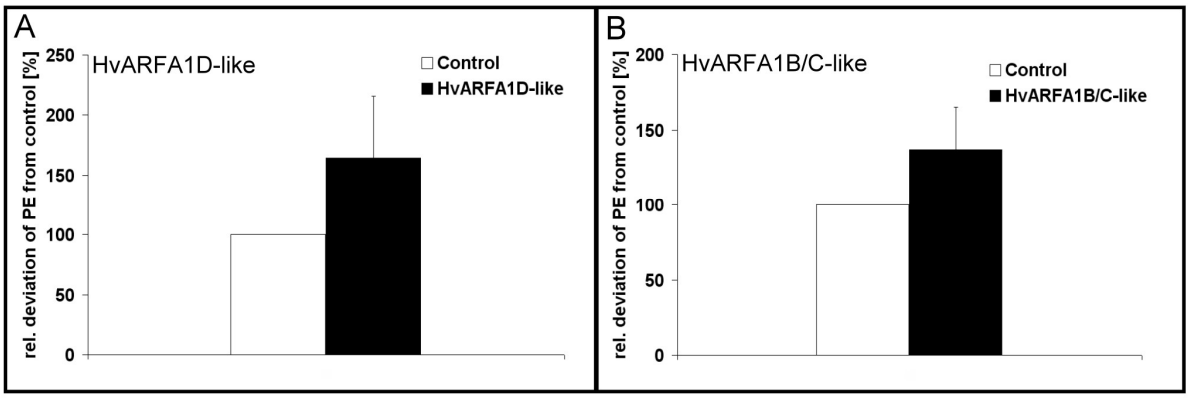

Figure 8: Over-expression experiments of *HvARFA1D-like* and *HvARFA1B/C-like*

Transient over-expression of both, **A:** *HvARFA1D-like* (*TA29797_4513*) and **B:** *HvARFA1B/C-like* (*TA29770_4513*), did not alter the PE of barley cv. 'Golden Promise' to *Bgh* significantly. The detached leaf segments were ballistically transformed with the transformation marker *GFP* (in pGY-1) and the over-expression constructs of *HvARFA1D-like* or *HvARFA1B/C-like* (in pGY-1) or the empty vector, respectively. The leaf segments were inoculated two dab and analyzed via fluorescence microscopy two dai. The PE (ratio of all attacked cells to cells attacked and penetrated) of the control was set to 100% and the OEx of *HvARFA1D-like*/*HvARFA1B/C-like* is given with the mean values of three independent experiments relative to the empty vector control. Bars represent standard errors.

Results

As shown in Figure 8, the over-expression of neither *HvARFA1D-like* nor *HvARFA1B/C-like* significantly influenced the penetration efficiency of *Bgh*. However, both constructs showed a tendency to supersusceptibility. During the plant defence reaction, various genes are up or down regulated (Göhre and Robatzek, 2008). Thus, the expression pattern of genes putatively involved in defence is of special interest and as the results above indicate an involvement of *HvARFA1D-like* and *HvARFA1B/C-like* in defence, their expression was analysed. I used a time-course inoculation experiment comprising infected and non-infected leaf samples of the susceptible cultivar 'Ingrid' WT and the *mlo*-resistant cultivar 'Ingrid-*mlo5*'. Both *HvARFA* genes were expressed in barley leaves as examined via semi-quantitative RT-PCR (Figure 9). *HvARFA1B/C-like* signals slightly increased after *Bgh* inoculation, especially in the 'Ingrid-*mlo5*'. In contrast, the expression of *HvARFA1D-like* shows no pathogen-induced changes.

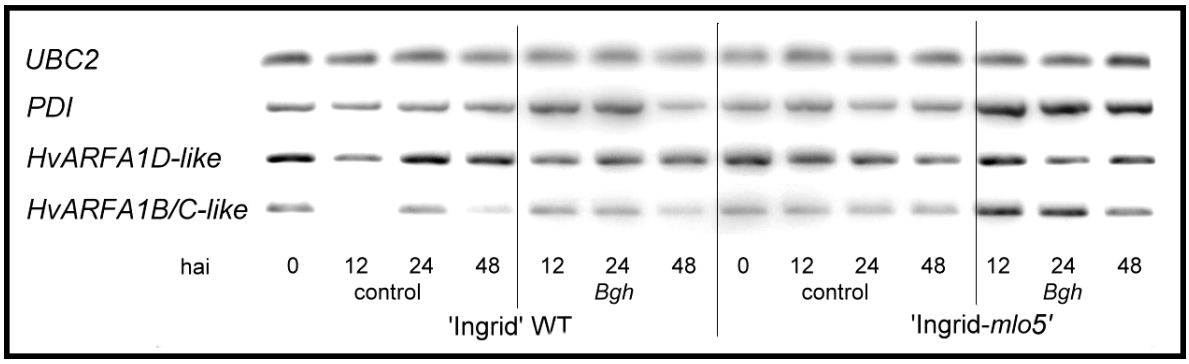

Figure 9: Expression of *HvARFA1D-like* /*HvARFA1B/C* in different barley genotypes

The barley cultivars 'Ingrid' and 'Ingrid-*mlo5*' were inoculated with *Bgh* and infected as well as mock-inoculated leaves were harvested at 12, 24 and 48 hai. The gene expression levels of *HvARFA1D-like* and *HvARFA1B/C-like* as well as control genes are shown as inverted ethidium bromide stained gel pictures. UBC2: *UBIQUITIN* (control for constitutive expression), PDI: *PROTEIN DISULFIDE ISOMERSE* (control for pathogen-induced gene expression)

The publically available expression database PLEXdb (http://www.plexdb.org) confirms a pathogen-inducible expression of *HvARFA1B/C-like* in the experiment BB10 (Meng *et al.,* 2009), which compares gene expression between four different barley genotypes. In this experiment the EST representing *HvARFA1D-like* seems to be slightly down regulated after inoculation, at least in some genotypes, which is not visible in the semi-quantitative experiment conducted in this work (see TableS5 for IDs used in PLEXdb and FigureS1 for expression summary).

3.2.3 The putative tethering complex subunit HvCOG3

The EST-sequence HA14A08r is the third-screening candidate, which influences the susceptibility of barley to *Bgh* significantly with $p < 0.05$ (Student's *t* test). Knock down of this gene enhanced the susceptibility of barley epidermal cells by 156% (Figure 10). In 10 independent TIGS experiments the SI varied between 20% enhanced resistance and 448% enhanced susceptibility. Analysis of the EST-sequence by nucleotide blast against the NCBI database revealed the *AK249208* gene to represent the corresponding full-length sequence. As there was no annotation available for this NCBI sequence I used the TIGR database to identify it as the "putative tethering factor Sec34" (TA38481_4513; not full-length). Sec34 is part of a complex, which localizes to Golgi bodies and is called COG complex for conserved oligomeric Golgi complex. As one subunit of this complex Sec34 was renamed into COG3 (Ungar *et al.,* 2002).

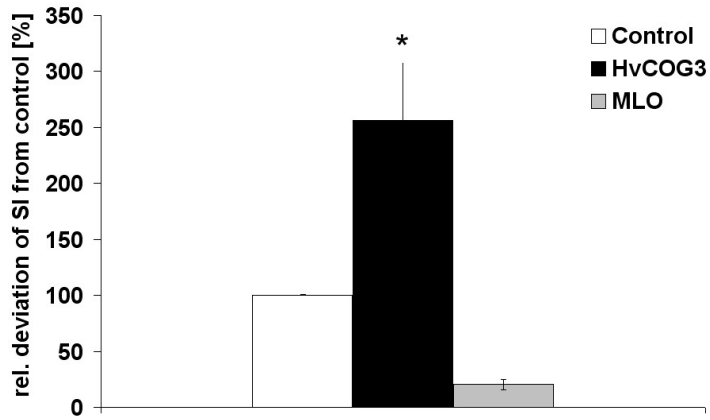

Figure 10: Transient knock down of *HvCOG3*

Transient RNAi of *HvCOG3* resulted in a significant induction of the susceptibility of barley cv. 'Golden Promise' to *Bgh* (+ 156%, Student's *t* test $p < 0.05$). The detached leaf segments were co-bombarded with the transformation marker *GFP* (in pGY-1) and the RNAi construct of *HvCOG3* (in pIPKTA30N) or the empty vector control, respectively. The leaves were inoculated two dab and analyzed using fluorescence microscopy two dai. The SI of the control was set to 100%. *HvCOG3*-RNAi and the *MLO*-RNAi control are given as mean values of ten independent TIGS experiments rel. to the empty vector control. The bars represent standard errors.

During the following investigations on *HvCOG3* and its surrounding protein framework, it appeared difficult to reproduce the screening RNAi-effect on the barley-*Bgh* interaction. However, the change from the pIPKTA30N vector based RNAi-system to the direct introduction of double stranded RNA verified the initial screening results. Introduction of dsRNA of *HvCOG3* enhanced the susceptibility of 'Golden Promise' epidermal cells by 21% with $p < 0.05$ (Student's *t* test). This strengthens the

reliability of the screening result although it is not clear why the vector based RNAi-system failed to reproduce the effect.

3.3 Investigations on *HvCOG3* effects in barley

To gain deeper insights into the possible functions of *HvCOG3* I isolated its full-length cDNA sequence out of RNA and introduced it into the plant over-expression vector pGY-1, under the control of the CaMV35s promoter (Schweizer *et al.,* 1999). The fluorescent microscopic analysis revealed a significant reduction of the penetration success of *Bgh* in epidermal cells of 'Golden Promise' with 71% of the empty vector control (Student's *t* test $p < 0.05$). The PE of the seven independent experiments ranged from 26% increased penetration to a reduction to 35% of the penetration level observed in the control (Figure 11A). As COG3 belongs to a complex in yeast and mammals (Ungar *et al.,* 2002) and as homologous genes for all complex subunits exist in barley (Figure 15), the observed over-expression effect of a single COG subunit was unexpected. In silico analysis of the protein sequence of HvCOG3, using the domain predicting program plantsp (http://plantsp.genomics.purdue.edu/cgi-bin/fscan/feature-scan.cgi) indicated a putative Rho-GAP domain for the c-terminal part of the protein (Figure 11C). A possible explanation for the reduced penetration efficiency of *Bgh* after *HvCOG3* over-expression could be that this putative Rho-GAP domain might indirectly regulate the activity of the complex. To test this hypothesis, I generated a pGY-1 construct over-expressing only the c-terminal part of the protein, which contains the putative Rho-GAP domain. After eight independent experiments, which varied between - 50% to + 523% penetration efficiency there was no significant effect observable (Figure 11B). Thus, it seems as if the putative Rho-GAP domain alone, which was predicted for HvCOG3, does not influence the outcome of the barley-*Bgh* interaction and that the N-terminus could be important for its funciton. Investigations on COG3 in yeast and animal cells showed that it localizes mainly to the cis-Golgi compartment in these organisms (Kim *et al.,* 2001; Suvorova *et al.,* 2001). To investigate the localization of COG3 in barley, I generated C- and N-terminal GFP-fusion constructs of *HvCOG3* and inserted them into the plant over-expression vector pGY-1. The over-expression of the N-terminal fusion construct in barley epidermal cells produced a rather weak and unspecific GFP-signal in the cytoplasm and showed only a weak co-localization with the Golgi-marker construct *GmMAN1-RFP* (Yang *et al.,* 2005; data not shown).

The C-terminal GFP-fusion construct did not to produce any detectable GFP signal (data not shown).

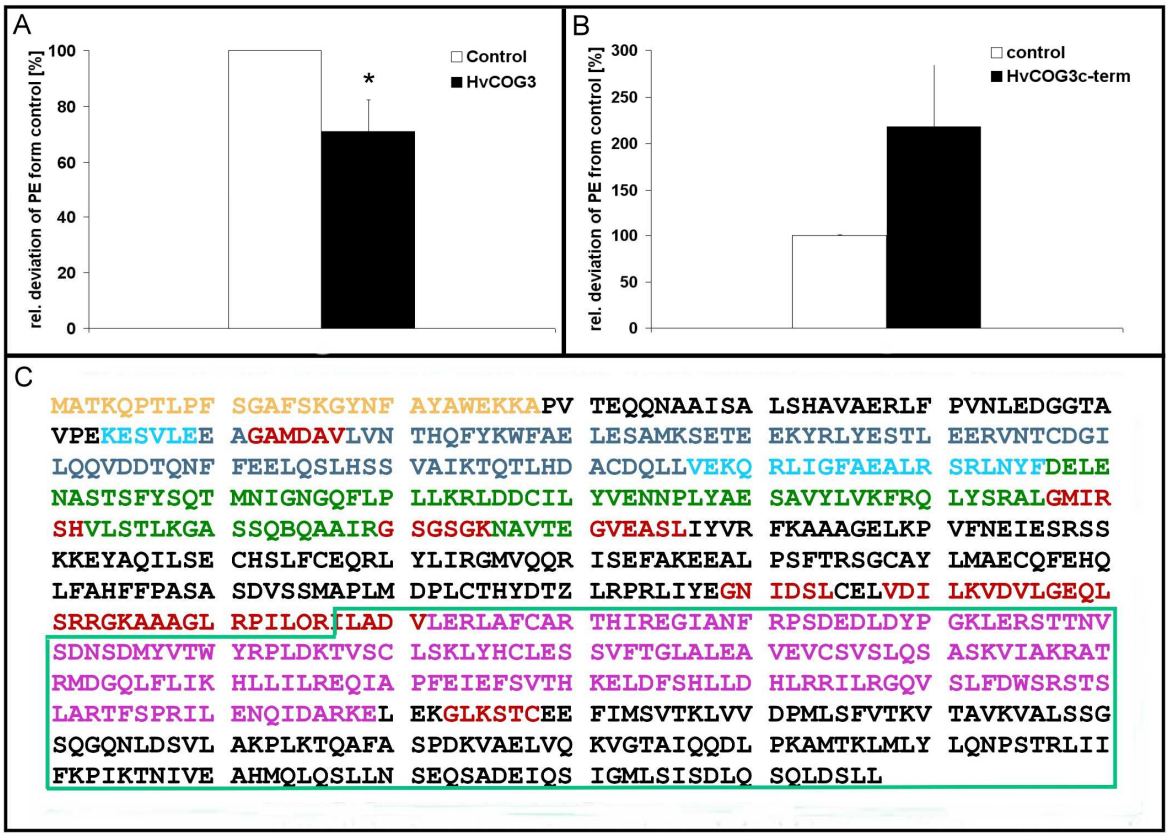

Figure 11: Over-expression of *HvCOG3* and its putative Rho-GAP domain

A: Transient over-expression of full-length *HvCOG3*. **B:** Transient over-expression of the *HvCOG3c-terminus*, containing the putative Rho-GAP domain. Over-expression of *HvCOG3* resulted in a significant increase in resistance of barley cv. 'Golden Promise' to *Bgh* (71% relative to the control, Student's *t* test $p < 0.05$); over-expression of the c-terminus had no significant effect. The detached leaf segments were co-bombarded with the transformation marker *GFP* (in pGY-1) and the over-expression construct of *HvCOG3*/the *HvCOG3* putative Rho-GAP domain (in pGY-1) or the empty vector, respectively. Inoculation took place two dab and two dai the experiments were evaluated microscopically. The PE of the control was set to 100%, while *HvCOG3* and *HvCOG3c-terminus* OEx are given as mean values of seven (**A**) or eight (**B**) independent experiments relative to the empty vector control. **C:** Protein sequence of HvCOG3. Purple font: predicted Rho-GAP domain (http://plantsp.genomics.purdue.edu/cgi-bin/fscan/feature_scan.cgi), Green box: over-expressed c-terminal part of *HvCOG3*

3.3.1 Effects of *HvCOG3* RNAi on barley epidermal cell function

The EST-sequence HA14A08r, which represents *HvCOG3,* belongs to the membrane trafficking and secretion candidate gene set. Therefore, the screening effect observed in cells with restricted *HvCOG3* function might be due to deficiencies in secretory transport processes. To investigate possible secretion defects in *HvCOG3* knock down cells I used a secreted GFP protein version (Sigpep-GFP). The Sigpep-GFP construct links an N-terminal signal peptide to GFP in pGY-1 and was generated in a previous work by J. Preuß (TUM, Phytopathology, Freising, Germany).

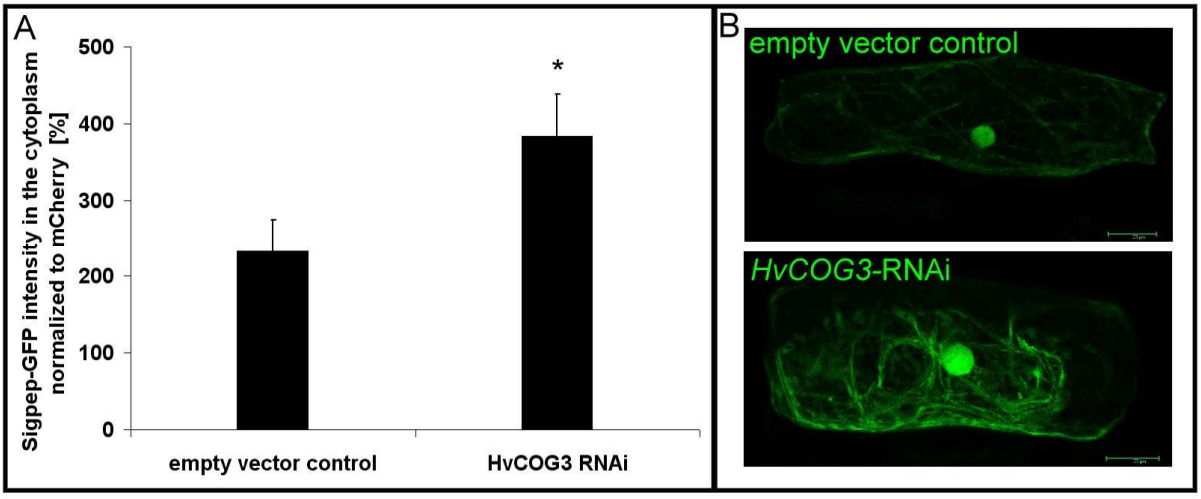

Figure 12: Analysis of secretion in *HvCOG3* RNAi cells

The accumulation of a secreted GFP-version in the cytoplasm of *HvCOG3* deficient cells was significantly enhanced. A secreted *GFP* construct, linking a signal peptide N-terminally to *GFP* (*Sigpep-GFP* in pGY-1) was co-expressed together with either the empty pIPKTA30N control or the *HvCOG3* RNAi construct (in pIPKTA30N) and the transformation marker mCherry (in pGY-1) in barley epidermal cells (cv. 'Golden Promise') and analyzed by confocal laser-scanning microscopy two dab. **A:** The GFP intensity detected in the cytoplasm was normalized to the fluorescence intensity of the cytoplasmic transformation marker mCherry for each of the 50 cells from three independent repetitions. The brighter GFP fluorescence in *HvCOG3* deficient cells is significantly higher compared to control cells (Student's *t* test $p < 0.05$). **B:** Confocal laser-scanning micrographs of barley epidermal cells expressing Sigpep-GFP together with either the empty vector (upper picture) or the *HvCOG3* RNAi construct (lower picture) two dab. A total of 50 cells were examined in three independent repetitions. All cells of the same experiment were imaged with the same excitation and detection settings.

In a transient assay, barley epidermal leaves were ballistically transformed with the cytoplasmic transformation marker mCherry, Sigpep-GFP and either the empty pIPKTA30N vector or the *HvCOG3*-RNAi construct (in pIPKTA30N). The transformed cells were analyzed using confocal laser-scanning microscopy two dab. As the Sigpep-GFP protein will be secreted due to the signal peptide, the GFP-signal inside the cells should be low. Indeed, in barley epidermal cells expressing the empty pIPKTA30N vector together with Sigpep-GFP the GFP intensity was very weak in most cases. In contrast, cells expressing the *HvCOG3*-RNAi construct clearly revealed brighter GFP fluorescence in the cytoplasm in comparison to the empty vector control (Figure 12B). To quantify this effect, the GFP fluorescence intensity was normalized to the fluorescence signal of mCherry for each cell, and this effect of *HvCOG3* RNAi was significant at $p < 0.05$ (Student's *t* test; Figure 12A). Several subunits of the COG complex have been reported to be important for the perpetuation of the Golgi structure in mammalian cells (Ungar *et al.,* 2002; Zolov and Lupashin, 2005). To examine a possible effect of *HvCOG3* RNAi on Golgi bodies of barley cells, I analyzed the frequency of bright shining Golgi bodies using a green fluorescent Golgi marker protein called sGFPHDEL (Eichmann, 2005). sGFPHDEL co-localizes with the Golgi marker protein GmMan:1 described by Yang *et al.* (2005) but provides much brighter fluorescent signals. In a ballistic transient transformation assay, barley epidermal cells were simultaneously transformed with either the empty pIPKTA30N vector or the *HvCOG3* RNAi construct (in pIPKTA30N) together with the sGFPHDEL construct (in pGY-1). The transformed cells were examined three dab using confocal laser-scanning microscopy. Figure 13B shows representative pictures of the distribution of Golgi body in control or *HvCOG3*-RNAi cells, respectively. To quantify the amount of Golgi bodies, bright shining Golgis per cell were counted, and classified into the following four categories: 0-10, 10-20, 20-50 or more than 50 detectable Golgi bodies per cell. The frequency at which cells were classified into the different categories is shown in Figure 13A. There are less bright shining Golgi bodies detectable in barley epidermal cells expressing the *HvCOG3*-RNAi construct. A χ^2 analysis was used to test for a significantly different distribution between the two constructs. This revealed that the two test series are significantly different form each other with a probability of 99.5%.

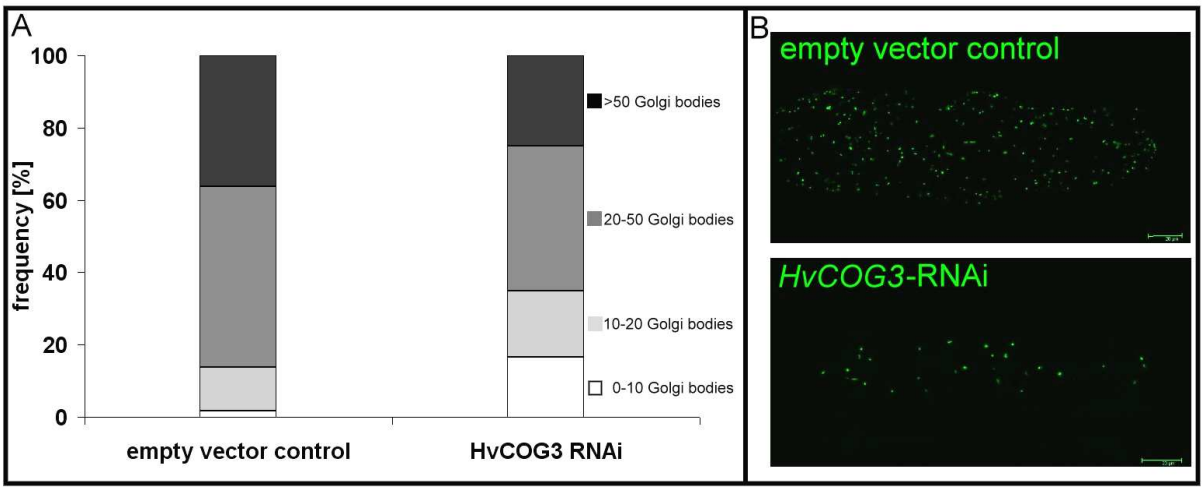

Figure 13: Analysis of Golgi bodies in *HvCOG3* knock down cells

The amount of bright shining Golgi bodies was significantly reduced in *HvCOG3* deficient cells. Barley epidermal cells (cv. 'Golden Promise') were simultaneously transformed with a green fluorescing Golgi marker protein (sGFPHDEL in pGY-1) and the empty pIPKTA30N or the *HvCOG3*-RNAi (in pIPKTA30N) construct. Transformed cells were analyzed three dab using confocal laser-scanning microscopy and the amount of bright fluorescing Golgi bodies per cell was examined. **A:** The analyzed cells were classified into four categories with different amounts of Golgi bodies. Statistical analysis using a χ^2 test showed that the two constructs exhibit a significantly different distribution concerning the amount of Golgi bodies per cell with a probability of 99.5%. **B:** Confocal laser-scanning micrographs of barley epidermal cells expressing sGFPHDEL together with either the empty vector (upper picture) or the *HvCOG3* RNAi construct (lower picture) three dab are shown. A total of 70 cells were examined in three independent repetitions. The detection settings were chosen on an intentionally low level, to obtain GFP signals only form clearly bright shining Golgi bodies. All cells of the same experiment were imaged with the same excitation and detection settings.

3.4 Investigations on the COG complex of barley

3.4.1 *In silico* studies

Because of the functional effects of *HvCOG3* knock down in barley, I started to investigate genes associated with COG3 in yeast or mammals. As already mentioned,

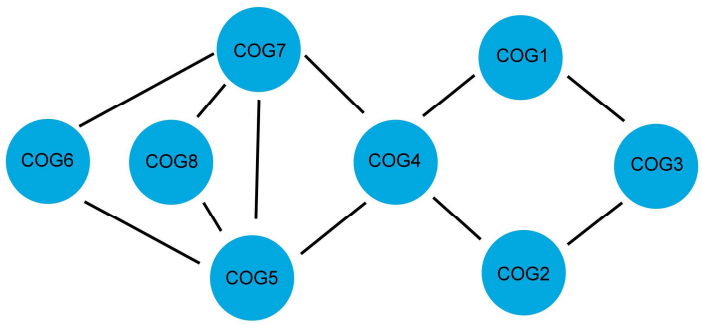

Figure 14: The yeast COG complex

Model of the yeast COG complex subunit architecture. Redrawn after Loh and Hong (2004)

COG3 exists in a complex together with seven other subunits in yeast and mammals (Ungar *et al.,* 2002). There was no information available concerning a COG complex in barley and therefore, I used the sequence information from the eight human COGs (Quental *et al.,* 2010) for a data base research in NCBI and TIGR. The obtained plant sequences were translated into the amino acid sequence and analyzed for similarities using the ClustalW2.0 program. All eight human COG protein sequences exhibit homologs in *Arabidopsis*, as published by Koumandou *et al.* (2007) and in addition in rice and barley. The similarities (ClustalW 2.0 scores) between the human and plant COG protein sequences varied between 18% and 35%, while the plant COG complex sequences were highly similar.

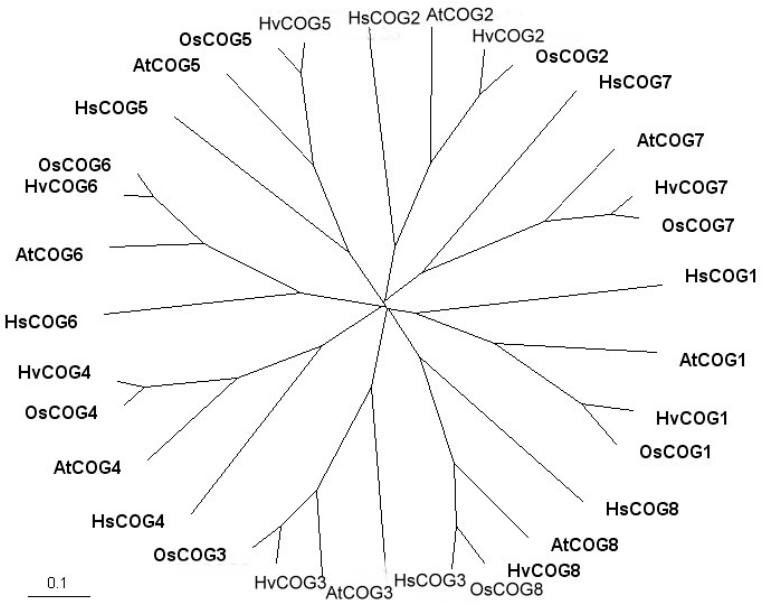

Figure 15: Phylogenetic tree of human, *Arabidopsis*, rice and barley COG subunits

The COG complex is highly conserved in plants. Nucleotide and protein sequences of the human (Hs), *Arabidopsis* (At), rice (Os) and barley (Hv) COG complex subunits were identified based on human COG sequence information published in Quental *et al.* (2010). The protein alignments were performed using the web-program ClustalW 2.0 (http://www.ebi.ac.uk/Tools/msa/clustalw2) and the phylogenetic tree was generated by the program TreeView.

The protein sequences from the COG subunits of rice and barley show between 82% and 91% similarity (see TableS5 for gene IDs of the human, *Arabidopsis*, rice and barley COG subunits). A phylogenetic tree was generated using TreeView to illustrate the relationships between the different COG proteins (Figure 15). The occurrence of all human COG subunits in plants indicates the existence of HvCOG3 in a complex similar to that known from yeast and mammals. This made the other COG subunits interesting candidates for further investigations.

3.4.2 Functional characterization of the different *HvCOG* subunits

I isolated cDNA fragments from the different *HvCOGs*, 300 – 700 bp in size, for the generation of RNAi constructs of the remaining barley COG subunits. The RNAi constructs (in pIPKTA30N) were ballistically introduced into barley epidermal cells (cv. 'Golden Promise') and analyzed microscopically for a putative effect on the interaction of barley with *Bgh*. To quantify the effects the susceptibility index was calculated two dai for five to six independent experiments per subunit (Figure 16).

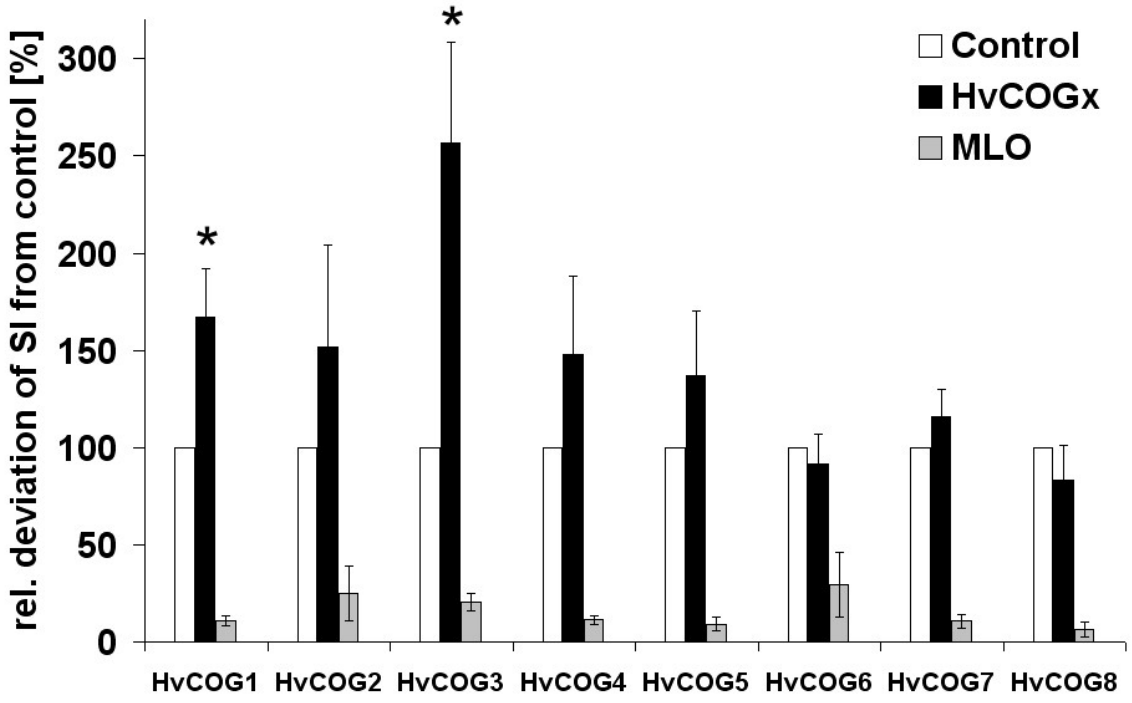

Figure 16: Knock down of the different COG subunits in barley epidermal cells

Beside *HvCOG3* also *HvCOG1* induces susceptibility in *HvCOG3* RNAi cells significantly (+ 67% Student's *t* test $p < 0.05$). Epidermal cells of barley cv. 'Golden Promise' were transiently transformed with the marker gene *GFP* (in pGY-1) and the RNAi construct of one of the different *HvCOG* subunit genes (in pIPKTA30N) via particle bombardment. The detached leaves were inoculated two dab and microscopical evaluation took place two dai. The susceptibility index of the empty vector control was set to 100% and the *HvCOGs* and *MLO*-RNAi are given as the mean values of five (*HvCOG4-8*) to six (*HvCOG1-2*) independent experiments. The bars represent standard errors. The *HvCOG3* knock down result from the screening was included in this graph for completeness.

Beside *HvCOG3* whose knock down already enhanced the susceptibility to the barley powdery mildew during the screening (Figure 10), one additional barley COG complex component, *HvCOG1,* significantly increased the amount of epidermal cells

that allow the establishment of a haustorium (Student's *t* test $p < 0.05$). The susceptibility index of the six independent experiments performed, varied between 1% and 173% elevated susceptibility. The knock down experiments of the other subunits revealed no significant impact on the success of *Bgh*. Nevertheless, TIGS of *HvCOG2*, *HvCOG4*, and *HvCOG5* at least tend to enhance the susceptibility of barley to *Bgh*, while knock down of *HvCOG6*, *HvCOG7* and *HvCOG8* do not seem to have any effect on the SI.

3.4.3 Gene expression analysis of *HvCOG* subunits

As the results described above indicate, the COG complex appears to be important for plant defence. One characteristic plant response to a pathogenic attack is the differential regulation of many genes (Bischof *et al.,* 2011). Using semi-quantitative RT-PCR, the *HvCOG* subunits were analysed for a differential expression in barley leaves inoculated with *Bgh*. I compared the expression of different barley COG subunits in a time-course inoculation experiment with susceptible and *mlo*-resistant barley ('Ingrid' MLO WT / 'Ingrid-*mlo5*') plants (Figure 17A).

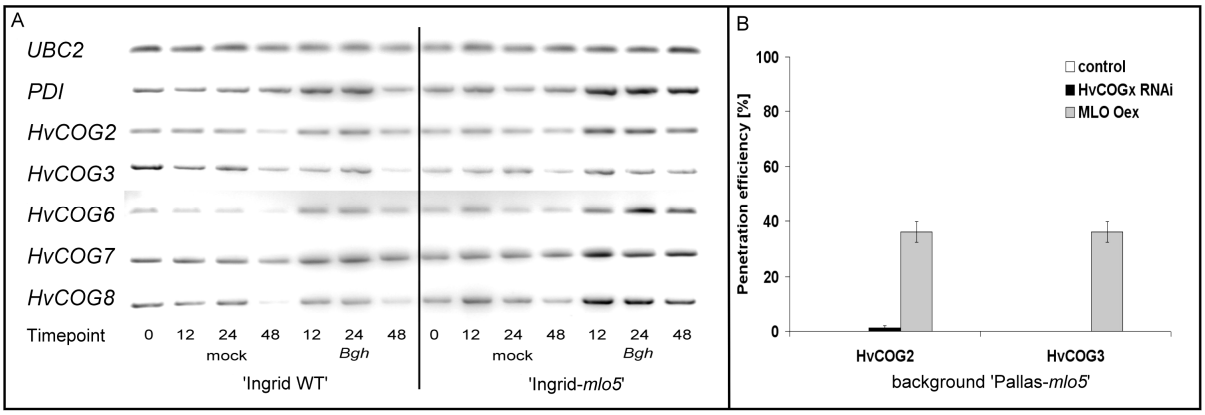

Figure 17: Analyses of *HvCOG* complex subunits in 'Ingrid' and 'Ingrid-*mlo5*'

A: 'Ingrid' WT and 'Ingrid-*mlo5*' plants were inoculated with *Bgh* and infected as well as mock-inoculated leaves were harvested at 12, 24 and 48 hai. A shows the inverted ethidium bromide stained gel pictures of *HvCOG2,3,6,7* and *8*. UBC2: *UBIQUITIN* (control for constitutive expression), PDI: *PROTEIN DISULFIDE ISOMERSE* (control for pathogen-induced gene expression) **B:** Transient knock down of *HvCOG2* and *HvCOG3* in 'Pallas-*mlo5*' background. *GFP* (in pGY-1) as transformation marker and either the empty vector control (pIPKTA30N), *HvCOG2*, *HvCOG3* (in pIPKTA30N) or *MLO* (in pGY-1) as positive control, were introduced into barley epidermal cells of 'Pallas-*mlo5*'. The leaves were inoculated two dab and analyzed microscopically two dai by calculating the PE. Between 50 and 87 individual interaction sites were analyzed per construct in four independent experiments. The bars represent standard errors.

Results

The gene expression of the complex components *HvCOG2* and *6-8* was clearly, *HvCOG3* slightly increased in the *mlo*-resistant barley plants after *Bgh* inoculation. In susceptible 'Ingrid' WT plants, the *Bgh* dependent induction was very weak but visible for *HvCOG2*, *6* and *7*. These results support that the HvCOG complex might be involved in penetration resistance. The COG complex subunits H*vCOG1*, *4* and *5* were not available at this point of the project. I used the publicly available expression database PLEXdb (http://www.plexdb.org) to support the observed pathogen-induced semi-quantitative gene expression pattern. The BB10 experiment displays four different barley genotypes inoculated and not inoculated at six different time points (Meng *et al.,* 2009). Analysis of the ESTs representing the different *HvCOG* subunits showed a clear pathogen-induced enhancement of *HvCOG1* and *HvCOG5-8*. For *HvCOG3* and *4* it was not as clear and COG2 displays a much lower expression level compared to the other subunits and an almost even expression (see TableS5 for IDs used in PLEXdb and FigureS1 for expression summary). Taken together, the gene expression results of the subunits semi-quantitatively analyzed here are largely in agreement with the data from the PLEXdb database experiment BB10 except that *HvCOG2* is not responding to pathogen infection in PLEXdb. In sum, these results indicate that the HvCOG complex might be involved in resistance. Because the semi-quantitative expression analysis indicated an enhancement of the *HvCOG* subunit gene expression in the 'Ingrid-*mlo5*' plants, I investigated a possible participation of the barley COG complex in *mlo*-mediated penetration resistance. Therefore, I knocked down two subunits, *HvCOG2* and *HvCOG3*, transiently in epidermal cells of the barley cultivar 'Pallas-*mlo5*' and analyzed them for differences in the penetration resistance against *Bgh*. As a positive control for resistance break down, the *HvMLO* gene was over-expressed to ensure the general viability of the fungus in the different experiments. In four independent repetitions, neither knock down of *HvCOG2* nor *HvCOG3* clearly influenced the *mlo*-mediated penetration resistance in 'Pallas-*mlo5*' plants (Figure 17B).

3.5 Investigations on potential interaction partners of HvCOG3

3.5.1 Functional analysis of potential HvCOG3 interaction partners

As the investigations on *HvCOG3* and the other subunits of the COG complex of barley indicate their importance for plant defence, the next step was a literature-based search for potential interaction partners of COG3. This let to ten proteins potentially interacting with COG3 in yeast or mammals, listed in Table 7. Three of them are subunits of the COG complex (see above). The corresponding homologous *Arabidopsis* sequences were identified in NCBI in a gene-annotation based search. The obtained *Arabidopsis* nucleotide sequences were used to identify the barley homologs via a nucleotide blast against the TIGR database (see TableS5 for gene IDs). All of the ten described COG3 interaction partners revealed a homologous sequence in barley, although for *HvGOS1-like* only the c-terminal part was available. The best-hit sequences were used for subsequent investigations. *HvYPT1-like*, *HvGOS1-like c-term*, *HvYKT6-like*, *HvSEC22-like* and *HvVTI1-like* were successfully isolated out of barley leaf cDNA and cloned into the plant expression vectors pIPKTA30N and in pGY-1 for RNAi and over-expression experiments, respectively. In addition to these non-COG complex subunits, COG3 interacts with several subunits in-between the COG complex (Table 7; see 3.4.2 for functional analysis).

Table 7: COG3 interacting proteins from yeast or mammals

Interaction partner	Description	Reference
YPT1	Rab protein	Suvorova *et al.,* 2002
SED5	t-SNARE	Suvorova *et al.,* 2002
GOS1	v-SNARE	Suvorova *et al.,* 2002
YKT6	v-SNARE	Suvorova *et al.,* 2002
SEC22	v-SNARE	Suvorova *et al.,* 2002
VTI1	v-SNARE	Suvorova *et al.,* 2002
COPIγ	COPI coatomer	Suvorova *et al.,* 2002
COG1	Complex component	Loh and Hong, 2004
SEC35 (=COG2)	Complex component	VanRheenen *et al.,* 1998
SGF1 (=COG4)	Complex component	Kim *et al.,* 2001

Results

Several attempts to isolate the homologues sequence of the t-SNARE SED5 failed, as well as the isolation of the full-length sequences of *HvCOG1*, *2* and *4*. The RNAi and over-expression constructs of the COPI coat subunit COPIγ were kindly provided by P. Schweizer (IPK, Gatersleben, Germany). The potential interaction partners were functionally characterized in transient knock down and over-expression experiments in detached barley leaves. Interestingly, the knock down and over-expression experiments of several potential interaction partners showed a significant impact on the susceptibility of barley cells to the powdery mildew fungus (Figure 18). Knock down of the small Rab-GTPase *HvYPT1-like* and the COPI coat subunit *HvCOPIγ-like* induced the susceptibility to *Bgh* to plus 29% and 48% relative to the empty vector control, respectively (Student's *t* test *HvYPT1-like*: $p < 0.05$; Student's *t* test *HvCOPIγ-like*: $p < 0.05$; Figure 18A).

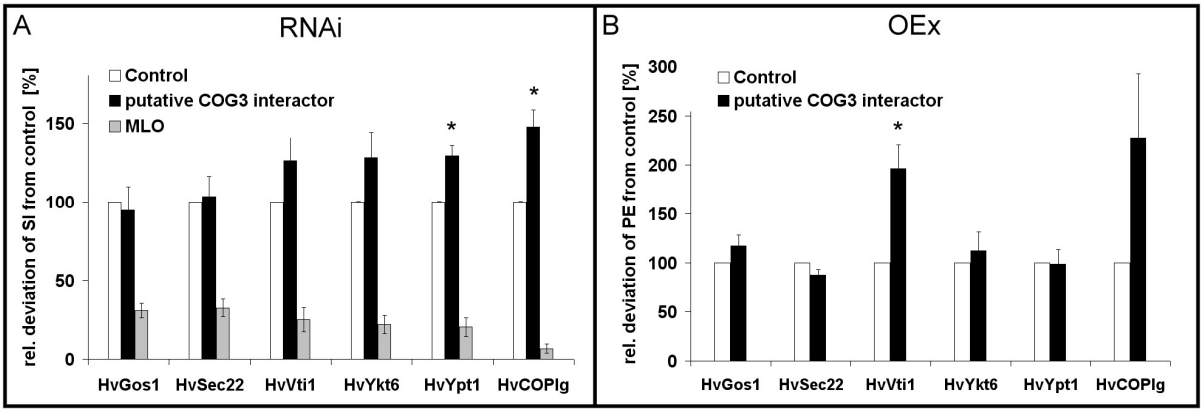

Figure 18: RNAi and over-expression of potential HvCOG3 interaction partners

Knock down of *HvYPT1-like* (+ 29% Student's *t* test $p < 0.05$) and *HvCOPIγ-like* (+ 48% Student's *t* test $p < 0.05$) and the over-expression of *HvVTI1-like* (+ 97% Student's *t* test $p < 0.05$) significantly altered the susceptibility of barley epidermal cells. Detached leaf segments of the barley cv. 'Golden Promise' were transiently transformed via particle bombardment. The transformation marker *GFP* (in pGY-1) and a potential interaction partner in either pGY-1 (for over-expression) or pIPKTA30N (for RNAi) or the empty vector controls, respectively were simultaneously expressed in barley epidermal cells. The leaf segments were inoculated two dab and the microscopic evaluation was conducted two dai. **A:** Knock down experiments: The SI of the empty vector control was set to 100% and the potential HvCOG3 interaction partners are given with the mean values of five to six independent experiments. The bars represent standard errors. **B:** Over-expression experiments: The PE of the control was assessed to 100% and the OEx results of the potential HvCOG3 interaction partners are given as the mean values of three to six independent experiments relative to the empty vector control. Bars represent standard errors.

The susceptibility indices varied between plus 8% and 48% for *HvYPT1-like* and plus 13% and 65% for *HvCOPIγ-like*, respectively. Additionally, one of the three subunits that interact with COG3 in between the yeast COG complex (COG1, 2 and 4) significantly altered the SI. Knock down of *HvCOG1* resulted in a significant increase of haustoria-containing cells as it was already described in section 3.4.2. However, the over-expression of neither *HvYPT1-like* nor *HvCOPIγ-like* significantly altered the penetration efficiency of *Bgh*.

Concerning the over-expression experiments of the other potential interaction partners, *HvVTI1-like* turned out to nearly double (plus 97%) the susceptibility of barley epidermal cells relative to the control (Student's *t* test $p < 0.05$). Cells that over-expressed *HvVTI1-like* showed between 38% and 285% more penetrated cells (Figure 18B). *HvCOG1, 2* and *4* were not over-expressed because I was not able to isolate full-length clones out of cDNA or RNA until now, presumably due to their very long sequences. In sum, interference with the expression of genes that are involved in the same transport step as HvCOG3 seems to affect plant defence severely as five of them enhance susceptibility when they are knocked down or over-expressed.

3.5.2 Further investigations on *HvCOPIγ-like*, *HvYPT1-like* and *HvVTI1-like*

As either knock down or over-expression of the three potential HvCOG3 interaction partners, *HvCOPIγ-like*, *HvYPT1-like* and *HvVTI1-like* led to enhanced susceptibility of barley epidermal cells to *Bgh*, further experiments were conducted to elucidate their function in more detail. A presumable dominant negative form of the Rab-GTPase *HvYPT1-like* was generated by site directed mutagenesis and functionally analyzed for an effect on the interaction of barley with *Bgh*. The experiments indicated a tendency towards more susceptibility, but the result was not statistically significant. In addition, *Arabidopsis* T-DNA insertion lines of the four different RabD-GTPases similar to the barley *YPT1-like* gene were investigated for an influence on the interaction with *Erysiphe cruciferarum*. No significant differences in fungal proliferation were observed between the insertion lines and the wild type Col-0 but a functional redundancy between the different RabD-GTPases cannot be excluded. To determine the subcellular localization *in planta* N-terminal fusion constructs of full length *HvYPT1-like* and *HvVTI1-like* were generated and inserted into the plant expression vector pGY-1. A C-terminal fusion construct of *HvCOPIγ-like* was obtained from P. Schweizer (IPK, Gatersleben, Germany).

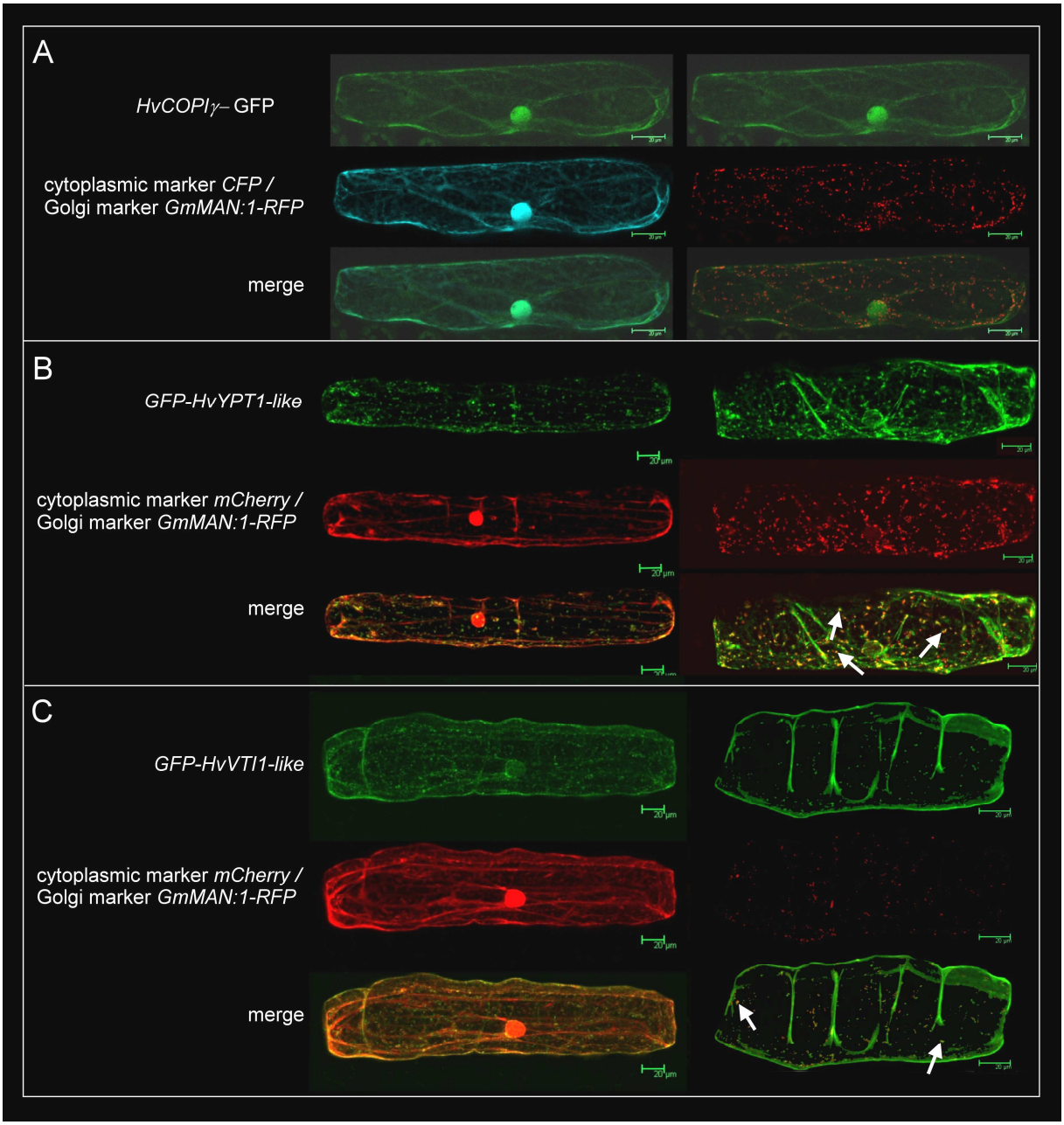

Figure 19: Subcellular localization of *HvCOPIγ-like*, *HvYPT1-like* and *HvVTI1-like*

Confocal laser scanning micrographs of barley epidermal cells (cv. 'Golden Promise') over-expressing GFP-fusion constructs of *HvCOPIγ-like* (A, green), *HvYPT1-like* (B, green) and *HvVTI1-like* (C, green) together with either a cytoplasmic and nuclear marker protein (A: *CFP* (blue); B and C: *mCherry* (red)) shown in the first column or the Golgi marker protein *GmMAN:1* (red), shown in the second column after transient particle transformation. Co-localization, indicated by overlapping fluorescence in the merged pictures, is shown in turquoise (A, first column) and or yellow/orange (A, second column, B and C). *HvCOPIγ* shows a weak co-localisation with *CFP* and seems to be diffusely distributed all over the cell, while *HvYPT1-like* and *HvVTI1-like* both co-localize partly with the *GmMAN:1* (arrows in the second column B and C)

Each construct was transformed transiently into barley epidermal cells by particle bombardment together with either mCherry/CFP (cyan fluorescent protein) as a cytosolic and nuclear marker protein or the Golgi marker protein GmMAN1-RFP (Yang *et al.,* 2005). The subcellular localization of the proteins was examined one to three days after particle bombardment using confocal laser-scanning microscopy.

The green fluorescing HvCOPIγ-like fusion protein showed a weak co-localization with the cytoplasmic and nuclear marker protein CFP but it seemed to be diffusely distributed all over the cell (Figure 19A). The GFP-fusion constructs of *HvYPT1-like* and *HvVTI1-like* both produced bright fluorescence signals and co-localized at least partly with the Golgi marker protein GmMAN:1 (arrows in Figure 19B and C). In addition, *GFP-HvVTI1-like* localized to the cell periphery (Figure 19C), most likely representing the plasma membrane. This was indicated as plasmolysis triggered by glycerol led to characteristic Hechtian strands, which become visible when the plasma membrane peals away form the cell wall due to protoplast shrinkage (Figure 20).

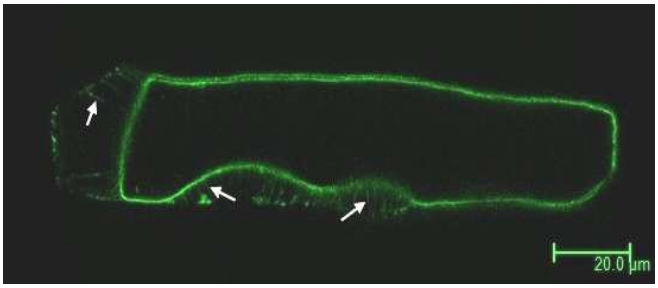

Figure 20: *GFP-HvVTI1*-like partly localizes to the plasma membrane
Glycerol mediated plasmolysis of cells transformed with *GFP-HvVTI1-like* triggers the formation Hechtian strands (indicated by arrows).

To examine a potential effect of *Bgh* challenge on the subcellular localization of the *HvVTI1-like* and *HvYPT1-like GFP*-fusion constructs, barley leaf segments expressing either *GFP-HvVTI1-like* or *GFP-HvYPT1-like* together with *mCherry* were inoculated four hours after bombardment with spores of *Bgh*. The GFP fluorescence signal was analyzed 24 to 48 hours after inoculation by confocal laser-scanning microscopy. Interestingly, the *GFP* signal of both, *GFP-HvVTI1-like* and *GFP-HvYPT1-like*, accumulates around the site of impeded and successful fungal attack (Figure 21; indicated by arrows). Especially in *GFP-HvVTI1-like* expressing cells with impeded fungal penetration, the *GFP*-fluorescence is very bright, indicating an accumulation at non-penetrated papilla (Figure 21A; left column, indicated by arrows). In addition, the small dots, which co-localized partly with the Golgi marker protein *GmMAN:1* (see Figure 19C, right column) were still visible. Concerning *GFP-*

HvYPT1-like, the fluorescence was clearly visible in successfully penetrated cells while in cells with impeded penetration, almost no redistribution of the GFP-tagged protein was observed. In addition, there were only surprisingly few cells successfully defending themselves against *Bgh* when *GFP-HvYPT1-like* is over-expressed. This might hint to a disruption of *HvYPT1-like* function due to the N-terminally fused *GFP*. Analysis of barley epidermal cells transiently transformed with *GFP-HvYPT1-like* concerning an effect on the interaction with *Bgh*, revealed significantly more successfully penetrated cells in comparison to the control (data not shown). This strengthens the result obtained during *HvYPT1-like* RNAi experiments.

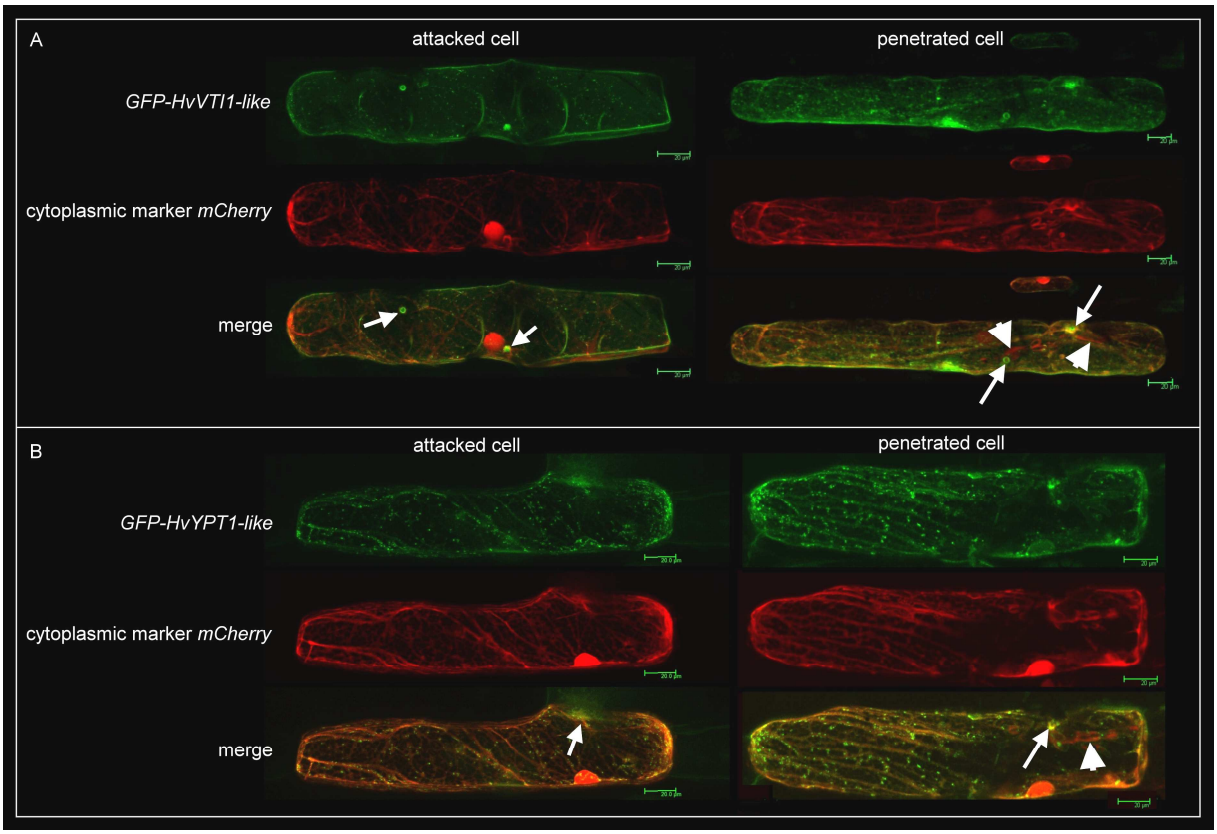

Figure 21: Subcellular localization of *HvVTI1-like* and *HvYPT1-like* after inoculation

Barley epidermal cells (cv. 'Golden Promise') were transiently transformed via particle bombardment with either *GFP-HvVTI1-like* (A, green) or *GFP-HvYPT1-like* (B, green) and *mCherry* (red). The leaf segments were inoculated with *Bgh* four hours after transformation and the *GFP*-fluorescence was examined two dai using confocal laser-scanning microscopy. Yellow/orange colour in the merged pictures indicate co-localization. Arrows indicate the site of fungal attack, arrow heads mark haustoria build by the fungus after successful penetration (right column).

4 Discussion

Membrane trafficking and secretion become a more and more recognized part of plant defence reactions. Many defence-related processes activate the protein secretory machinery or induce other membrane trafficking processes. For example, a pathogenic attack leads to the reorganization of cellular components, enabling the polarized delivery of toxic compounds with harmful effects on the invading pathogen to the site of attempted penetration. In addition, cell surface proteins, important for defence, are transported to the plasma membrane and plasma membrane resident proteins are redistributed, concentrating in defence signalling platforms, all aiming in the restriction of the pathogens colonization success. Many proteins of the well-studied transport and secretory machinery of yeast are conserved in other eukaryote kingdoms, including plants. However, their precise functions in plants are often unknown and their possible involvement in plant-pathogen interactions is an emerging field of research (Hückelhoven and Panstruga, 2011). The present study focused on candidate genes of barley that are presumably participating in membrane trafficking processes. They were functionally analyzed for a possible involvement in the interaction of barley with its powdery mildew fungus *Bgh* via a transient knock down screening. In a second part, candidate genes whose knock down altered the susceptibility of barley to *Bgh* significantly were subject to further investigations. Knock down of one candidate, *HvCOG3*, promoted the colonization of barely leaves by *Bgh* and was of special interest during the second part of this work. In yeast and mammalian cells COG3 is described as a Golgi resident protein, which is involved in the retrograde transport of proteins in between the different Golgi stacks and from the Golgi back to the ER. To gain deeper insights into the role of this gene in barley it was investigated in more detail by different molecular and cell biological methods, starting to elucidate the function of this gene and its potential physiological context in barley.

4.1 Identification of promising candidates using TIGS

To identify candidate genes that affect the outcome of the barley-*Bgh* interaction the TIGS system developed by Douchkov *et al.* (2005) was adapted. TIGS is based on the generation of constructs using the Gateway cloning system and the calculation of the susceptibility index instead of penetration efficiency as used previously (e.g. by

Hückelhoven *et al.,* 2003). This time-optimised procedure enables a transient high throughput screening for genes that function in susceptibility or resistance of barley to *Bgh*. As the *β-glucuronidase* (*GUS*) reporter gene, which is used by Douchkov and colleagues, did not stain transformed barley leaves reliably in our hands, we used *GFP* as reporter in our screening experiments. Over all candidates, about two-thirds induced susceptibility in TIGS experiments. This distribution maybe reflects the overall importance of secretory and membrane trafficking processes for plant defence. However, only three of the 107 tested genes revealed a significant effect. This might be due to the variation of the SI of cells transformed with the empty pIPKTA30N control vector, making it difficult to obtain candidates with significant effects on the barley-*Bgh* interaction.

4.2 Candidate genes, which influence the susceptibility of barley to *Bgh*

4.2.1 A putative exocyst subunit

Transient gene silencing of the candidate HD14N02r significantly enhanced the susceptibility of barley epidermal cells to *Bgh*. Database research supported, that this EST-sequence belongs to a gene, which contains a putative EXO70 domain. EXO70 is one subunit of the exocyst complex, which was originally identified in budding yeast and was shown to consist of eight subunits: SEC3, SEC5, SEC6, SEC8, SEC10, SEC15, EXO70 and EXO84 (TerBush *et al.,* 1996; Kee *et al.,* 1997). The exocyst complex is important for the tethering of secretory vesicles to the plasma membrane and all subunits accumulate at areas of active secretion (Munson and Novick, 2006; Zhang *et al.,* 2010). In yeast mutants with defects in exocyst subunits, secretory vesicles still reach the site of secretion, but accumulate there because fusion with the plasma membrane is inhibited (Munson and Novick, 2006; Zhang *et al.,* 2010). Further on, it is believed, that the exocyst complex defines the sites for polarized secretion. Two subunits, SEC3 and EXO70, act as landmarks for sites of active secretion and the other subunits of the complex are transported to these sites via secretory vesicles (Finger e*t al.,* 1998; Boyd *et al.,* 2004). Thus, the assembly of the exocyst complex itself could tether vesicles, containing a subset of the exocyst subunits, to the plasma membrane, which comprises the other subunits (Munson and Novick, 2006). On the other hand, the exocyst complex subunit SEC6 interacts with

the SNARE protein SEC9 (Sivaram *et al.,* 2005). In addition, SEC1 (an SM-protein) was shown to link the exocyst-mediated vesicle tethering to the final SNARE-mediated fusion process. It was shown to interact with Sec9 and the exocyst (Wiederkehr *et al.,* 2004) and this interaction of the exocyst with the SNARE-based fusion machinery indicates an active contribution to the fusion process (Munson and Novick, 2006). In yeast, final fusion of post-Golgi secretory vesicles involves the interaction between the t-SNAREs Sso1/2 and Sec9 and the v-SNARE Snc1/2 (Brennwald and Rossi, 2007). Figure 22 shows a schematic model of the exocyst function and its involved interaction partners.

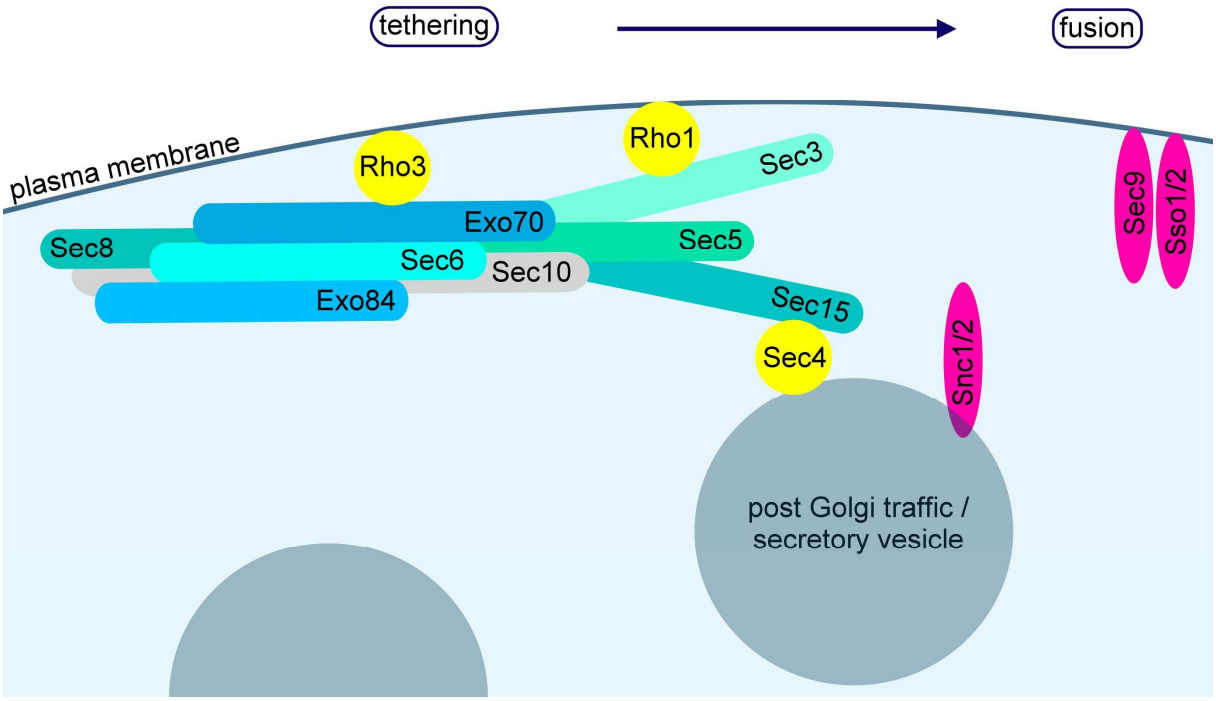

Figure 22: Model of exocyst function in yeast.

The eight subunit containing exocyst complex is responsible for the tethering of post Golgi secretory vesicles to the plasma membrane prior to SNARE protein (pink) mediated fusion of the two membranes. The tethering process involves several small GTPases: Rho1 + 3 and the Rab-GTPase Sec4 (yellow) (combined yeast model information from Brennwald and Rossi, 2007 and Munson and Novick, 2006).

The exocyst complex is conserved between the different eukaryotic kingdoms. All eight subunits of the exocyst have been reported in mammalian cells (Hsu *et al.,* 1996; Kee *et al.,* 1997), *Arabidopsis* (Elias *et al.,* 2003), rice, poplar and moss (Chong *et al.,* 2009). In *Arabidopsis* cells, an exocyst like structure, which tethers vesicles to membranes has been observed during cell plate formation and pollen

development (Otegui and Staehelin, 2004; Segui-Simarro *et al.,* 2004). In yeast and human, each of the eight exocyst-subunits is encoded by a single gene while *Arabidopsis* comprises one SEC6 and one SEC8 gene, two genes for SEC3, SEC5, SEC10, and SEC15, three EXO84 genes and as many as 23 EXO70 encoding genes (Zhang *et al.,* 2010). Synek *et al.* (2006), who identified these 23 EXO70 subunits of *Arabidopsis*, divided them phylogenetically in three main groups, which were further classified into nine clusters (EXO70 A to I). The protein sequence corresponding to the barley *AK362856* gene, which enhanced susceptibility to *Bgh* in the TIGS (Figure 6A) was phylogenetically grouped using ClustalW and TreeView. This analysis revealed that it clusters into the EXO70G group of *Arabidopsis* as shown in Figure 6B. Synek *et al.* (2006) speculate that the *Arabidopsis* group EXO70A, which is most similar to the yeast and human EXO70 subunit, represents those EXO70 proteins, which fullfill a function in exocyst tethering while other EXO70 proteins might act independently of the other exocyst subunits. Another explanation would be that plants have evolved different EXO70 proteins for different purposes of secretion and that each of them creates a unique exocyst complex, specialized for different exocytosis events (Synek *et al.,* 2006). This fits to the idea of the plant exocyst to perform tethering in several types of secretion, since different tethering complexes contribute to site-specific secretion in mammalian cells whereas in plants only the exocyst tethering factor is known (Zhang *et al.,* 2010). Like in mammals, the exocyst complex of plants has been linked to polarized secretion as subunits, including EXO70A1, localize to the growing tips of pollen tubes (Hála *et al.,* 2008), are involved in root hair elongation (Wen *et al.,* 2005) and play a role in plant cytokinesis (Fendrych *et al.,* 2010). Polarized secretion is an important process in plant-pathogen interactions (Hückelhoven, 2007b; Frei dit Frey and Robatzek, 2009) and one may suggest that the exocyst might be involved in tethering of vesicles to the plasma membrane, which deliver components for defence. Although all exocyst subunits are present in plants, there is only limited information available about their individual functions. Especially the role of the highly expanded EXO70 family is still unclear. In 2010, Li *et al.* investigated the expression level of the EXO70 gene family in different *Arabidopsis* tissues and organs. Interestingly, they found a cell-type specific expression of all EXO70 genes, except one, in polarized tissues like root hairs or elongating pollen tubes. Due to the diverse expression patterns of the different EXO70 genes they strengthen the hypothesis of Synek *et al.* (2006) that this diversity

might reflect the function of different EXO70 subunits in different exocytosis events (Li *et al.,* 2010). In addition, they suggest functions of EXO70 genes in cell type specific exocytosis, tip growth and cell differentiation. Interestingly, one of the EXO70G genes of *Arabidopsis* seems to be involved in the formation of xylem elements in vascular bundles, a process that requires cell elongation, secondary cell wall thickening and programmed cell death (Li *et al.,* 2010). Similar processes are known to be also important in plant defence. A possible involvement of the exocyst complex in pathogen defence has been addressed by Pecenková *et al.* in 2011, where they examined the role of the *EXO70B2* and *EXO70H1* genes in the interaction of *Arabidopsis* with *P. syringae* and *Bgh*. Analysis of mutant lines revealed an enhanced susceptibility to *P. syringae* and inoculation of especially *EXO70B2* mutant lines demonstrated altered papilla formation. In these plants extensive vesicle-like halos appeared around the papilla, which indicate that docking of defence-related vesicles is somehow compromised in *Arabidopsis* plants lacking *EXO70B2*. These data indicate a role of the *Arabidopsis* exocyst complex in the defence of bacterial as well as fungal pathogens (Pecenková *et al.,* 2011). The finding that transient knock down of a putative barley *EXO70* gene enhanced the susceptibility of barely to *Bgh* (Figure 6A) fits to this hypothesis of the importance of the exocyst complex in plant defence. The EXO70G group, where the putative barley *EXO70* gene branches to (Figure 6B), was not analyzed by Pecenková et al. (2011), but maybe an exocyst complex containing an EXO70 protein from the G-group is important for the tethering of defence-associated vesicles to the plasma-membrane especially in the compatible interaction of barley with its adapted pathogen *Bgh*. In this work, the putative barley *EXO70* gene was not investigated into more detail due to the lack of a full-length sequence at the end of the screening. However, it would be interesting e.g. to monitor *EXO70* RNAi cells for secretory and especially tethering defects or to examine the extension and possible function of the *EXO70* gene family in barley concerning pathogen defence.

4.2.2 ADP RIBOSYLATION FACTORS

Two ARF-GTPases (HO30E03S (*HvARFA1B/C-like)* and HO02D01S (*HvARFA1D-like*)) enhanced the susceptibility of barley to *Bgh* when they were knocked down during the screening (Figure 7A). ARF-GTPases play an important role in vesicle transport. They are responsible for the formation of COPI and clathrin coated vesicles. An ARF-GEF mediates the conversion into their active GTP bound form,

which leads to membrane association of the ARF-GTPase. At the membrane, they recruit the coat complexes and thus initiate vesicle budding. In addition, ARF-GTPases function in scission of the vesicle, which is driven by the interplay of GEFs and GAPs and they are important for uncoating of COPI vesicles, depending on the GAP-induced GTP hydrolysis (Reinhard *et al.,* 2003; Pucadyil and Schmid, 2009). The *Arabidopsis* genome encodes twelve ARF isoforms and eight ARF-GTPases have been reported for barley (Vernoud *et al.,* 2003; Böhlenius *et al.,* 2010). *In silico* analysis of the protein sequences of the ARF-GTPases used here, revealed that they belong to the HvARFA1 group defined by Böhlenius *et al.* (2010). HvARFA1B/C-like shares 97% homology with HvARFA1B/C while HvARFA1D-like is identical to HvARFA1D (Figure 7C). *Arabidopsis* plants without functional ARF-GTPases show multiple severe defects in plant development because cell production and cell size are decreased (Gebbie *et al.,* 2005). In addition, Gebbie and colleagues (2005) suggested defects in hormone or other signalling pathways, because flowering time, apical dominance and fertility were also affected. Interestingly, altered cell size and expansion have been linked to *Bgh* susceptibility in barley (Pathuri *et al.,* 2008, 2009). There is not much information available about the specific cellular function or localization of the different plant ARF-GTPases but AtARFA1C has been shown to localize to the Golgi compartments and endocytic organelles in both, *Arabidopsis* and onion, and mutant plants exhibit defects in root hair development (Xu and Scheres, 2005). Their distinct localization has been reported to depend on interactions with effectors, but also on specific protein domains and further binding partners e.g. on the Golgi surface (Matheson *et al.,* 2008). The barley HvARFA1B/1C-GTPase has been shown to localize to MVB-like endomembranes (Böhlenius *et al.,* 2010). In the literature, several hints exist for an involvement of ARF-GTPases in host-pathogen interactions. For example, the mammalian bacterial pathogen *Legionella pneumophila*, which induces the formation of special bacteria-containing vacuoles in the host cell, possesses an effector called RalF, which activates host ARF1. This pathogen-induced activation recruits ARF1 to the vacuoles where the bacteria proliferate. If ARF1 is inactivated, the formation of these bacteria containing vacuols is inhibited which indicates the importance of ARF1 for the pathogenesis (Alix *et al.,* 2011). Coemans *et al.* (2008) investigated tobacco ARF1 and showed that the over-expression of ARF1 leads to the induction of cell death. In addition, they found a strongly increased expression of ARF1 after treatment of tobacco plants with non-

host but not after treatment with adapted pathogens. Consistent with the gene expression data, silencing of *ARF1* resulted in a disturbed non-host resistance of tobacco against *Pseudomonas cichorii* (Coemans *et al.,* 2008). In barley, RNAi silencing as well as the expression of a dominant negative *HvARFA1B/1C* construct resulted in increased susceptibility to the adapted powdery mildew fungus *Bgh* (Böhlenius *et al.,* 2010). This importance of HvARFA1B/1C for penetration resistance is genetically linked to penetration resistance mediated by HvROR2. The authors suggest that the accumulation of HvROR2 at or in papilla depends on HvARFA1B/1C containing MVB and that HvARF1B/1C is responsible for callose deposition into papillae while HvROR2 is responsible for the timing of callose deposition (Böhlenius *et al.,* 2010). In gene expression experiments Böhlenius and colleagues (2010) showed, that all tested barley ARF-GTPases except *HvARFA1D* are expressed in the epidermal cell layer, which constitutes the interface of the interaction between barley and *Bgh*. Although the HvARFA1D could not be amplified out of cDNA by Böhlenius *et al*. (2010), the EST clone used here derived form an epidermis EST library (Zhang *et al.,* 2004). In inoculated whole leaf samples, used for semi-quantitative gene expression studies in this work, the expression of *HvARFA1D-like* seemed to be unaffected by *Bgh* challenge, while the *HvARFA1B/C-like* expression was slightly enhanced, especially in resistant ‘Ingrid-*mlo5*’ plants (Figure 9). The upregulation of *HvARFA1B/C-like* was confirmed by publicly available expression data (PLEXdb experiment BB10). Interestingly, the transcript level of *HvARFA1B* was reduced between 8 and 16 hai, but the HvARFA1C expression was unchanged in quantitative PCR experiments (Böhlenius *et al.,* 2010). Concerning *HvARFA1D-like*, which was not analyzed by Böhlenius et al. (2010), the BB10 experiment indicated a slight reduction of gene expression after *Bgh* treatment in some but not all genotypes, which is also not the case in the ‘Ingrid’/’Ingrid-*mlo5*’ inoculation time course experiment in this work. Taken together, the functional analysis and gene expression data of this work together with the work of Böhlenius *et al.* (2010) on HvARFA1B/1C strongly support the hypothesis of ARF1-GTPases playing an important role in plant defence. However, there is a high sequence similarity among the four barley ARFA-GTPases and as the RNAi-constructs used in this work are rather long, each of the two screening ARF-GTPases that significantly alter the susceptibility of barley to *Bgh*, may knock down off-target barley ARFA family members. Depending on the stringency of the amount of contiguous homolog nucleotides defined to be necessary

for effective RNAi, it is likely that the constructs will knock down additional ARF-GTPases outside the ARFA-GTPase group. Therefore, it is not possible yet to relate the screening results to one individual GTPase due to the potential co-silencing of various other ARF-GTPases. The fungal toxin brefeldin A (BFA) inhibits the function of specific, BFA sensitive ARF-GEFs and is used as an inhibitor of vesicle formation, leading to the inhibition of secretion and endocytosis (Robinson *et al.,* 2008). Recently, it was shown for *Vitis vinifera*, that BFA treatment increases susceptibility of a nonadapted powdery mildew fungus while it reduces the penetration efficiency of the adapted powdery mildew. The authors conclude that vesicle trafficking is important for nonhost penetration resistance, maybe by the endocytosis of MAMP receptors or secretion of cell wall material for defence. On the other side, the adapted powdery mildew species might employ the host vesicle trafficking machinery e.g. for the formation of the host derived extrahaustorial membrane or the host dependent internalization of pathogen derived effectors (Feechan *et al.,* 2011).

4.2.3 COG3, the COG complex and potentially associated proteins

The main focus of this work was on HvCOG3 and its surrounding protein environment. In the RNAi screening, knock down of *HvCOG3* (HA14A08r) enhanced the susceptibility of barley epidermal cells to *Bgh* significantly (Figure 10). Due to this knock down effect of *HvCOG3*, I additionally analyzed this gene for a putative over-expression effect. The evaluation of this experiments revealed a significant reduction in the penetration efficiency of *Bgh* into transiently transformed barley cells (Figure 11A). Wuestehube *et al.* (1996) were the first researchers who identified COG3 in yeast. It was called SEC34 at that time due to the observed secretory defects. COG3 was isolated in a screen for yeast mutants that are compromised in the transport from the ER to the Golgi as indicated by the accumulation of secretory proteins that exhibited ER modifications but lacked Golgi modifications. In addition, they showed that the *sec34* yeast mutant cells grow more slowly compared to wild type cells, they have deficiencies in the transport of soluble and integral membrane proteins and accumulate vesicles. In 1999, VanRheenen *et al.* described COG3 as a protein of 93 kD, which is peripherally associated with membranes. COG3 is found throughout the Golgi apparatus but mainly localizes to the cis-Golgi compartment (Kim *et al.,* 2001; Suvorova *et al.,* 2001). During this work, an N-terminal and a C-terminal GFP fusion construct of the barley *COG3* gene was generated but both failed to produce satisfactory fluorescence signals. The C-terminal fusion construct lacked any

detectible fluorescence signal. The N-terminal fusion protein was localized diffusely throughout the transformed barley cells and showed only a very weak co-localization with the Golgi marker protein, maybe due to over-expression side effects or a false processing of the N-terminal GFP fusion construct.

COG3 exists in a large multimeric complex of approximately 750 kD together with COG2 (=SEC35; VanRheenen *et al.,* 1999). Over the years, several research groups independently identified and worked with additional subunits of the COG complex, which led to various names for the different complex components. In 2002, Ungar *et al.* introduced the term COG complex (conserved oligomeric Golgi complex) for this COG3 containing complex, consisting of the subunits COG1 to COG8 as basis for a uniform nomenclature. In Table 8 the different historical names of the yeast and mammalian COG subunits are summarized according to Ungar *et al.* (2002).

Table 8: Historical names of yeast and mammalian COG complex subunits

Current name	Former names
COG1	Cod3p, LdlBp, Sec36p, Tfi1p
COG2	Sec35, LdlCp
COG3	Sec34, GRD20
COG4	Cod1p, Sec38p, Sgf1p, Tfi3p
COG5	Cod4p, GTC-90, Api4p
COG6	Cod2p, Sec37p, Tfi2p
COG7	Cod5p
COG8	Dor1

According to Ungar *et al.* (2002)

The COG complex is conserved between different kingdoms. The whole complex exists in several taxa like yeast and human, the amoeba *Dictyostelium discoideum* as well as in *Phytophthora ramorum* and *Arabidopsis thaliana*. Several other taxa contain at least some subunits of the COG complex (Koumandou *et al.,* 2007). *In silico* analysis done in this work revealed homologous sequences for all COG complex subunits in the rice and barely genomes (Figure 15). The fact, that COG3 exists in a complex in many genera and that all subunits exist in barley makes it difficult to interpret the observed over-expression effect (Figure 11A), as the over-expression of single complex components is not necessarily expected to cause strong effects by its own. One possible explanation for this over-expression effect could be that COG3 is kind of a bottleneck in between the complex and that it is the

limiting factor of complex activity. The domain-predicting program PlantsP (http://plantsp.genomics.purdue.edu/cgi-bin/fscan/feature_scan.cgi) detects a potential Rho GAP domain at the c-terminus of the barley COG3 protein (Figure 11C). Given that there is indeed a functional GAP domain present in HvCOG3, its over-expression could lead to reduced activity of a target GTPase. Interestingly, there is a GTPase interacting with COG3 in yeast, the Rab protein YPT1 (Suvorova *et al.,* 2002). It might be that the amount of available COG3 regulates the efficiency of vesicle tethering to the cis-Golgi membrane. If the target GTPase of COG3 is a negative regulator of vesicle transport, the over-expression of *HvCOG3* might convert this GTPase into its inactive state more frequently, thereby allowing enhanced transport activity. Vice versa, under-expression of *HvCOG3* would leave this GTPase more often in its active state, which would slow down transport activity. As a result, *HvCOG3* over-expression might enhance the transport of important defence compounds while knock down might reduce transport of these molecules. If HvCOG3 is a target of *Bgh*, HvCOG3 could control a GTPase that positively regulates vesicle trafficking. This hypothesis was addressed by the over-expression of only the c-terminal, potential GAP domain containing, part of COG3. However, the result of the transient experiments does not support this hypothesis as no significant effect was observed (Figure 11B). However, the over-expression of the truncated *COG3 c-terminal* part revealed a tendency for a dominant negative effect. Alternatively, the N-terminus might be important for COG3 function. Another hypothesis for the over-expression effect of *HvCOG3* might be, that the amount of available HvCOG3 is monitored by the cell and that the availability of the other COG complex components is adjusted to the level of COG3. As a consequence, COG3 over-expression would enhance the amount of the whole complex and therefore allow alleviated vesicle tethering what in turn might enforce transport while knock out would impede transport. This hypothesis is supported by the observation of Zolov a Lupashin (2005) that a reduction in the amounts of the mammalian COG3 reduces the protein contents of other components of the COG complex. The stable transgenic barley plants, expressing an epidermis specific *HvCOG3* RNAi construct, which have been generated in this project in cooperation with G. Hänsel (IPK, Gatersleben), would be useful to test this hypothesis.

The eight subunits of the COG complex are organized in two globular domains (Ungar *et al.,* 2002). In 2004, Loh and Hong developed a model for the molecular

organization of the mammalian COG complex based on co-immunoprecipitation studies. They proposed two globular loops, the first comprising COG1, 2, 3 and 4 and the second consisting of COG4, 5, 6, 7, and 8, with the COG4 protein connecting the two loops. Later on, two other groups specified the human COG complex architecture in further investigations. They predicted the COG complex to comprise three subcomplexes, one containing COG2, 3 and 4, one containing COG5, 6 and 7 and that these two subdomains are linked by a heterodimer consisting of COG1 and 8 (Ungar *et al.,* 2005; Oka *et al.,* 2005). Thus, the actual structure of the COG complex still needs to be elucidated in more detail. The functional characterization of all the barley COG complex subunits via TIGS also revealed the lack of functional *HvCOG1* to significantly enhance the success of *Bgh* on transiently transformed epidermal cells. The other subunits failed to produce significant effects, but the KD of *HvCOG2*, *4* and *5* also tended to increase susceptibility. According to Lees *et al.* (2010), the COG complex can be divided into an essential subunit loop consisting of COG1, 2, 3 and 4 (Wuestehube *et al.,* 1996; Whyte and Munro 2001; Giaever *et al.,* 2002; Deutschbauer *et al.,* 2005) and a nonessential subunit loop consisting of COG5, 6, 7 and 8 (Whyte and Munro, 2001). It is interesting to note that the subunits with significant RNAi effects, *HvCOG1* and *HvCOG3* are among the essential subunits and *HvCOG2* and *4* also tend towards more susceptibility when knocked down. In addition, the fact that COG3 is an essential gene in yeast and that there is only one homologues gene in barley, might explain the impossibility to generate viable transgenic barley plants with constitutively silenced *HvCOG3* (G. Hensel, IPK Gatersleben, Germany, personal communication). The semi-quantitative gene expression analysis of different COG subunits revealed a clear induction in 'Ingrid-*mlo5*' background, and a slight induction for most of the analyzed subunits in 'Ingrid-WT' plants (Figure 17). These results were generally supported by gene expression data form PLEXdb, where most subunits were clearly induced after pathogen treatment except *HvCOG2*, which is only very weakly expressed and the induction is not as clear for *HvCOG3* and *4*. Taken together, at least some of the HvCOG complex subunits are differentially expressed after powdery mildew treatment, supporting the functional characterization results, which indicate a significant change in susceptibility when *HvCOG1* or *3* are knocked down. The knock down of *HvCOG2* or *HvCOG3* in *mlo5* background did not hamper the *mlo5* mediated penetration resistance. Thus, the *mlo5* resistance seems to be independent form a functional

COG complex although the expression of most COG subunits is increased in these *mlo5* resistant plants.

Ongoing work on the different COG complex components, let to the replacement of the hypothesis of Wuestehube *et al.* (1996), that COG3 functions in ER to Golgi transport, with a role of the COG complex in retrograde intra Golgi and in endosome to Golgi trafficking (e.g. Kim *et al.,* 2001; Whyte and Munro, 2001; Suvorova *et al.,* 2002; Zolov and Lupashin, 2005). This idea is supported by several findings. For example, in COG subunit deficient mammalian cells, key enzymes of the Golgi glycosylation machinery were mislocalized (Shestakova *et al.,* 2006; Pokrovskaya *et al.,* 2011). Indeed, Pokrovskaya *et al.* (2011) showed that some subunits localize to trafficking structures that also carry glycosyl transferases, indicating the importance of the COG complex for the functionality of the Golgi glycosylation machinery. In humans, this glycosylation defects that are caused by mutations in subunits of the COG complex, lead to congenital disorders of glycosylation, a genetic disease with severe effects on the physical and mental development (Smith and Lupashin, 2008). In mammalian cells the amount of some integral Golgi membrane proteins (MANNOSIDASEII, GOS28, GS15, GPP130, CASP, GIANTIN and GOLGIN-84) was reduced when a functional COG1 or COG2 is missing, also indicating that a functional COG complex is important for correct transport and localization Golgi proteins (Oka *et al.,* 2004). Furthermore, the COG complex interacting framework is also associated with retrograde trafficking. Subunits of the COG complex were shown to interact with yeast SNARE proteins that are involved in retrograde transport (including SED5, SEC22, YKT6, GOS1 and VTI1) and with subunits of COPI vesicles but not with COPII vesicle subunits (Suvorova *et al.,* 2001; Suvorova *et al.,* 2002). Finally, Zolov and Lupashin (2005) nicely demonstrated that COG3 deficient HeLa cells are capable for the transport of a GFP-tagged vesicular somatic virus G protein (marker for anterograde transport) to the cell surface while these cells were unable to accumulate the retrograde marker substance Shiga toxin around the nucleus. It is now widely accepted that the COG complex functions in retrograde traffic and plays an important role in Golgi glycosylation, at least in yeast and human cells (Ungar *et al.,* 2006) although there are also reports indicating an additional role in anterograde transport (VanRheenen *et al.,* 1998).

Whyte and Munro (2001) found that several components of the COG complex have homologies with components of well-known tethering factors, namely the exocyst and

the Vps52/53/54 (GARP) complex. Further evidence for an involvement of the complex in vesicle tethering comes from Shestakova *et al.* (2007) who showed that the interaction of the GOG complex with a cis-Golgi t-SNARE complex (including Sed5/Syntaxin5) enhances the stability of this SNARE complex in yeast and mammals. They also showed that the mobility of SNARE molecules is reduced in COG7 knock down cells. Further on, the COG complex interacts with many proteins implicated in the vesicle fusion machinery, supporting a function in tethering. For example, the mammalian COG complex (namely COG4 subunit) interacts with the SM protein Sly1, which plays an important role in SNARE complex regulation. This interaction is required for the formation of the SYNTAXIN5, GS28, YKT6 (t-SNAREs) and GS15 (v-SNARE) containing SNARE complex which acts in intracellular vesicle docking (Shestakova *et al.,* 2007; Laufman *et al.,* 2009).

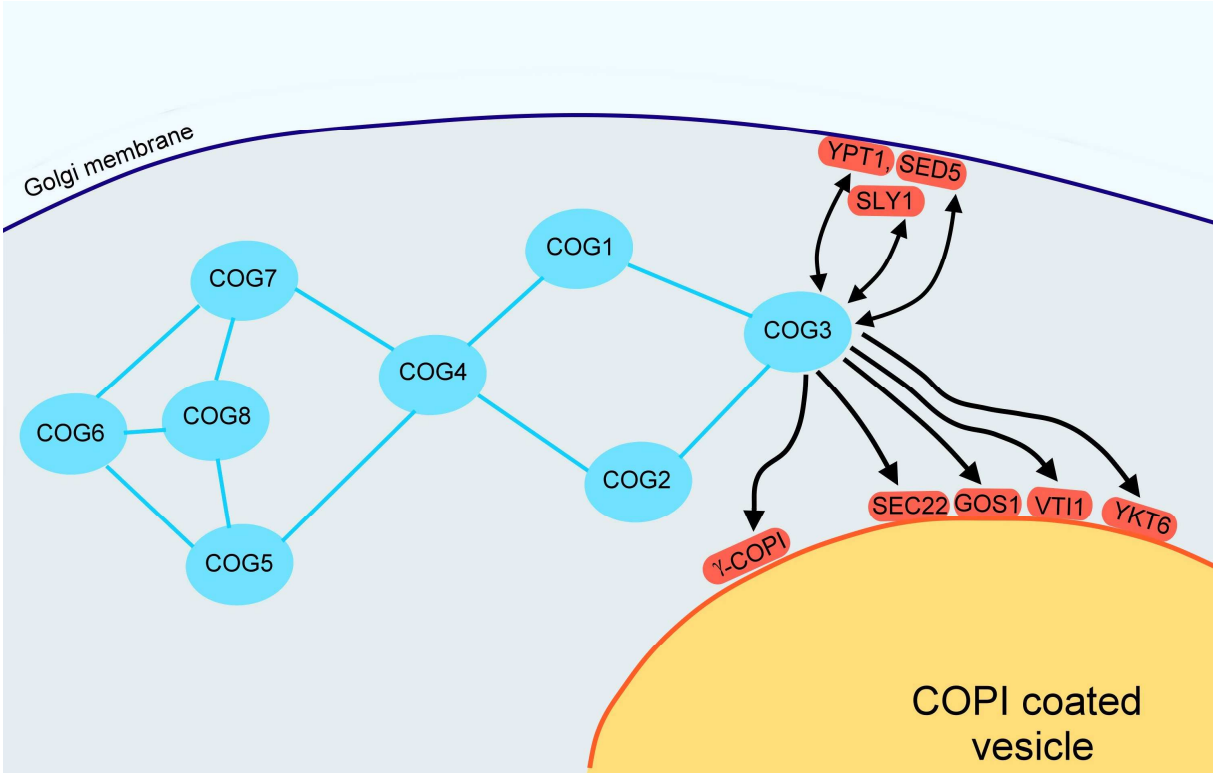

Figure 23: Interaction network of the yeast COG complex

In yeast and mammalian cells, the COG complex (turquoise) interacts with different components of the vesicle trafficking machinery like Rabs, SNAREs, vesicle coats and coil coiled tethering factors. Here, interactions between the COG complex subunit COG3 and its known yeast interaction partners are indicated by arrows.

Beside the above described cellular effects of *HvCOG3* knock down, some potential interaction partners of HvCOG3 have been analyzed during this work for an

involvement in the interaction of barley with *Bgh*. In yeast, COG3 interacts with at least seven proteins from the vesicle trafficking machinery: the Rab-GTPase YPT1, the t-SNARE SED5, the COPI vesicle subunit COPIγ and the v-SNAREs GOS1, YKT6, SEC22 and VTI1 (Suvorova *et al.,* 2002; Table 7). The interactions of COG3 in yeast are summarized in Figure 23. Their most similar barley homologues were functionally characterized via TIGS and over-expression experiments, except of SED5, which could not be isolated. Three of them altered the outcome of the barley *Bgh* interaction significantly. Knock down of *HvCOPIγ-like* enhanced the penetration success of *Bgh* significantly (Figure 18A). COPIγ is one subunit of COPI vesicles which are responsible for the retrograde transport and recycling of proteins in between the Golgi and form the Golgi to the ER (e.g. McMahon and Mills, 2004). Interestingly, D. Douchkov (IPK, Gatersleben), who provided the *HvCOPIγ-like* constructs analyzed here, already found an increase in susceptibility after *HvCOPIγ-like* knock down when they inoculated transiently transformed cells with the non-adapted wheat powdery mildew fungus. The fact that *HvCOG3* and *HvCOPIγ-like* knock down enhances the susceptibility to *Bgh* suggests that the retrograde trafficking machinery is important for a functional plant defence system. Knock down of *HvCOG3* may reduce the tethering efficiency of COPI coated vesicles while knock down of *HvCOPIγ-like* may disturb proper COPI vesicle transport. Thus, both proteins might influence the same transport process, which is important for defence. It would be interesting, to transiently knock down *HvCOPIγ-like* in barley simultaneously with *HvCOG3* to elucidate if they act in the same pathway or if there is an additive effect. An *HvCOPIγ-like–GFP* fusion construct revealed a weak co-localization with the cytoplasmic and nuclear marker protein but was diffusely distributed all over the cell (Figure 19A). As coat components of vesicles are recruited from the cytoplasm to the sites of vesicle formation, the observed *HvCOPIγ-like–GFP* localization might be due to a strong production of the protein after over-expression. Thus, the surplus of the coat subunit could lead to the observed localization. It might be reasonable to use a weaker promoter for the localization experiments to gain the authentic localization. A targeted yeast two-hybrid experiment with *HvCOG3* and *HvCOPIγ–like* revealed no interaction, as the transformed yeast colonies failed to grow on the interaction selective medium. Thus, the barley *HvCOG3* and *HvCOPIγ-like* do not interact at least in the artificial yeast system (data not shown).

The second gene of potential *HvCOG3* interaction partners that influences the barley *Bgh* interaction is the small GTPase *HvYPT1-like*. In yeast cells, YPT1 is a small Rab-GTPase involved in several tethering events. It interacts with the tethering complex TRAPP, which seems to be a GEF for YPT1 (Jones *et al.,* 2000), while the COG complex is an effector (specifically interacting with the GTP bound from) for YPT1, functioning in retrograde transport (Suvorova *et al.,* 2002). In case of the TRAPP complex, YPT1 is important for anterograde ER to Golgi transport, where it aids uncoating of COPII vesicles (Hutagalung and Novick, 2011). In mammals, two additional Rab GTPases (Rab6 and Rab41) have been reported to interact with the COG complex, namely with subunit COG6 (Fukuda *et al.,* 2008). Knock down of the most similar barley homolog of the yeast YPT1 induces the susceptibility of transiently transformed epidermal cells to *Bgh* (Figure 18). In plants there is not much information available concerning *YPT1* homologs. The *Arabidopsis* genome encodes 57 Rab-GTPases, which are divided into eight subgroups, AtRabA to AtRabH (Vernoud *et al.,* 2003). The RAB-D class of Rab-GTPases is most closely related to the yeast YPT1 and human Rab1 proteins. It is further divided into two subclasses, RAB-D1 and RAB-D2. The *Arabidopsis* RAB-D1 class comprises only one gene (*At3g11730*) while the RAB-D2 class is represented by three genes (*RAB-D2A*: *At1g02130*; *RABD2B*: *At5g47200*; and *RABD2C*: *At4g17530*) with potential functional redundancy (Rutherford and Moore, 2002; Pinheiro *et al.,* 2009). Double mutant combinations of all three *RAB-D2* genes are viable; only the triple mutant is lethal (Pinheiro *et al.,* 2009). A *GFP* fusion construct of the barley *YPT1-like*, which induced the susceptibility to *Bgh*, was partly co-localized with the Golgi marker protein GmMAN:1 and in addition found in the cytoplasm of barley epidermal cells (Figure 19B). Fluorescent fusion proteins of the AtRAB-D1 and AtRAB-D2a proteins both localized to Golgi bodies and the TGN in *Arabidopsis* cells (Zheng *et al.,* 2005; Pinheiro *et al.,* 2009). Thus, the localization of the barley GFP-HvYPT1-like protein is in agreement with the localization observed in *Arabidopsis*. Additionally, non co-localizing parts might represent the TGN as well. The additional cytoplasmic localization observed in *GFP-HvYPT1*-like expressing barley cells was also present in *Arabidopsis* and Pinheiro *et al.* (2009) suggested that the cytoplasmic fluorescence is caused by saturated labelling of Golgi bodies/TGN in these cells. Interestingly, in *Bgh* attacked barley epidermal cells expressing the *HvYTP1-like* fusion construct, the GFP fluorescence concentrates around the sites of penetration (Figure 21B). As this

accumulation is not very strong, one cannot be sure whether this accumulation is due to a specific recruitment of HvYPT1-like proteins to the plant-pathogen interface or if it represents general cytoplasmic accumulation around the attack. Both RAB-D classes interfere with trafficking from the ER to the Golgi, as *Arabidopsis* plants expressing a dominant negative mutant form of AtRAB-D1 as well as AtRAB-D2a accumulate secreted GFP and other cargo molecules in an ER-like structure inside the cells (Batoko *et al.,* 2000; Pinheiro *et al.,* 2009). Nevertheless, AtRAB-D1 and AtRAB-D2a seem to influence different interactors, because the wild type protein of AtRAB-D1 was not able to compensate the dnAtRAB-D2a caused defect and vice versa (Pinheiro *et al.,* 2009). This role in anterograde ER to Golgi transport might not be the only function of the AtRAB-D subclass. Given that one of these GTPases interacts with the *Arabidopsis* COG3 like the yeast YPT1 interacts with COG3 (Suvorova *et al.,* 2002), there might be an additional role in retrograde trafficking through a cooperation with the COG complex. Due to the observed RNAi effect of the barley YPT1 homolog, T-DNA insertion lines for the RAB-D class of *Arabidopsis* have been treated with the *Arabidopsis* powdery mildew *Erysiphe cruciferarum* and analyzed for a potential effect on its proliferation. None of the tested T-DNA insertion lines caused significant effects on the fungal development in preliminary experiments but as a functional redundancy of the different AtRAB-D proteins is very likely, a function in the plant powdery-mildew interaction is still possible.

Beside the knock down of *HvCOPIγ-like* and *HvYPT1-like* over-expression of a third potential interaction partner of HvCOG3, *HvVTI1*-like, induced the susceptibility of barley to *Bgh* (Figure 18). VTI1 is a v-SNARE protein that is required for vesicle fusion at different transport steps. In yeast, this SNARE protein functions in the transport from the TGN to the prevacuolar compartment, in transport to the vacuole and in retrograde transport to the cis-Golgi (Fischer von Mollard *et al.,* 1997; Lupashin *et al.,* 1997; Fischer von Mollard and Stevens, 1999). In *Arabidopsis*, VTI1 is represented by a gene family with four members: *AtVTI11*, *AtVTI12* and *AtVTI13* *AtVTI14*. *AtVTI13* was not detectable in RT-PCR experiments and *AtVTI14* only in suspension-cultured cells but *AtVTI11* and *AtVTI12* are highly expressed throughout the plant (Surpin *et al.,* 2003; Uemura *et al.,* 2004). Zheng *et al.* (1999) suggested a role for the AtVTI11 v-SNARE protein in vesicle transport form the TGN to the prevacuolar compartment. They reported AtVTI11 to localize to the TGN and the PVC. A comprehensive localization study on *Arabidopsis* SNARE proteins using

transient expression of fluorescent fusion proteins revealed AtVTI11, AtVTI12 and AtVTI13 to localize mainly to the TGN. Additionally, AtVTI11 and AtVTI13 are also found in the PVC while AtVIT12 is localized to the plasma membrane. This suggests a function of AtVTI11 and AtVTI13 in anterograde transport from the TGN to the PVC/vacuole and for AtVTI12 an involvement in retrograde transport from the PVC to the TGN but also in transport to the plasma membrane (Uemura *et al.,* 2004). Localization experiments of the putative barley VTI1-like GFP-fusion protein revealed punctuate structures that partly co-localized with the Golgi marker protein GmMAN:1 and additionally labelled the plasma membrane (Figure 19C). It might be speculated, that the structures not co-localizing with GmMAN:1 may represent PVC and that the observed plasma membrane localization might partly reflect over-expression effects, because over-expressed SNARE proteins often localize to the plasma membrane. Alternatively, the tested barley *HvVTI1-like* GFP fusion construct is similar to AtVTI12 (Uemura *et al.,* 2004). Inoculated barley cells expressing the *GFP-HvVTI1-like* construct accumulated the fusion protein at the attempted fungal penetration site in or around papillae (Figure 21). This fungus-induced re-localization of HvVTI1-like is an additional interesting hint for an involvement of this protein in the barley-*Bgh* interaction. It might be that HvVTI1-like is involved in the transport of molecules necessary for fungal success from the Golgi to the plasma membrane or that it might interfere with penetration defence when over-expressed. This might explain the enhanced penetration success of the fungus in cells over-expressing *HvVTI1-like*.

5 Summary

The plant-pathogen interface is a highly dynamic area where many membrane transport and trafficking processes take place that influence the outcome of the interaction between the plant and the pathogen. In the first part of this work, a transient induced gene silencing (TIGS) approach was used to screen 107 barley ESTs for a potential involvement in the interaction of barley with its adapted powdery mildew fungus *Blumeria graminis* f.sp. *hordei* (*Bgh*). The ESTs were predominantly selected due to their annotation, which indicated an involvement in protein transport and secretory processes. The screening revealed three barley genes, which enhanced the penetration success of *Bgh* into barley epidermal cells significantly when they were knocked down: *AK369764* (*HvARFA1B/C-like*), *AK362856 (*putative *EXO70-like)* and *AK249208* (*HvCOG3*). The second part of this work was focused on a more detailed investigation of *HvCOG3,* starting to elucidate its function in barley. In yeast and mammals COG3 is described as part of a Golgi resident eight subunit-containing tethering complex that is responsible for retrograde trafficking/recycling in-between the Golgi complex and from the Golgi back to the ER. In contrast to the enhanced susceptibility during the knock down screening, over-expression of *HvCOG3* rendered barley epidermal cells more resistant. In addition, HvCOG3 might be important for secretion and involved in the stability of Golgi bodies as indicated by secretory pathway analysis of HvCOG3 deficient barely cells, a result that fits well to known effects of COG deficient yeast/mammalian cells. Beside *HvCOG3* itself, *HvCOG1*, which is a predicted component of the same tethering complex as COG3, significantly enhanced the susceptibility of barley to *Bgh*. Beside the barley COG complex components, the putative protein environment of HvCOG3 was analyzed based on information from the yeast COG3 interactome. Like knock down of *HvCOG1* and *HvCOG3, HvCOPIγ-like*, a subunit of COPI vesicles involved in retrograde trafficking and *HvYPT1-like*, a Rab GTPase involved in several tethering events enhanced the susceptibility of barley to *Bgh* when knocked down. The same is true for over-expressing *HvVTI1-like*, a v-SNARE protein potentially interacting with *HvCOG3*. In addition, *HvVTI1-like* seemed to accumulate around the site of fungal attack in cells expressing a *GFP-HvVTI1-like* fusion construct. Taken together, the results obtained during this work strongly indicate the importance of a functional secretory system, including early retrograde transport, for effective defence in barley.

6 Zusammenfassung

Die Berührungsstelle zwischen Pflanze und Pathogen ist ein extrem dynamischer Bereich in welchem eine Vielzahl von Transport- und Sekretionsprozessen stattfinden. Im ersten Teil der vorliegenden Arbeit wurden durch transient induziertes Gensilencing (TIGS) 107 EST Sequenzen aus Gerste auf einen potentiellen Effekt auf die Interaktion zwischen Gerste und dem adaptierten Mehltaupilz *Blumeria graminis* f.sp. *hordei* (*Bgh*) hin untersucht. Die analysierten EST Sequenzen wurden überwiegend aufgrund ihrer Annotation im Bereich Membrantransport und Sekretion ausgewählt. Das Ausschalten dreier Gerstengene führte während der TIGS Untersuchung zu einer signifikanten Erhöhung der Anfälligkeit von Gerstenepidermiszellen gegenüber *Bgh*: *AK369764* (*HvARFA1B/C-like*), *AK362856 (*putative *EXO70-like)* und *AK249208* (*HvCOG3*). Im zweiten Teil dieser Arbeit wurde HvCOG3, welches in Hefe und tierischen Zellen beschrieben wird, als ein im Golgiapparat angesiedeltes Protein, das Teil eines acht Untereinheiten umfassenden Tetheringkomplexes ist, auf seine Funktion in Gerste näher untersucht. In Hefe und im tierischen System ist der COG Komplex am retrograden Transport bzw. am Recycling von Proteinen im Golgiapparat beteiligt und am Transport vom Golgi zum ER. Während das Ausschalten von *HvCOG3* während des Screenings zu einer erhöhten Anfälligkeit der Gerste gegenüber Mehltau führte, verlieh die Überexpression von HvCOG3 den Gerstenzellen eine erhöhte Resistenz. Außerdem führte auch das Ausschalten einer weiteren COG Komplexuntereinheit, *HvCOG1*, wie bereits *HvCOG3* selbst, zu einer signifikanten Erhöhung der Anfälligkeit. Neben den acht verschiedenen COG Komplexuntereinheiten wurden potentielle Interaktionspartner von HvCOG3, die auf Basis von Informationen über Hefe COG3 identifiziert worden waren, bezüglich ihres Einflusses auf die Gerste-*Bgh* Interaktion analysiert. Hier führte das Ausschalten von *HvCOPIγ-like*, welches ein Baustein der Hülle von COPI Vesikeln ist, die in retrograde Transportprozesse involviert sind, und das Ausschalten von *HvYPT1-like*, einer kleinen GTPase die an verschiedenen Tetheringvorgängen beteiligt ist, zu einer erhöhten Anfälligkeit von Gerste gegenüber Mehltau. Außerdem erhöhte die Überexpression von *HvVTI1-like*, eines v-SNAREs, die Penetrationsrate. Die Expression eines *GFP-HvVTI1-like* Fusionskonstrukts in inokulieren Gerstenzellen führt zu einer Akkumulation des Fusionsproteins um die Interaktionsstelle. Zusammengenommen lassen die hier erhaltenen Ergebnisse auf die Wichtigkeit eines funktionierenden Sekretionssystems, einschließlich des retrograden Transportes, für eine effektive Penetrationsabwehr in Gerste schließen.

7 References

Aguilera-Romero, A., Kaminska, J., Spang, A., Riezmann, H. and Muniz, M. (2008): The yeast p24 complex is required for the formation of COPI retrograde transport vesicles from the Golgi apparatus. *Journal of Cell Biology 180(4): 713-720*

Aist, J.R. (1976): Papillae and related wound plugs of plant cells. *Annual Reviews Phytopathology 14: 145-163*

Alfano, J.R. (2009): Roadmap for future research on plant pathogen effectors. *Molecular Plant Pathology 10(6): 805-813*

Alix, E., Mukherjee, S. and Roy, C.R. (2011): Host-pathogen interactions: Subversion of membrane transport pathways by vacuolar pathogens. *Journal of Cell Biology 195(6): 943-952*

Alvarez, M.E. (2000): Salicylic acid in the machinery of hypersensitive cell death and disease resistance. *Plant Molecular Biology 44: 429-442*

An, Q., Ehlers, K., Kogel, K.H., van Bel, A.J. and Hückelhoven, R. (2006a): Multivesicular compartments proliferate in susceptible and resistant MLA12-barley leaves in response to infection by the biotrophic powdery mildew fungus. *New Phytologist 172(3): 563-576*

An, Q., Hückelhoven, R., Kogel, K.-H. and van Bel, A.J.E. (2006): Multivesicular bodies participate in a cell wall-associated defence response in barley leaves attacked by the pathogenic powdery mildew. *Cellular Microbiology 8(6): 1009-1019*

Angers, C.G. and Merz, A.J. (2011): New links between vesicle coats and Rab-mediated vesicle targeting. *Seminars Cell and Developmental Biology 22: 18-26*

Angot, A., Peeters, N., Lechner, E., Vailleau, F., Baud, C., Gentzbittel, L., Sartorel, E., Genschik, P., Boucher, C. and Genin, S. (2006): *Ralstonia solanacearum* requires F-box-like domain-containing type III effectors to promote disease on several host plants. *PNAS 103(39): 14620-14625*

Apel, K. and Hirt, H. (2004): Reactive oxygen species: Metabolism, oxidative stress, and signal transduction. *Annual Reviews Plant Biology 55: 373-399*

Asai, T., Tena, G., Plotnikova, J., Willmann, M.R., Chiu, W.-L., Gomez-Gomez, L., Boller, T., Ausubel, F.M. and Sheen, J. (2002): MAP kinase signalling cascade in *Arabidopsis* innate immunity. *Nature 415: 977-983*

Assad, F.F., Qiu, J.L., Youngs, H., Ehrhardt, D., Zimmerli, L., Kalde, M., Wanner, G., Peck, S.C., Edwards, H., Ramonell, K., Somerville, C.R. and Thordal-Christensen, H. (2004): The PEN1 syntaxin defines a novel cellular

compartment upon fungal attack and is required for the timely assembly of papilla. *Molecular Biology of the Cell 15(11): 5118-5129*

Bassham, D.C., Brandizzi, F., Otegui, M.S. and Sanderfoot, A.A. (2008): The Secretory System of *Arabidopsis*. *ASPB, The Arabidopsis Book 6*

Batoko, H., Zheng, H.Q., Hawes, C. and Moore, I. (2000): A rab1 GTPase is required for transport between the endoplasmic reticulum and Golgi apparatus and for normal Golgi movement in plants. *Plant Cell 12(11): 2201-2218*

Bednarek, P., Kwon, C. and Schulze-Lefert, P. (2010): Not a peripheral issue secretion in plant-microbe interactions. *Current Opinion in Plant Biology 13(4): 378-387*

Bednarek, P., Pislewska-Bednarek, M., Svatos, A., Schneider, B., Doubsky, J., Mansurova, M., Humphry, M., Consonni, C., Panstruga, R., Sanchez-Vallet, A., Molina, A. and Schulze-Lefert, P. (2009): A glucosinolate metabolism pathway in living plant cells mediates broad-spectrum antifungal defence. *Science 323: 101-106*

Bélanger, R.R., Bushnell, W.R., Dik, A.J. and Carver, T.L.W. (2002): The powdery mildews: A comprehensive Treatise. St. Paul, MN: Am. Phytopathol. Soc.

Bent, A.F. and Mackey, D. (2007): Elicitors, effectors, and R genes: The new paradigm and a lifetime supply of questions. *Reviews Phytopathology 45: 399-436*

Bhat, R.A., Miklis, M., Schmelzer, E., Schulze-Lefert, P. and Panstruga, R. (2005): Recruitment and interaction dynamics of plant penetration resistance components in a plasma membrane microdomain. *PNAS 102(8): 3135-3140*

Bischof, M., Eichmann, R. and Hückelhoven, R. (2011): Pathogenesis-associated transcriptional patterns in Triticeae. *Journal of Plant Physiology 168(1): 9-19*

Bittel, P. and Robatzek, S. (2007): Microbe-associated molecular patterns (MAMPs) probe plant immunity. *Current Opinion in Plant Biology 10(4): 335-341*

Block, A., Li, G., Qing Fu, Z. and Alfano, J.R. (2008): Phytopathogen type III effector weaponry and their plant targets. *Current Opinion in Plant Biology 11(4): 396-403*

Bogdanove, A.J. and Martin, G.B. (2000): AvrPto-dependent Pto-interacting proteins and AvrPto interacting protein in tomato. *PNAS 97(16): 8836- 88340*

Böhlenius, H., Morch, S.M., Godfrey, D., Nielsen, M.D. and Thordal-Christensen, H. (2010): The MVB-localized GTPase ARFA1b-1c is important for callose deposition and ROR2 syntaxin-dependent preinvasive basal defense in barley. *Plant Cell 22(11): 3831-3844*

Bonifacino, J.S. and Glick, B.S. (2004): The Mechanisms of Vesicle budding and fusion. *Cell 116(2): 153-166*

References

Boyd, C., Hughes, T., Pypaert, M. and Novick, P. (2004): Vesicles carry most exocyst subunits to exocytic sites marked by the remaining two subunits, Sec3p and Exo70p. *Journal of Cell Biology 167(5): 889–901*

Brennwald, P. and Rossi, G. (2007): Spatial regulation of exocytosis and cell polarity: yeast as a model for animal cells. *FEBS Letters 581(11): 2119-2124*

Bröcker, C., Engelbrecht-Vandré, S. and Ungermann C. (2010): Multisubunit tethering complexes and their role in membrane fusion. *Current Biology 20(21): 943-952*

Buchanan, B., Gruissem, W. and Jones, R. (2002): Protein Sorting and Vesicle Traffic. Biochemistry & Molecular Biology of Plants, pp 160-201 American Society of Plant Physiologists, Rockville, MD

Büttner, D. and Yang He, S. (2007): Type III protein secretion in plant pathogenic bacteria. *Plant Physiology 150(4): 1656-1664*

Cai, H., Reinisch, K. and Ferro-Novick, S. (2007): Coats, tethers, Rabs, and SNAREs work together to mediate the intracellular destination of a transport vesicle. *Developmental Cell 12(5): 671-682*

Carver, T.L.W. and Bushnell, W.R. (1983): The probable role of primary germ tubes in water uptake before infection by *Erysiphe graminis*. *Physiological Plant Pathology 23: 229-240*

Carver, T.L.W. and Ingerson, S.M. (1987): Responses of *Erysiphe graminis* germlings to contact with artificial and host surfaces. *Physiological and Molecular Plant Pathology 30: 359-372*

Chinchilla, D., Zipfel, C., Robatzek, S., Kemmerling, B., Nürnberger, T., Jones, J.D., Felix, G. and Boller, T. (2007): A flagellin-induced complex of the receptor FLS2 and BAK1 initiates plant defence. Nature 448: 497-500

Chisholm, S.T., Coaker, G., Day, B. and Staskawicz, B.J. (2006): Host-microbe interactions: Shaping the evolution of the plant immune response. *Cell 124(4): 803-814*

Chong, Y.T., Gidda, S.K., Sanford, C., Parkinson, J., Mullen, R.T. and Goring, D.R. (2009): Characterization of the *Arabidopsis thaliana* exocyst complex gene families by phylogenetic, expression profiling, and subcellular localization studies. *New Phytologist 185(2): 401-419*

Clay, N.K., Adio, A.M., Denoux, C., Jander, G. and Ausubel, F.M. (2009): Glucosinolate metabolites required for an *Arabidopsis* innate immune response. *Science 323: 95-101*

Coemans, B., Takahashi, Y., Berberich, T., Ito, A., Kanzaki, H., Matsumura, H., Saitoh, H., Tsuda, S., Kamoun, S., Sági, L., Swennen, R. and Terauchi, R. (2008): High-throughput in planta expression screening identifies an ADP-ribosylation factor (ARF1) involved in non-host resistance and R gene-mediated resistance. *Molecular Plant Pathology 9(1): 25-36*

Collins, N.C., Thordal-Christensen, H., Lipka, V., Bau, S., Kombrink, E., Qiu, J.-L., Hückelhoven, R., Stein, M., Freialdenhoven, A., Somerville, S. and Schulze-Lefert, P. (2003): SNARE-protein-mediated disease resistance at the plant cell wall. *Nature 425(6961): 973-977*

Cottam, N.P. and Ungar, D. (2011): Retrograde vesicle transport in the Golgi. *Protoplasma DOI: 10.1007/s00709-011-0361-7*

Dacks, J.B., Poon, P.P. and Field, M.C. (2008): Phylogeny of endocytic components yields insight into the process of nonendosymbiotic organelle evolution. *PNAS 105(2): 588-593*

Dangl, J.L. and Jones, J.D.G. (2001): Plant pathogens and integrated defence responses to infection. *Nature 411(6839): 826-833*

Danna, C.H., Millet, Y.A., Koller, T., Han, S.-W., Bent, A.F., Roland, T.C. and Ausubel, F.M. (2011): The *Arabidopsis* flagellin receptor FLS2 mediates the perception of *Xanthomonas* Ax21 secreted peptides. *PNAS 108(22): 9286-9291*

Day, B., Dahlbeck, D., Huang, J., Chisholm, S.T., Li, D. and Staskawicz, B.J. (2005): Molecular basis for the RIN4 negative regulation of RPS2 disease resistance. *The Plant Cell 17(4): 1292-1305*

de Wit, P.J.G.M. (2007): How plants recognize pathogens and defend themselves. *Cellular and Molecular Life Sciences 64(21): 2726-2732*

Deutschbauer, A.M., Jaramillo, D.F., Proctor, M., Kumm, J., Hillenmeyer, M.E., Davis, R.W., Nislow, C. and Giaever, G. (2005): Mechanisms of haploinsufficiency revealed by genome-wide profiling in yeast. *Genetics 169(4): 1915–1925*
DOI: 10.1007/s00709-011-0361-7

Donohoe, B.S., Kang, B.-H. and Staehelin, L.A. (2007): Identification and characterization of COPIa- and COPIb-type vesicle classes associated with plant and algal Golgi. *PNAS 104(1): 163-168*

Dou, D., Kale, S.D., Wang, X., Jiang, R.H.Y., Bruce, N.A., Arredondo, F.D., Zhang, X. and Tyler, B.M. (2008): RXLR-mediated entry of *Phytophthora sojae* effector Avr1b into soybean cells does not require pathogen-encoded machinery. *The Plant Cell 20(7): 1930-1947*

References

Douchkov, D., Nowara, D., Zierold, U. and Schweizer, P. (2005): A high-throughput gene-silencing system for the functional assessment of defense-related genes in barley epidermal cells. *Molecular Plant-Microbe Interactions 18(8): 755-761*

Eichmann, R. (2005): Molecular analyses on the mechanism of nonhost resistance of barley (*Hordeum vulgare L.*) to the wheat powdery mildew fungus (*Blumeria graminis f.sp. tritici*). Dissertation, Justus-Liebig-Universität Giessen, Faculty of Agricultural and Nutritional Sciences, Home Economics and Environmental Management

Eichmann, R. and Hückelhoven, R. (2008): Accommodation of powdery mildew fungi in intact plant cells. *Journal of Plant Physiology 165(1): 5-18*

Eichmann, R., Bischof, M., Weis, C., Shaw, J., Lacomme, C., Schweizer, P., Duchkov, D., Hensel, G., Kumlehn, J. and Hückelhoven R. (2010): BAX INHIBITOR-1 is required for full susceptibility of barley to powdery mildew. *Molecular Plant-Microbe Interactions* 23: 1217-1127.

Elias, M., Drdoba, E., Ziak, D., Bavlnka, B., Hala, M., Cvrckova, F., Soukupova, H. and Zarsky, V. (2003): The exocyst complex in plants. *Cell Biology International 27(3): 199-201*

Fasshauer, D., Sutton, R.B., Brunger, A.T. and Jahn, R. (1998): Conserved structural features of the synaptic fusion complex SNARE proteins reclassified as Q- and R-SNAREs. *PNAS 95(26): 15781-15786*

Feechan, A., Kabbara, S. and Dry, I.B. (2011): Mechanisms of powdery mildew resistance in the Vitaceae family. *Molecular Plant Pathology 12(3): 263-274*

Felix, G., Duran, J.D., Volko, S. and Boller, T. (1999): Plants have a sensitive perception system for the most conserved domain of bacterial flagellin. *The Plant Journal 18 (3): 265-376*

Fendrych, M., Synek, L., Pecenková, T., Toupalová, H., Cole, R., Drdová, E., Nebesárová, J., Sedinová, M., Hála, M., Fowler, J.E. and Zársky, V. (2010): The *Arabidopsis* exocyst complex is involved in cytokinesis and cell plate maturation. *Plant Cell 22(9): 3053-3065*

Field, B., Jordán, F. and Osbourn, A. (2006): First encounters - deployment of defence-related natural products by plants. *New Phytologist 172(2): 193-207*

Finger, F.P., Hughes, T.E. and Novick, P. (1998): Sec3p is a spatial landmark for polarized secretion in budding yeast. *Cell 92(4): 559–571*

Fischer von Mollard, G. and Stevens, T.H. (1999): The Saccharomyces cerevisiae v-SNARE Vti1p is required for multiple membrane transport pathways to the vacuole. *Molecular Biology of the Cell 10(6): 1719-1732*

Fischer von Mollard, G., Nothwehr, S.F. and Stevens, T.H. (1997): The yeast v-SNARE Vti1p mediates two vesicle transport pathways through interactions with the t-SNAREs Sed5p and Pep12p. *Journal of Cell Biology 137(7): 1511-1524*

Flor, H.H. (1942): Inheritance of pathogenicity in *Melampsora lini*. *Phytopath*ology *32: 653–669.*

Francis, S.A., Dewey, F.M. and Gurr, S.J. (1996): The role of cutinase in germling development and infection by *Erysiphe graminis* f.sp. *hordei*. *Physiological and Moledular Plant Pathology 49(3): 201-211*

Frei dit Frey, N. and Robatzek, S. (2009): Trafficking vesicles pro or contra pathogens. *Current Opinion in Plant Biology 12(4): 437-443*

Freialdenhoven, A., Peterhänsel, C., Kurth, J., Kreuzaler, F. and Schulze-Lefert, P. (1996): Identification of genes required for the function of non-race-specific mlo resistance to powdery mildew in barley. *The Plant Cell 8(1): 5-14*

Fukuda, M., Kanno, E., Ishibashi, K. and Itoh, T. (2008): Large scale screening for novel rab effectors reveals unexpected broad Rab binding specificity. *Molecular Cell Proteomics 7(6): 1031-1042*

Gebbie, L.K., Burn, J.E., Hocart, C.H. and Williamson, R.E. (2005): Genes encoding ADP-ribosylation factors in *Arabidopsis thaliana* L. Heyn.; genome analysis and antisense suppression. *Journal of Experimental* Botany 56(414): 1079-1091

Geldner, N., Anders, N., Wolters, H., Keicher, J., Kornberger, W., Muller, P., Delbarre, A., Ueda, T., Nakano, A. and Jürgens, G. (2003): The *Arabidopsis* GNOM ARF-GEF mediates endosomal recycling, auxin transport, and auxin-dependent plant growth. *Cell 112(2): 219-230*

Giaever, G. et al. (2002): Functional profiling of the *Saccharomyces cerevisiae* genome. *Nature 418: 387–391*

Gil, F. and Gay, J.L. (1977): Ultrastructural and physiological properties of the host interfacial components of haustoria of *Erysiphe pisi* in vivo and in vitro. *Physiological Plant Pathology 10: 1-12*

Goel, A.K., Lundberg, D., Torres, M.A., Matthews, R., Akimoto-Tomiyama, C., Farmer, L., Dangl, J.L. and Grant, S.R. (2008): The *Pseudomonas syringae* type III effector HopAM1 enhances virulence on water-stressed plants. *Molecular Plant-Microbe Interactions 21(3): 361-370*

Göhre, V. and Robatzek, S. (2008): Breaking the barriers: microbial effector molecules subvert plant immunity. *Annual Reviews Phytopathology 46: 189-215*

Goméz-Goméz, L. and Boller, T. (2000): FLS2: An LRR receptor-like kinase involved in the perception of the bacterial elicitor flagellin in *Arabidopsis. Molecular Cell 5: 1003-1011*

References

Grant, S.R., Fischer, E.J., Chang, J.H., Mole, B.M. and Dangl, J.L. (2006): Subterfuge and manipulation: Type III effector proteins of phytopathogenic bacteria. *Annual Reviews Microbiology 60: 425-449*

Gross, A., Kapp, D., Nielsen, T. and Niehaus, K. (2005): Endocytosis of *Xanthomonas campestris* pathovar *campestris* lipopolysaccharides in non-host plant cells of *Nicotiana tabacum*. *New Phytologist 165(1): 215-226*

Guermonprez, H., Smertenko, A., Drosnier, M.T., Durandet, M., Vrielynck, N., Guerche, P., Hussey, P. J., Satiat-Jeunemaitre, B. and Bonhomme, S. (2008): The POK AtVPS52 protein localizes to several distinct post-Golgi compartments in sporophytic and gametophytic cells. *Journal of Experimental Botany 59(11): 3087-3098*

Gutierrez, J.R., Bahmuth, A.L., Ntoukakis, V., Mucyn, T.S., Gimernez-Ibanez, S., Jones, A.M.E. and Tathjen, J.P. (2010): Prf immune complexes of tomato are oligomeric and contain multiple Pto-like kinases that diversify effector recognition. *The Plant Journal 61(3): 507-518*

Hála, M., Cole, R., Synek, L., Drdová, E., Pecenková, T., Nordheim, A., Lamkemeyer, T., Madlung, J., Hochholdinger, F., Fowler, J.E. and Zárský, V. (2008): An exocyst complex functions in plant cell growth in *Arabidopsis* and tobacco. *Plant Cell 20(5): 1330-1345*

Hammer, J.A. and Wu, X.S. (2002): Rabs grab motors: defining the connections between Rab GTPases and motor proteins. *Current Opinion in Cell Biology 14(1): 69-75*

Hanton, S.L., Matheson, L.A. and Brandizzi, F. (2006): Seeking a way out: export of proteins from the plant endoplasmic reticulum. *TRENDS in Plant Science 11(7): 335-343*

Hawes, C., Osterrieder, A., Hummel, E. and Sparkes, I. (2008): The plant ER-Golgi interface. *Traffic 9(10): 1571-1580*

He, P., Shan, L. and Sheen, J. (2007): Elicitation and suppression of microbe-associated molecular pattern-triggered immunity in plant-microbe interactions. *Cellular Microbiology 9(6):1385-1396*

Heath, M.C. (2000): Hypersensitive response-related death. *Plant Molecular Biology 44(3): 321-334*

Heese, A., Hann, D.R., Gimenez-Ibanez, S., Jones, A.M.E., He, K., Schroeder, J.I., Peck, S.C. and Rathjen, J.P. (2007): The receptor-like kinase SERK3/BAK1 is a central regulator of innate immunity in plants. *PNAS 14(29): 12217-12222*

Himmelbach, A., Zierold, U., Hensel, G., Riechen, R., Douchkov, D., Schweizer, P. and Kumlehn, J. (2007): A set of molecular binary vectors for transformation of cereals. *Plant Physiology 145(4): 1192-1200*

Hsu, S.C., Ting, A.E., Hazuka, C.D., Davanger, S., Kenny, J.W., Kee, Y. and Scheller, R.H. (1996): The mammalian brain rSec6/8 complex. *Neuron 17(6): 1209–1219*

Hückelhoven, R. (2007a): Cell Wall-Associated mechanisms of disease resistance and susceptibility. *Annual Reviews Phytopathology 45: 101-127*

Hückelhoven, R. (2007b): Transport and secretion in plant-microbe interactions. *Current Opinion in Plant Biology 10(6): 573-579*

Hückelhoven, R. and Panstruga, R. (2011): Cell biology of the plant-powdery mildew interaction. *Current Opinion in Plant Biology 14(6): 738-746*

Hückelhoven, R., Dechert, C. and Kogel, K.H. (2003): Over-expression of barley BAX inhibitor 1 induces breakdown of mlo-mediated penetration resistance to *Blumeria graminis*. *PNAS 100(9): 5555-5560*

Hückelhoven, R., Fodor, J., Preis, C. and Kogel, K.-H. (1999): HR and papilla formation in barley attacked by PM are associated with Hydrogen peroxide but not with SA accumulation. *Plant Physiology 119(4): 1251-1260*

Hutagalung, A.H. and Novick, P. J. (2011): Role of Rab GTPases in membrane traffic and cell physiology. *Physiological Reviews 91(1): 119-149*

Hwang, I. and Robinson, D.G. (2009): Transport vesicle formation in plant cells. *Current Opinion in Plant Biology 12(6): 660-669*

Ihlow, A., Schweizer, P. and Seiffert, U. (2008): A high-througput screening system for barley/powdery mildew interactions based on automated analysis of light micrographs. *BMC Plant Biology 8(6) doi:10.1186/1471-2229-8-6*

Ingle, R.A., Carstens, M. and Denby, K.J. (2006): PAMP recognition and the plant-pathogen arms race. *BioEssays 28(9): 880-889*

Inuma, T., Khodaparast, S.A. and Takamatsu, S. (2007): Multilocus phylogenetic analysis within *Blumeria graminis*, a powdery mildew fungus of cereals. *Molecular Phylogenetics and Evolution 44(2): 741-751*

Ishikawa, T., Machida, C., Yoshioka, Y., Ueda, T., Nakano, A. and Machida, Y. (2008): EMBRYO YELLOW gene, encoding a subunit of the conserved oligomeric Golgi complex, is required for appropriate cell expansion and meristem organization in *Arabidopsis thaliana*. *Genes to Cells 13(6): 521-535*

Jahn, R. and Scheller, R.H. (2006): SNAREs — engines for membrane fusion. *Nature Reviews Molecular Cell Biology 7(9): 631-643*

References

Jia, Y., McAdams, S.A., Bryan, G.T., Hershey, H.P. and Valent, B. (2000): Direct interaction of resistance gene and avirulence gene products confers rice blast resistance. *EMBO 19(15): 4004-4014*

Jones, J.D.G. and Dangl, J.L. (2006): The plant immune system. *Nature 444(7117): 323-329*

Jones, S., Newman, C., Liu, F. and Segev, N. (2000): The TRAPP complex is a nucleotide exchanger for Ypt1 and Ypt31/32. *Molecular Biology of the Cell 11(12): 4403-4411*

Kaku, H., Nshizawa, Y., Ishii-Minami, N., Akimoto-Tomiyama, C., Dohmae, N., Takio, K., Minami, E. and Shibuya, N. (2006): Plant cells recognize chitin fragments for defence signalling through a plasma membrane receptor. *PNAS 103(29): 11086-11091*

Kay, S., Hahn, S., Marois, E., Hause, G. and Bonas, U. (2007): A bacterial effector acts as a plant transcription factor and induces a cell size regulator. *Science 318(5850): 648-651*

Kee, Y., Yoo, J.S., Hazuka, C.D., Peterson, K.E., Hsu, S.C. and Scheller, R.H. (1997): Subunit structure of the mammalian exocyst complex. *PNAS 94(26): 14438-14443*

Keinath, N.F., Kierszniowska, S., Lorek, J., Bourdais, G., Kessler, S.A., Shimosato-Asano, JH., Grossniklaus, U., Schulze, W.X., Robatzek, S. and Panstruga, R. (2010): PAMP (Pathogen-associated Molecular Pattern)-induced changes in plasma membrane compartmentalization reveal novel components of plant immunity. *Journal of Biological Chemistry 285(50): 39140-39149*

Kim, D.-W., Massey, T., Sacher, M., Pypaert, M. and Ferro-Novick, S. (2001): Sgf1, a new component of the Sec34/Sec35 complex. *Traffic 2(11): 820-830*

Kim, D.W., Sacher, M., Scarpa, A., Quinn, AM. and Ferro-Novick, S. (1999): High-copy suppressor analysis reveals a physical interaction between Sec34p and Sec35p, a protein implicated in vesicle docking. *Molecular Biology of the Cell. 10(10): 3317-3329*

Kim, M.G., da Cunha, L., McFall, A.J., Belkhadir, Y., DebRoy, S., Dangl, J.L. and Mackey, D. (2005): Two *Pseudomonas syringae* type III effectors inhibit RIN4-regulated basal defence in *Arabidopsis*. *Cell 121(5): 749-759*

Klade, M., Nühse, T.S., Findlay, K. and Peck, S.C. (2007): The syntaxin SYP132 contributes to plant resistance against bacteria and secretion of pathogenesis-related protein 1. *PNAS 104(28): 11850-11855*

Kobayashi, Y., Kobayashi, I., Funaki, Y., Fujimoto, S., Takemoto, T. and Kunoh, H. (1997): Dynamic reorganization of microfilaments and microtubules is necessary for the expression of non-host resistance in barley coleoptile cells. *The Plant Journal 11(3): 525-537*

Koh, S., André, A., Edwards, H., Ehrhardt, D. and Somerville, S. (2005): *Arabidopsis thaliana* subcellular responses to compatible *Erysiphe cichoracearum* infections. *The Plant Journal 44(3): 516-529*

Kombirnk, A., Sánchez-Vallet, A. and Thomma, B.P. (2011): The role of chitin detection in plant-pathogen interactions. *Microbes and Infection 13(14-15*): *1168-1176*

Koumandou, V.L., Dacks, J.B., Coulson, R.M. and Field, M.C. (2007): Control systems for membrane fusion in the ancestral eukaryote; evolution of tethering complexes and SM proteins. *BMC Evolutionary Biology 7: 29*

Kunoh, H. (2002): Localized induction of accessibility and inaccessibility by powdery mildew. In The Powdery Mildews: A Comprehensive Treatise, ed. Belanger, R.R., Bushnell, W.R., Dik, A.J., Carver, T.L.W., pp. 126-133. St. Paul, MN: Am. Phytopathol. Soc.

Kunze, G., Zipfel, C., Robatzek, S., Niehaus, K., Boller, T. and Felix, G. (2004): The N terminus of bacterial elongation factor Tu elicits innate immunity in *Arabidopsis* plants. *The Plant Cell 16(12): 3496-3507*

Kwon, C., Bednarek, P. and Schulze-Lefert, P. (2008a): Secretory pathways in plant immune responses. *Plant Physiology 147(5): 1575-1583*

Kwon, C., Neu, C., Pajonk, S., Yun, H.S., Lipka, U., Humphry, M., Bau, S., Straus, M., Kwaaitaal, M., Rampelt, H., El Kasmi, F., Jürgens, G., Parker, J., Panstruga, R., Lipka, V. and Schulze-Lefert, P. (2008b): Co-option of a default secretory pathway for plant immune responses. *Nature 451(7180): 835-840*

Lahaye, T. and Bonas, U. (2001): Molecular secrets of bacterial type III effector proteins. *TRENDS in Plant Science 6(10): 479-485*

Lamb, C. and Dixon, R.A. (1997): The oxidative burst in plant disease resistance. *Annual Reviews Plant Physiology Plant Molecular Biology 48: 251-275*

Latijnhouwers, M., Gillespie, T., Boevink, P., Kriechbaumer, V., Hawes, C. and Carvalho, C.M. (2007): Localization and domain characterization of *Arabidopsis* golgin candidates. *Journal of Experimental Botany 58(15/16): 4373-7386*

Latijnhouwers, M., Hawes, C. and Carvalho, C. (2005): Holding it all together? Candidate proteins for the plant Golgi matrix. *Current Opinion in Plant Biology 8(6): 632-639*

References

Laufman, O., Hong, W. and Lev, S. (2011): The COG complex interacts directly with Syntaxin 6 and positively regulates endosome-to-TGN retrograde transport. *Journal of Cell Biology 194(3): 459-472*

Laufman, O., Kedan, A., Hong, W. and Lev, S. (2009): Direct interaction between the COG complex and the SM protein, Sly1, is required for Golgi SNARE pairing. *EMBO Journal 28(14): 2006-2017*

Lees, J.A., Yip, C.K., Walz, T. and Hughson, F.M. (2010): Molecular organization of the COG vesicle tethering complex. *Nature Structural and Molecular Biology 17(11): 1292-1297*

Lherminier, J., Elmayan, T., Fromentin, J., Elaraqui, K.T., Vesa, S., Morel, J., Verrier, J.-L., Cailleteau, B., Blein, J.-P. and Simon-Plas, F. (2009): NADPH oxidase-mediated reactive oxygen species production subcellular localization and reassessment of its role in plant defence. *Molecular Plant-Microbe Interactions 22(7): 868-881*

Li, S., van Os, G.M., Ren, S., Yu, D., Ketelaar, T., Emons, A.M. and Liu, C.M. (2010): Expression and functional analyses of **EXO70** genes in *Arabidopsis* implicate their roles in regulating cell type-specific exocytosis. *Plant Physiology 154(4): 1819-1830*

Lipka, V., Dittgen, J., Bednarek, P., Baht, R., Wiermer, M., Stein, M., Landtag, J., Brandt, W., Rosahl, S., Scheel, D., Llorente, F., Molina, A., Parker, J., Somerville, S. and Schulze-Lefert, P. (2005): Pre- and postinvasion defences both contribute to nonhost resistance in *Arabidopsis*. *Science 310: 1180-1183*

Lipka, V., Kwon, C. and Panstruga, R. (2007): SNARE-Ware: The role of SNARE-domain proteins in plant biology. *Annual Reviews Cell and Developmental Biology 23: 147-174*

Lodish, H., Berk, A., Zipursky, S.L., Matsudaira, P., Baltimore, D. and Darnell, J. (2000): Protein Sorting: Organelle Biogenesis and Protein Secretion. In Molecular Cell Biology W. H. Freeman New York:

Loh, E. and Hong, W. (2004): The binary interacting network of the conserved oligomeric Golgi tethering complex. *Journal of Biological Chemistry 279(23): 24640-24648*

Lu, D., Lin, W., Gao, X., Wu, S., Cheng, C., Avila, J., Heese, A., Devarenne, T.P., He, P. and Shan, L. (2011): Direct ubiquitination of pattern recognition receptor FLS2 attenuates plant innate immunity. *Science 332(6036): 1439-1442*

Lupashin, V.V., Pokrovskaya, I.D., McNew, J.A. and Waters, M.G. (1997): Characterization of a novel yeast SNARE protein implicated in Golgi retrograde traffic. *Molecular Biology of the Cell 8(12): 2659-2676*

Malsam, J., Kreye, S. and Söller, T.H. (2008): Membrane fusion: SNAREs and regulation. *Cellular and Molecular Life Science 65(18): 2814-2832*

Marti, L., Fornaciari, S., Renna, L., Stefano, G. and Brandizzi, F. (2010): COPII-mediated traffic in plants. *TRENDS in Plant Science 15(9): 522-528*

Matheson, L.A., Suri, S.S., Hanton, S.L., Chatre, L. and Brandizzi, F. (2008): Correct targeting of plant ARF GTPases relies on distinct protein domains. *Traffic 9(1): 103-120*

McMahon, H.T. and Mills, I.G. (2004): COP and clathrin-coated vesicle budding: different pathways, common approaches. *Current Opinion in Cell Biology 16(4): 379-391*

Meng, Y., Moscou, M.J., Wise, and R.P. (2009): *Blufensin1* negatively impacts basal defense in response to barley powdery mildew. *Plant Physiology 149(1): 271-285*

Meyer, D., Pajonk, S., Micali, C., O´Connell, R. and Schulze-Lefert, P. (2008): Extracellular transport and integration of plant secretory proteins into pathogen-induced cell wall compartments*. The Plant Journal 57(6): 968-999*

Micali, C.O., Neumann, U., Grunewald, D., Panstruga, R. and O´Connell, R. (2010): Biogenesis of a specialized plant-fungal interface during host cell internalization of *Golovinomyces orontii* haustoria. *Cellular Microbiology 13(2): 210-226*

Miya, A., Albert, P., Shinya, T., Desaki, Y., Ichimura, K., Shirasu, K., Nanusaka, Y., Kawakami, N., Kaku, H. and Shibuya, N. (2007): CERK1, a LysM receptor kinase, is essential for chitin elicitor signalling in *Arabidopsis*. *PNAS 104(49): 19613-19618*

Moreau, P., Brandizzi, F., Hanton, S., Chatre, L., Melser, S., Hawes, C. and Satiat-Jeunemaitre, B. (2007): The plant ER–Golgi interface: a highly structured and dynamic membrane complex. *Journal of Experimental Botany 58(1): 49-64*

Mudget, M. B. (2005): New insights to the function of phytopathogenic bacterial type III effectors in plants. *Annual Reviews of Plant Biology 56: 509-531*

Munson, M. and Novick, P. (2006): The exocyst defrocked, a framework of rods revealed. *Nature Structural and Molecular Biology 13(7): 577-581*

Mur, L.A.J., Kenton, P., Lloyd, A.J., Ougham, H. and Prats, E. (2008): The hypersensitive response the centenary is upon us but how much do we know? *Journal of Experimantal Botany 59(3): 501-520*

Nanda, A.K., Andrio, E., Marino, D., Pauly, N. and Dunand, C. (2010): Reactive oxygen species during plant-microorganism early interactions. *Journal of Integrative Plant Biology 52(2): 195-204*

References

Nomura, K., DebRoy, S., Lee, Y.H., Pumplin, N., Jones, J. and He, S.Y. (2006): A bacterial virulence protein suppresses host innate immunity to cause plant disease. *Science 313(5784): 220-223*

Nühse, T.S., Boller, T. and Peck, S.C. (2003): A plasma membrane syntaxin is phosphorylated in response to the bacterial elicitor flagellin. *Journal of Biological Chemistry 278(46): 45248-45254*

Nürnberger, T., Brunner, F., Kemmerling, B. and Piater, L. (2004): Innate immunity in plants and animals: striking similarities and obvious differences. *Immunological Reviews 198: 249-266*

Oka, T., Ungar, D., Hughson, F.M. and Krieger, M. (2004): The COG and COPI complexes interact to control the abundance of GEARs, a subset of Golgi integral membrane proteins. *Molecular Biology of the Cell 15(5): 2423-2435*

Oka, T., Vasile, E., Penman, M., Novina, C.D., Dykxhoorn, D.M., Ungar, D., Hughson, F.M. and Krieger, M. (2005): Genetic analysis of the subunit organization and function of the conserved oligomeric golgi (COG) complex: studies of COG5- and COG7-deficient mammalian cells. *Journal of Biological Chemistry 280(38): 32736-32745*

Otegui, M.S. and Staehelin, L.A. (2004): Electron tomographic analysis of post-meiotic cytokinesis during pollen development in *Arabidopsis thaliana*. *Planta 218(4): 501-515*

Pathuri, I.P., Eichmann, R. and Hückelhoven, R. (2009): Plant small monomeric G-proteins (RAC/ROPs) of barley are common elements of susceptibility to fungal leaf pathogens, cell expansion and stomata development. *Plant Signal Behaviour 4(2):109-110*

Pathuri, I.P., Zellerhoff, N., Schaffrath, U., Hensel, G., Kumlehn, J., Kogel, K.H., Eichmann, R. and Hückelhoven, R. (2008): Constitutively activated barley ROPs modulate epidermal cell size, defense reactions and interactions with fungal leaf pathogens. *Plant Cell Reports 27(12): 1877-1887*

Pecenková, T., Hála, M., Kulich, I., Kocourková, D., Drdová, E., Fendrych, M., Toupalová, H. and Zársky, V. (2011): The role for the exocyst complex subunits Exo70B2 and Exo70H1 in the plant-pathogen interaction. *Journal of Experimental Botany 62(6): 2107-2116*

Pelham, H.R.B. (2001): SNAREs and the specificity of membrane fusion. *TRENDS in Cell Biology 11(3): 99-101*

Peng, M. and Kuc, J. (1992): Peroxidase-generated hydrogen peroxide as a source of antifungal activity in vitro and on tobacco leaf disks. *Phytopathology 82: 696-699*

Petutschnig, E.K., Jones, A.M., Serazetdinova, L., Lipka, U. and Lipka, V. (2010): The lysin motif receptor-like kinase (LysM-RLK) CERK1 is a major chitin-binding protein in *Arabidopsis thaliana* and subject to chitin-induced phosphorylation. *Journal of Biological Chemistry 285(37): 28902-28911*

Pike, L.J. (2006): Rafts defined: a report on the Keystone symposium on lipid rafts and cell function. *Journal of Lipid Research 47(7): 1597-1698*

Pinheiro, H., Samalova, M., Geldner, N., Chory, J., Martinez, A. and Moore, I. (2009): Genetic evidence that the higher plant Rab-D1 and Rab-D2 GTPases exhibit distinct but overlapping interactions in the early secretory pathway. *Journal of Cell Science 122(29): 3749-3758*

Pitzschke, A., Schikora, A. and Hirt, H. (2009): MAPK cascade signalling networks in plant defence. *Current Opinion in Plant Biology 12(4): 421-426*

Pokrovskaya, I.D., Willett, R., Smith, R.D., Morelle, W., Kudlyk, T. and Lupashin, V.V. (2011): Conserved oligomeric Golgi complex specifically regulates the maintenance of Golgi glycosylation machinery. *Glycobiology 21(12): 1554-1569*

Pritchard, L. and Birch, P. (2011): A systems biology perspective on plant-microbe interactions biochemical and structural targets of pathogen effectors. *Plant Science 180(4): 584-603*

Pryce-Jones, E., Carver, T. and Gurr, S.J. (1999): The roles of cellulase enzymes and mechanical force in host penetration by *Erysiphe graminis* f.sp. *hordei*. *Physiological and Molecular Plant Pathology 55: 175-182*

Pucadyil, T.J. and Schmid, S.L. (2009): Conserved functions of membrane active GTPases in coated vesicle formation. *Science 325(5945): 1217-1220*

Quental, R., Azevedo, L., Matthiesen, R. and Amorim, A. (2010): Comparative analyses of the conserved oligomeric Golgi (COG) complex in vertebrates. *BMC Evolutionary Biology 10: 212-220*

Quental, R., Azevedo, L., Matthiesen, R. and Amorim, A. (2010): Comparative analyses of the Conserved Oligomeric Golgi (COG) complex in vertebrates. *BMC Evolutionary Biology 10: 212*

Reinhard, C., Schweikert, M., Wieland, F.T. and Nickel, W. (2003): Functional reconstitution of COPI coat assembly and disassembly using chemically defined components. *Proc Natl Acad Sci U S A 100(14): 8253-8257*

Ridout, C.J., Skamnioti, P., Porritt, O., Sacristan, S., Jones, J.D.G. and Brown, J.K.M. (2006): Multiple avirulence paralogues in cereal powdery mildew fungi may contribute to parasite fitness and defeat of plant resistance. *The Plant Cell 18(9): 2402-2414*

References

Robatzek, S. (2007): Vesicle trafficking in plant immune responses. *Cellular Microbiology 9(1): 1-8*

Robatzek, S., Chinchilla, D. and Boller, T. (2006): Ligand-induced endocytosis of the pattern recognition receptor FLS2 in *Arabidopsis*. *Genes and Development 20(5): 537-542*

Robinson, D.G., Herranz, M.-C., Bubeck, J., Pepperkok, R. and Ritzenthaler, C. (2007): Membrane dynamics in the early secretory pathway. *Critical Reviews in Plant Science 26: 199-255*

Robinson, D.G., Langhans, M., Saint-Jore-Dupas, C. and Hawes, C. (2008): BFA effects are tissue and not just plant specific. *TRENDS in Plant Science 13(8): 405-408*

Rojo, E. and Denecke, J. (2008): What is moving in the secretory pathway of plants. *Plant Physiology 147(4): 1493-1503*

Rojo, E., Zouhar, J., Kovaleva, V., Hong, S. and Raikhel, N.V. (2003): The AtC-VPS protein complex is localized to the tonoplast and the prevacuolar compartment in *Arabidopsis*. *Molecular Biology of the Cell 14(2): 361-369*

Ron, M. and Avni, A. (2004): The receptor for the fungal elicitor ethylene-inducing Xylanase is a member of a resistance-like gene family in tomato. *The Plant Cell 16(6): 1604-1615*

Ron, M. and Avni, A. (2004): The receptor for the fungal elicitor ethylene-inducing xylanase is a member of a resistance-like gene family in tomato. *Plant Cell 16(6): 1604-1615.*

Roux, M., Schwessinger, B., Albrecht, C., Chinchilla, D., Jones, A., Holton, N., Malinovsky, F.G., Tör, M., de Vries, S. and Zipfel, C. (2011): The *Arabidopsis* leucine-rich repeat receptor-like kinases BAK1/SERK3 and BKK1/SERK4 are required for innate immunity to Hemibiotrophic and Biotrophic pathogens. *Plant Cell 23(6): 2440-2455*

Rutherford, S. and Moore, I. (2002): The *Arabidopsis* Rab GTPase family: another enigma variation. *Current Opinion in Plant Biology 5(6): 518-528*

Saenz, G. S. and Taylor, J. W. (1999): Phylogeny of the *Erysiphales* (powdery mildews) inferred from internal transcribed spacer ribosomal DNA sequences. *Canadian Journal of Botany* 77: *150-168*

Schultheiss, H., Dechert, C., Kogel, K.-H. and Hückelhoven, R. (2002): A small GTPbinding host protein is required for entry of powdery mildew fungus into epidermal cells of barley. *Plant Physiology 128: 1447-1454*

Schultheiss, H., Dechert, C., Kogel, K.-H. and Hückelhoven, R. (2003): Functional analysis of barley RAC/ROP G-protein family members in susceptibility to the powdery mildew fungus. Plant Journal 36: 589-601.

Schweizer, P., Pokorny, J., Abenderhalden, O. and Dudler, R. (1999): A transient assay system for the functional assessment of defence-related genes in wheat. *Molecular Plant-Microbe Interactions 12: 647-654*

Seguí-Simarro, J.M., Austin, J.R., White, E.A. and Staehelin, L.A. (2004): Electron tomographic analysis of somatic cell plate formation in meristematic cells of *Arabidopsis* preserved by high-pressure freezing. *Plant Cell 16(4): 836-856*

Sels, J., Mathys, J., De Coninck, B.M.A., Cammue, B.P.A. and De Bolle, M.F.C. (2008): Plant pathogenesis-related (PR) proteins: A focus on PR peptides. *Plant Physiology and Biochemistry 46(11): 941-950*

Shahollari, B., Peskan-Gerghöfer, T. and Oelmüller, R. (2004): Receptor kinases with leucine-rich repeats are enriched in Triton X-100 insoluble plasma membrane microdomains from plants. *Physiologia Plantarum 122(4): 397-403*

Shestakova, A., Suvorova, E., Pavliv, O., Khaidakova, G. and Lupashin, V. (2007): Interaction of the conserved oligomeric Golgi complex with t-SNARE Syntaxin5a/Sed5 enhances intra-Golgi SNARE complex stability. *Journal of Cell Biology 179(6): 1179-1192*

Shestakova, A., Zolov, S. and Lupashin, V. (2006): COG complex-mediated recycling of Golgi glycosyltransferases is essential for normal protein glycosylation. *Traffic 7(2): 191-204*

Shimizu, T., Nakano, T., Takamizawa, D., Desaki, Y., Ishii-Minami, N., Nishizawa, Y., Minami, E., Okada, K., Yamane, H., Kaku, H. and Shibuya, N. (2010): Two LysM receptor molecules, CEBiP and OsCERK1 cooperatively regulate chitin elicitor signalling in rice. *The Plant Journal 64(2): 204-214*

Sivaram, M.V., Saporita, J.A., Furgason, M.L., Boettcher, A.J. and Munson, M. (2005): Dimerization of the exocyst protein Sec6p and its interaction with the t-SNARE Sec9p. *Biochemistry 44(16): 6302-6311*

Smith, R.D. and Lupashin, V.V. (2008): Role of the conserved oligomeric Golgi (COG) complex in protein glycosylation. *Carbohydrate Research 343(12): 2024-2031*

Sohda, M., Misumi, Y., Yamamoto, A., Nakamura, N., Ogata, S., Sakisaka, S., Hirose, S., Ikehara, Y. and Oda, K. (2010): Interaction of Golgin-84 with the COG complex mediates the intra-Golgi retrograde transport. *Traffic 11(12): 1552-1566*

Sohda, M., Misumi, Y., Yoshimura, S., Nakamura, N., Fusano, T., Ogata, S., Sakisaka, S. and Ikehara, Y. (2007): The interaction of two tethering factors, p115 and COG complex, is required for Golgi integrity. *Traffic 8(3): 270-284*

Söllner, T. (2002): Vesicle tethers promoting fusion machinery assembly. *Developmental Cell 2(4): 377-387*

References

Söllner, T., Whiteheart, S.W., Brunner, M., Erdjument-Bromage, H., Geromanos, S., Tempst, P. and Rothmann, J.E. (1993): SNAP receptors implicated in vesicle targeting and fusion. *Nature 362(6418): 318-323*

Speth, E.B., Imboden, L., Hauck, P. and He, S.Y. (2009): Subcellular localization and functional analysis of the *Arabidopsis* GTPase RabE. *Plant Physiology 149(4): 1824-1837*

Springer, S., Spang, A. and Schekman, R. (1999): A Primer on Vesicle Budding. *Cell 97(2): 145-148*

Stanislas, T., Bouyssie, D., Rossignol, M., Vesa, S., Fromentin, J., Morel, J., Pichereaux, C., Monsarrat, B. and Simon-Plas, F. (2009): Quantitative proteomics reveals a dynamic association of proteins to detergent-resistant membranes upon elicitor signalling in tobacco. *Molecular and Cellular Proteomics 8(9): 2186-2198*

Stein, M., Dittgen, J., Sánchez-Rodriguez, C., Hou, B.-H., Molina, A., Schulze-Lefert, P., Lipka, V. and Somerville, S. (2006): *Arabidopsis* PEN3 PDR8, an ATP binding cassette transporter, contributes to nonhost resistance to inappropriate pathogens that enter by direct penetration. *The Plant Cell 18(3): 731-746*

Stenmark, H. (2009): Rab GTPases as coordinators of vesicle traffic. *Nature Reviews Molecular Cell Biology 10(8): 513-525*

Stergiopoulos, I. and de Wit, P.J.G.M. (2009): Fungal effector proteins. *Annual Reviews Phytopathology 47: 233-263*

Stukkens, Y., Bultrey, A., Grec, S., Trombik, T., Vanham, D. and Boutry, M. (2005): NpPDR1, a pleiotropic drug resistance-type ATP-binding cassette transporter from *Nicotiana plumbaginifolia*, plays an major role in plant pathogen defence. *Plant Physiology 139(1): 341-352*

Südhof, T.C. and Rothman, J.E. (2009): Membrane fusion: Grappling with SNARE and SM proteins. *Science 323(5913): 474-477*

Surpin, M., Zheng, H., Morita, M.T., Saito, C., Avila, E., Blakeslee, J.J., Bandyopadhyay, A., Kovaleva, V., Carter, D., Murphy, A., Tasaka, M. and Raikhel, N. (2003): The VTI family of SNARE proteins is necessary for plant viability and mediates different protein transport pathways. *Plant Cell 15(12): 2885-2899*

Sutton, B.R., Fasshauer, D., Jahn, R. and Brunger, A.T. (1998): Crystal structure of a SNARE complex involved in synaptic exocytosis at 2.4. A resolution. *Nature, 395(6700): 347-353*

Suvorova, E.S., Duden, R. and Lupashin, V.V. (2002): The Sec34/Sec35p complex, a Ypt1p effector required for retrograde intra-Golgi trafficking, interacts with Golgi SNAREs and COPI vesicle coat proteins. *Journal of Cell Biology 157(4): 631-643*

Suvorova, E.S., Kurten, R.C. and Lupashin, V.V. (2001): Identification of a human orthologue of Sec34p as a component of the cis-Golgi vesicle tethering machinery. *Journal of Biological Chemistry 276(25): 22810-22818*

Synek, L., Schlager, N., Eliás, M., Quentin, M., Hauser, M.T. and Zárský, V. (2006): AtExo70A1, a member of a family of putative exocyst subunits specifically expanded in land plants, is important for polar growth and plant development. *Plant Journal 48(1): 54-72*

Sztul, E. and Lupashin, V. (2006): Role of tethering factors in secretory membrane traffic. *Am. J. Physiol. Cell Physiol. 290(1): 11-26*

Sztul, E. and Lupashin, V. (2009): Role of vesicle tethering factors in the ER-Golgi membrane traffic. *FEBS Letters 583(23): 3770-3783*

Takemoto, D., Jones, D.A. and Hardham, A.R. (2003): GFP-tagging of cell components reveals the dynamics of subcellular reorganization in response to infection of *Arabidopsis* by oomycete pathogens. *The Plant Journal 33(4): 775-792*

Tanaka, S., Ichikawa, A., Yamada, K., Tsuji, G., Nishiuchi, T., Mori, M., Koga, H., Nishizawa, Y., O´Connell, R. and Kubo, Y. (2010): HvCEBiP, a gene homologous to rice chitin receptor CEBiP, contributes to basal resistance of barley to *Magnaporthe oryzae*. *BMC Plant Biology 10: 288-299*

TerBush, D.R., Maurice, T., Roth, D. and Novick, P. (1996): The Exocyst is a multiprotein complex required for exocytosis in *Saccharomyces cerevisiae*. *EMBO Journal 15(23): 6483-6494*

Thellmann, M., Rybak, K., Thiele, K., Wanner, G. and Assaad, F.F. (2010): Tethering factors required for cytokinesis in *Arabidopsis*. *Plant Physiology 154(2): 720-732*

Thordal-Christensen, H. (2003): Fresh insights into processes of nonhost resistance. *Current Opinion in Plant Biology 6(4): 351-357*

Toonen, R.F.G. and Verhage, M. (2007): Munc18-1 in secretion: Lonely Munc joins SNARE team and takes control. *TRENDS in Neuroscience 30(11): 564-572*

Tör, M., Lotze, M.T. and Holton, N. (2009): Receptor-mediated signalling in plants: molecular patterns and programmes. *Journal of Experimental Botany 60(13): 3645-3654*

Torres, M.A. (2010): Ros in biotic interactions. *Physiologia Plantarum 138(4): 414-429*

References

Uemura, T., Ueda, T., Ohniwa, R.L., Nakano, A., Takeyasu, K. and Sato, M.H. (2004): Systematic analysis of SNARE molecules in *Arabidopsis*: Dissection of the post-Golgi network in plant cells. *Cell Structure and Function 29(2): 49-65*

Ungar, D., Oka, T., Brittle, E.E., Vasile, E., Lupashin, VV., Chatterton, J.E., Heuser, J.E., Krieger, M. and Waters, M.G. (2002): Characterization of a mammalian Golgi-localized protein complex, COG, that is required for normal Golgi morphology and function. *Journal of Cell Biology 157(3): 405-415*

Ungar, D., Oka, T., Krieger, M. and Hughson, F.M. (2006): Retrograde transport on the COG railway. *TRENDS in Cell Biology 16(2): 113-120*

Ungar, D., Oka, T., Vasile, E., Krieger, M. and Hughson, F.M. (2005): Subunit architecture of the conserved oligomeric Golgi complex. *Journal of Biological Chemistry 280(38): 32729-32735*

van der Biezen, E.A. and Jones, J.D. (1998): Plant disease-resistance proteins and the gene-for-gene concept. *TRENDS Biochemical Science 23(12): 454-456*

van der Hoorn, R.A.L. and Kamoun, S. (2008): From Guard to Decoy - A New model for perception of plant pathogen effectors. *The Plant Cell 20(8): 2009-2017*

Van Loon, L.C. and Van Strien, E.A. (1999): The families of pathogenesis-related proteins, their activities, and comparative analysis of PR-1 type proteins. *Physiological and Molecular Plant Pathology 55: 85-97*

VanRheenen, S.M., Cao, X., Lupashin, VV., Barlowe, C. and Waters, M.G. (1998): Sec35p, a novel peripheral membrane protein, is required for ER to Golgi vesicle docking. *Journal of Cell Biology 141(5): 1107-1119*

VanRheenen, S.M., Cao, X., Sapperstein, S.K., Chiang, E.C., Lupashin, V.V., Barlowe, C. and Waters, M.G. (1999): Sec34p, a protein required for vesicle tethering to the yeast Golgi apparatus, is in a complex with Sec35p. *Journal of Cell Biology 147(4): 729-742*

Varlamov, O., Volchuk, A., Rahimian, V., Doege, C.A., Paumet, F., Eng, W.S., Arango, N., Parlati, F., Ravazzola, M., Orci, L., Söllner, T.H. and Rothman, J.E. (2003): i-SNAREs: inhibitory SNAREs that fine-tune the specificity of membrane fusion. *Journal of Cell Biology 164(1): 79-88*

Vernoud, V., Horton, A.C., Yang, Z. and Nielsen, E. (2003): Analysis of the small GTPase gene superfamily of *Arabidopsis*. *Plant Physiology 131(3): 1191-1208*

Viotti, C., Bubeck, J., Stierhof, Y.D., Krebs, M., Langhans, M., van den Berg, W., van Dongen, W., Richter, S., Geldner, N., Takano, J., Jürgens, G., de Vries, S.C., Robinson, D.G. and Schumacher, K. (2010): Endocytic and secretory traffic in *Arabidopsis* merge in the Trans-Golgi network/Early Endosome, an independent and highly dynamic organelle. *The Plant Cell 22(4): 1344-1357*

Wan, J., Zhang, X.C., Neece, D., Ramonell, K.M., Clough, S., Kim, S.Y., Stacey, M.G. and Stacey, G.A. (2008): LysM receptor-like kinase plays a critical role in chitin signalling and fungal resistance in *Arabidopsis*. *Plant Cell 20(2): 471-481.*

Wang, W., Wen, Y., Berkey, R. and Xiao, S. (2009): Specific targeting of the *Arabidopsis* resistance protein RPW8.2 to the interfacial membrane encasing the fungal haustorium renders broad-spectrum resistance to powdery mildew. *Plant Cell 21(9): 2898-8913*

Wen, T.J., Hochholdinger, F., Sauer, M., Bruce, W. and Schnable, P.S. (2005): The roothairless1 gene of maize encodes a homolog of sec3, which is involved in polar exocytosis. *Plant Physiology 138(3):1637-1643*

Wendehenne, D., Pugin, A., Klessig, D.F. and Durner, J. (2001): Nitric oxide: comparative synthesis and signalling in animal and plant cells. *Trends Plant Science 6(4):177-183*

Whisson, S.C., Boevink, P.C., Moleleki, L., Avrova, A.O., Morales, J.G., Gilroy, E.M., Armstrong, M.R., Grouffaud, S., van West, P., Chapman, S., Hein, I., Toth, I.K., Pritchard, L. and Birch, P.R.J. (2007): A translocation signal for delivery of oomycete effector proteins into host plant cells. *Nature 450(7166): 115-118*

Whyte, J.R. and Munro, S. (2001): The Sec34/35 Golgi transport complex is related to the exocyst, defining a family of complexes involved in multiple steps of membrane traffic. *Developmental Cell 1(4): 527-537*

Whyte, J.R. and Munro, S. (2002): Vesicle tethering complexes in membrane traffic. *Journal of Cell Science 115(13): 2627-2637*

Wiederkehr, A., De Craene, J.O., Ferro-Novick, S. and Novick, P. (2004): Functional specialization within a vesicle tethering complex: bypass of a subset of exocyst deletion mutants by Sec1p or Sec4p. *Journal of Cell Biology 167(5): 875–887*

Wuestehube, L.J., Duden, R., Eun, A., Hamamoto, S., Korn, P., Ram, R. and Schekman, R. (1996): New mutants of Saccharomyces cerevisiae affected in the transport of proteins from the endoplasmic reticulum to the Golgi complex. *Genetics 142(2): 393-406*

Wyand, R.A. and Brown, J.K. (2003): Genetic and forma specialis diversity in Blumeria graminis of cereals and its implications for host-pathogen co-evolution. *Molecular Plant Pathology 4(3): 187-198*

Xu, J. and Scheres, B. (2005): Dissection of *Arabidopsis* ADP-RIBOSYLATION FACTOR 1 function in epidermal cell polarity. *Plant Cell 17(2): 525-536*

Yamaguchi, Y., Huffaker, A., Bryan, A.C., Tax, F.E. and Ryan, C.A. (2010): PEPR2 is a second receptor for the Pep1 and Pep2 peptides and contributes to defense responses in *Arabidopsis*. *Plant Cell 22(2): 508-522*

References

Yang, Y.D., Elamawi, R., Bubeck, J., Pepperkok, R., Ritzenthaler, C. and Robinson, D.G. (2005): Dynamics of COPII vesicles and the Golgi apparatus in cultured *Nicotiana tabacum* BY-2 cells provides evidence for transient association of Golgi stacks with endoplasmic reticulum exit sites. *Plant Cell, 17(5): 1513-1531*

Zeier, J., Delledonne, M., Mishina, T., Severi, E., Sonoda, M. and Lamb, C. (2004): Genetic elucidation of nitric oxide signalling in incompatible plant-pathogen interactions. *Plant Physiology 136(1): 2875-2886*

Zeyen, R.J., Carver, T.L.W. and Lyngkjaer, M.F. (2002): Epidermal cell papillae. In The Powdery Mildews: A Comprehensive Treatise, ed. Belanger, R.R., Bushnell, W.R., Dik, A.J., Carver, T.L.W., pp. 107-124. St. Paul, MN: Am. Phytopathol. Soc.

Zhang, H., Sreenivasulu, N., Weschke, W., Stein, N., Rudd, S., Radchuk, V., Potokina, E., Scholz, U., Schweizer, P., Zierold, U., Langridge, P., Varshney, R.K., Wobus, U. and Graner, A. (2004): Large-scale analysis of the barley transcriptome based on expressed sequence tags. *Plant Journal 40(2): 276-290*

Zhang, Y., Liu, C.M., Emons, A.M. and Ketelaar, T. (2010): The plant exocyst. *Journal of Integrative Plant Biology 52(2): 138-146*

Zheng, H., Camacho, L., Wee, E., Batoko, H., Legen, J., Leaver, C.J., Malhó, R., Hussey, P.J. and Moore, I. (2005): A Rab-E GTPase mutant acts downstream of the Rab-D subclass in biosynthetic membrane traffic to the plasma membrane in tobacco leaf epidermis. *Plant Cell 17(7): 2020-2036*

Zheng, H., von Mollard, G.F., Kovaleva, V., Stevens, T.H. and Raikhel, N.V. (1999): The plant vesicle-associated SNARE AtVTI1a likely mediates vesicle transport from the trans-Golgi network to the prevacuolar compartment. *Molecular Biology of the Cell 10(7): 2251-2264*

Zipfel, C. (2008): Pattern-recognition receptors in plant innate immunity. *Current Opinion in Immunology 20(1): 10-16*

Zipfel, C. and Felix, G. (2005): Plants and animals: a different taste for microbes? *Current Opinion in Plant Biology 8(4): 353-360*

Zipfel, C., Kunze, G., Chinchilla, D., Caniard, A., Jones, J.D.G., Boller, T. and Felix, G. (2006): Perception of the Bacterial PAMP EF-Tu by the Receptor EFR restricts *Agrobacterium*-mediated Transformation. *Cell 125(4): 749-760*

Zipfel, C., Robatzek, S., Navarro, L., Oakeley, E.J., Jones, J.D.G., Felix, G. and Boller, T. (2004): Bacterial disease resistance in *Arabidopsis* through flagellin perception. *Nature 428(6984): 764-767*

Zolov, S.N. and Lupashin, V.V. (2005): Cog3p depletion blocks vesicle-mediated Golgi retrograde trafficking in HeLa cells. *Journal of Cell Biology 168(5): 747-759*

8 Appendix

Table S1: Multi-subunit tethering complexes (MTC)
According to Bröcker *et al.,* 2010; modified

MTC	Subunits	Interaction partners			Localization	Functions between
		Small GTPase	SNARE	Coat		
Dsl1p	Dsl1 Dsl3 (Sec39) Tip20	Ypt1?	Use1, Sec20	COPI	ER	Golgi to ER
COG	Cog1 Cog2 Cog3 Cog4 Cog5 Cog6 Cog7 Cog8	Ypt1	Sec22 Gos1 Sed5 Ykt6 Vti1	COPI	Golgi	Endosome to Golgi
GARP	Vps51/Ang2 Vps52 Vps53 Vps54	Ypt6	Tlg1		TGN	Ensosome to TGN
Exocyst	Sec3 Sec5 Sec6 Sec8 Sec10 Sec15 EXO70 EXO84	Sec4 RalA Rho1 Rho3	Sso1/2 Snc1/2 Sec9		Plasma membrane	Vesicle to plasma membrane
CORVET	Vps8 Vps3 Vps11 Vps16 Vps18 Vps33	Vps21 (Rab5)			Endosome	TGN to early endosome
HOPS	Vps41 Vps39 Vps11 Vps16 Vps18 Vps33	Ypt7 (Rab7)	Vam3 Vam7 Vti1 Nyv1	AP subunit	vacuole	MVB to vacuole Vacuole-vacuole
TRAPPI	Bet3 Bet5 Trs23 Trp31 Trs33	Ypt1		COPII	Golgi	ER to Golgi
TRAPPII	TRAPPI subunits and Trs65 Trs120 Trs130 Tca17	Ypt1 Ypt31/32		COPI	Golgi	Endosome to Golgi
TRAPIII	TRAPPI subunits and Trs85	Ypt1			Phagophore	Golgi to lysosome

Table S2: Membrane trafficking candidates

Internal ID	EST-ID	Vector	Fragment size (bp)	Screening effect relative to the empty vector control (control set to 0%)	Protein blast domain prediction by NCBI
1	GAN002A06f	pCR blunt	410	-	PRONE Superfamily
2	GBN005A07u	pCR blunt	360	-	Exo70 Superfamily
3	GBN005P11u	pCR blunt	267	-	VHS and GAT domain predicted
4	GBN008O23u	pCR blunt	497	-	TBC Superfamily
5	HA01K19r	pBluescript SK+	400	-	No putative conserved domains
6	HA14A08r	pBluescript SK+	451	156,452	Sec34 family
7	HA15J01r	pBluescript SK+	490	52,704	Sec1 Family
8	HA16C04r	pBluescript SK+	354	33,565	Ras-like-GTPase Superfamily Arl5/Arl18
9	HA18P09r	pBluescript SK+	602	21,275	Ras-like-GTPase Superfamily Arl5/Arl18
10	HA24I11r	pBluescript SK+	644	113,581	ProneSuperfamily
11	HB17K16r	pBluescript SK+	602	-4,408	WD40 Superfamily
12	HB19C23r	pBluescript SK+	645	-10,795	C2 domain containing Oryza sativa
13	HB20L08r	pBluescript SK+	476	30,097	VHS and GAT domain predicted
14	HB28E03r	pBluescript SK+	494	-2,428	WD40 Superfamily and ACE Superfamily
15	HC06C03y	pSPORT	195	13,905	C2 Superfamily
16	HC07C06w	pSPORT	609	37,110	no significant similarity found
17	HC13C10w	pSPORT	698	14,924	VHS and GAT domain predicted
18	HD12L16r	pBluescript SK+	339	65,772	PH and Rho-GAP domain predicted Sorghum bicolor
19	HD14N02r	pBluescript SK+	603	172,823	Exo70 Superfamily
20	HF02O10r	pBluescript SK+	619	90,297	Sec15 Superfamily
21	HF02O10r	pBluescript SK+	619	-	Sec15 Superfamily
22	HF06K21r	pBluescript SK+	714	-	Sec1 Superfamily
23	HF08K21r	pBluescript SK+	688	-41,970	PH and Rho-GAP domain predicted Oryza sativa
24	HF24H17r	pBluescript SK+	698	20,991	OTU Superfamily
25	HH01C09w	pSPORT	612	31,511	C2 Superfamily
26	HH05H03w	pSPORT	644	31,806	No significant similarity found
27	HH06L20y	pSPORT	646	-4,783	Ras-like-GTPase Superfamily Arf1-5 like
28	HH06P13w	pSPORT	506	-19,263	ARF-GAP Superfamily
29	HI01H03T	pBluescript SK+	306	-37,083	No significant similarity found

30	HI05P18r	pBluescript SK+	617	-12,321	Sec10 Exocyst component Oryza sativa
31	HI14L24r	pBluescript SK+	638	-	WD40 Superfamily
32	HM10F01w	pBluescript SK+	663	-36,234	GDI Superfamily GDP dissociation inhibitor
33	HM11A23r	pBluescript SK+	622	195,245	no significant similarity found
34	HM11L23r	pBluescript SK+	641	2,242	No significant similarity found
35	HO02A12S	pBluescript SK+	589	-	C2 Superfamily Tricinctum aestivum
36	HO02D01S	pBluescript SK+	494	173,530	Ras-like-GTPase Superfamily Arf1-5 like
37	HO03F09w	pBluescript SK+	383	-4,667	C2 Superfamily
38	HO04C21w	pBluescript SK+	732	13,145	Sec14 Superfamily
39	HO04E07S	pBluescript SK+	553	-43,827	C2 Superfamily
40	HO04I09S	pBluescript SK+	627	58,235	TBC Superfamily
41	HO05H10S	pBluescript SK+	465	-	VHS and GAT domain predicted
42	HO05L22S	pBluescript SK+	616	-	Sec14 Superfamily
43	HO06I15S	pBluescript SK+	356	-	C2 Superfamily
44	HO07H23S	pBluescript SK+	656	-16,823	Exo70 Superfamily
45	HO07N23S	pBluescript SK+	633	7,434	Armadillo/beta-catenin-like repeats Sorghum bicolor
46	HO10F09S	pBluescript SK+	530	-	No putative conserved domains
47	HO10F11S	pBluescript SK+	458	-37,810	C2 Superfamily
48	HO10F23S	pBluescript SK+	504	-	Sec6 Superfamily Exocyst component
49	HO10F23w	pBluescript SK+	804	67,391	Sec6 Superfamily Exocyst component
50	HO11J13S	pBluescript SK+	562	-2,367	Cyclophilin Superfamily
51	HO11M02S	pBluescript SK+	560	-10,805	Ras-like-GTPase Superfamily Arf1-5 like
52	HO12A13S	pBluescript SK+	515	-75,976	PRONE Superfamily
53	HO12I08S	pBluescript SK+	565	84,436	VHS and GAT domain predicted
54	HO12M05S	pBluescript SK+	575	110,170	Ras-like-GTPase Superfamily Arf1-5 like
55	HO13J21S	pBluescript SK+	506	-23,422	ARF-GAP C2 domain containing
56	HO13K18S	pBluescript SK+	530	-	C2 Superfamily
57	HO14O24S	pBluescript SK+	573	-	Ras-like-GTPase Superfamily Arl1
58	HO14P08w	pBluescript SK+	659	39,873	TBC Superfamily
59	HO15C01S	pBluescript SK+	550	59,118	Rho-GAP Superfamily
60	HO15C01w	pBluescript SK+	768	77,572	Rho-GAP Superfamily
61	HO16B02w	pBluescript SK+	570	-22,393	C2 Superfamily Tricinctum aestivum
62	HO16J18w	pBluescript SK+	743	115,101	No significant similarity found
63	HO16O17S	pBluescript SK+	647	-	No significant similarity found

64	HO16O17w	pBluescript SK+	697	-	No significant similarity found
65	HO17J03S	pBluescript SK+	705	-	Sec14 Superfamily
66	HO18B23S	pBluescript SK+	679	34,598	Sec14 Superfamily
67	HO18N20w	pBluescript SK+	708	46,394	PKC-like Superfamily
68	HO18P20S	pBluescript SK+	630	-1,505	Ras-like-GTPase Superfamily Arf1-5 like
69	HO19E12w	pBluescript SK+	742	29,526	TBC Superfamily
70	HO19M12S	pBluescript SK+	532	32,670	C2 Superfamily
71	HO20H05S	pBluescript SK+	582	46,991	Sec14 Superfamily
72	HO20M06S	pBluescript SK+	660	54,155	WD40 Superfamily Oryza sativa
73	HO20M15S	pBluescript SK+	432	65,924	TBC Superfamily
74	HO23M07S	pBluescript SK+	559	26,499	VHS and GAT domain predicted
75	HO24G19S	pBluescript SK+	578	36,361	C2 Superfamily
76	HO24P03S	pBluescript SK+	441	9,004	Ras-like-GTPase Superfamily Arf1-5 like
77	HO25P07S	pBluescript SK+	671	-3,393	VHS domain predicted
78	HO26C01S	pBluescript SK+	745	46,755	Ras-like-GTPase Superfamily Arf1-5 like
79	HO27A21w	pBluescript SK+	719	-	VHS and GAT domain predicted
80	HO27H21w	pBluescript SK+	640	-34,355	No putative conserved domains
81	HO28A15S	pBluescript SK+	633	-23,869	Sec14 Superfamily
82	HO28B22S	pBluescript SK+	701	-1,983	No putative conserved domains
83	HO28K18S	pBluescript SK+	283	20,749	Exo70 Superfamily
84	HO28L01S	pBluescript SK+	560	-8,071	C2 Superfamily
85	HO29C15w	pBluescript SK+	668	5,694	No significant similarity found
86	HO30E03S	pBluescript SK+	435	75,908	Ras-like-GTPase Superfamily Arf1-5 like
87	H030K09S	pBluescript SK+	286	75,325	heat shock 70 kDa protein
88	HO30O16S	pBluescript SK+	412	-11,012	Exo70 Superfamily
89	HO31A04w	pBluescript SK+	604	-	No significant similarity found
90	HO31E21S	pBluescript SK+	521	41,741	No putative conserved domains
91	HO32A03S	pBluescript SK+	647	-	Sec14 Superfamily
92	HO33C08S	pBluescript SK+	609	44,318	Exo70 Superfamily
93	HO33C08w	pBluescript SK+	583	-	Exo70 Superfamily
94	HO33K13S	pBluescript SK+	656	-	TBC Superfamily
95	HO36L09S	pBluescript SK+	565	-	TBC Superfamily
96	HO36O15S	pBluescript SK+	715	-	Sec1 Superfamily
97	HO37E20S	pBluescript SK+	755	46,074	ARF-GAP C2 domain containing

98	HO37H01S	pBluescript SK+	607	33,708	Sec15 Superfamily
99	HO37H01S	pBluescript SK+	607	-33,310	Sec15 Superfamily
100	HP01L19w	pBluescript SK+	441	38,010	Ras-like-GTPase Superfamily Arf10-like
101	HP06J11T	pBluescript SK+	516	-	C2 Superfamily
102	HS04L21r	pBluescript SK+	514	-	C2 Superfamily
103	HS06F17r	pBluescript SK+	442	84,926	Sec14 Superfamily
104	HS06I01r	pBluescript SK+	365	-22,542	WD40 and ACE1-Sec16-like
105	HT01N03T	pBluescript SK+	587	-27,685	GDI Superfamily GDP dissociation inhibitor
106	HT01N03w	pBluescript SK+	638	31,192	GDI Superfamily GDP dissociation inhibitor
107	HT07K06r	pBluescript SK+	616	0,612	TBC Superfamily
108	HT11P11u	pBluescript SK+	573	-	Exo70 Superfamily
109	HU03J06u	pBluescript SK+	600	-	TBC Superfamily
110	HU10G14r	pBluescript SK+	622	-	ARF-GAP Superfamily
111	HU12C13u	pBluescript SK+	485	55,880	No putative conserved domains
112	HU13A03r	pBluescript SK+	743	42,084	GDI Superfamily GDP dissociation inhibitor
113	HV02H11r	pBluescript SK+	628	-	ENTH epsin related Tricinctum aestivum
114	HV02I09r	pBluescript SK+	374	-4,891	No significant similarity found.
115	HV06B16r	pBluescript SK+	599	3,731	No domain found
116	HV14H17u	pBluescript SK+	571	-	Exo70 Superfamily
117	HW01E01V	lambda ZAP	516	-	Exo70 Superfamily
118	HW03B20T	lambda ZAP	631	-	WD40 Superfamily
119	HW03G11T	lambda ZAP	477	-	No putative conserved domains
120	HW04A03u	lambda ZAP	439	-	Topoisomerase II-associated protein PAT1
121	HW06E02V	lambda ZAP	564	-	TBC Superfamily
122	HX03G01r	pBluescript SK+	525	-	C2 Superfamily
123	HX04B21r	pBluescript SK+	505	-7,525	Sec14 Superfamily
124	HX07G06r	pBluescript SK+	475	-	No significant similarity found
125	HX09O10w	pBluescript SK+	687	-	Exo70 Superfamily
126	HY01G15T	lambda ZAP	687	-	Sec14 Superfamily
127	HY08J06u	lambda ZAP	482	-	Sec15 Superfamily
128	HY08J06u	lambda ZAP	482	-	Sec15 Superfamily
129	HY09E18V	lambda ZAP	561	-	WD40 Superfamily
130	HZ36O17r	pBluescript SK+	167	-	VHS and GAT domain predicted
131	HZ39G02r	pBluescript SK+	266	-	PI3K-like domains

132	HZ39O05r	pBluescript SK+	673	-	C2 Superfamily
133	HZ45A16r	pBluescript SK+	583	-37,433	Exo70 Superfamily
134	HZ48G21r	pBluescript SK+	311	-	Sec1 Superfamily
135	HZ51H12r	pBluescript SK+	517	3,378	Exo70 Superfamily

Table S3: Yeast two hybrid candidates

Internal ID	Gene ID	Vector	Fragment size (bp)	Screening effect relative to the empty vector control
c6	NM_115079.3	pGADT7-Rec	787	-6,812849784
c11	TC140154	pGADT7-Rec	706	47,90830797
c22	NM_120583.4	pGADT7-Rec	715	-
c123	TC132044	pGADT7-Rec	670	-
c140	TC132044	pGADT7-Rec	743	46,87764851
c141	TC139926	pGADT7-Rec	717	88,11578078
c146	TC141472	pGADT7-Rec	771	60,51876228
c179	TC152090	pGADT7-Rec	765	10,80952381
c184	XM_001261396.1	pGADT7-Rec	690	55,49400341
c189	NM_130176.2	pGADT7-Rec	674	-34,30515063
c350	XM_001590703.1	pGADT7-Rec	641	-
c356	NM_111057.3	pGADT7-Rec	699	-
c364	DQ235271.1	pGADT7-Rec	488	26,29074665
c380	NM_111141.2	pGADT7-Rec	560	38,1604892
c382	TC138926	pGADT7-Rec	716	57,148895
c400	NM_124328.2	pGADT7-Rec	747	7,476415094
c427	TC133000	pGADT7-Rec	658	66,54727105
c510	AK249699.1	pGADT7-Rec	656	-0,097087379
c520	XM_001585972.1	pGADT7-Rec	696	-28,45633258
c537	NM_001112067.1	pGADT7-Rec	554	8,284023669

Table S4: Differentially expressed candidates

Internal ID	Gene ID	Vector	Fragment size (bp)	Screening effect relative to the empty vector control
12925	AK362661	BI-1 RacB Array	619	23,92400789
19046	AK367393.1	BI-1 RacB Array	523	29,17122
26912	AK251832.1	BI-1 RacB Array	630	6,11649445
29410	XM_003576960.1	BI-1 RacB Array	394	5,531118285

Table S5: Gene IDs for HvCOGs, potential HvCOG3 interaction partners and screening the HvARFs

Candidate	Gene IDs					
	Human	*Arabidopsis*	Rice	Barley	PlexDB ID/Contig	
HvCOG1	NP_061184	AT5G16300	NM_001050954	AK370785	Barley1_13332	Contig13332_at
HvCOG2	NP_031383	AT4G24840	NM_001058433	AK370312	Barley1_11948	Contig11948_at
HvCOG3	NP_113619	AT1G73430	NM_001068479	AK249208	Barley1_07930	Contig7930_at
HvCOG4	NP_056201	AT4G01400	NM_001186014	AK356539	Barley1_11310	Contig11310_at
HvCOG5	NP_006339	AT1G67930	NM_001061925	AK252011	Barley1_13262	Contig13262_at
HvCOG6	NP_065802	AT1G31780	AC107226	AK354922	Barley1_10684	Contig10684_at
HvCOG7	NP_705831	AT5G51430	AP003635	AK363189	Barley1_14245	Contig14245_at
HvCOG8	NP_115758	AT5G11980	NM_001073472	AK248490	Barley1_09113	Contig9113_at
HvARFA1D-like	-	-	-	AK251040	Barley1_00093	Contig93_at
HvARFA1B/C-like	-	-	-	AK369764	Barley1_00395	Contig395_s_at
HvGOS1	YHL031c	AT2G45200	NP_001045755	TA36193_4513	Barley1_12134	Contig12134_at
HvYKT6	YKL196c	AT5G58180	NP_001045489	TA38338_4513	Barley1_08337	Contig8337_at
HvSEC22	YLR268w	AT1G11890	EEC80182	TA49055_4513	Barley1_18727	Contig18727_at
HvVTI1	YMR197c	AAF24062	NP_001043348	TA38030_4513	Barley1_09598	Contig9598_at
HvYPT1	YFL038c	AT1G0213	NP_001043336	TA34665_4513	Barley1_04865	Contig4865_s_at

- = not used during this work

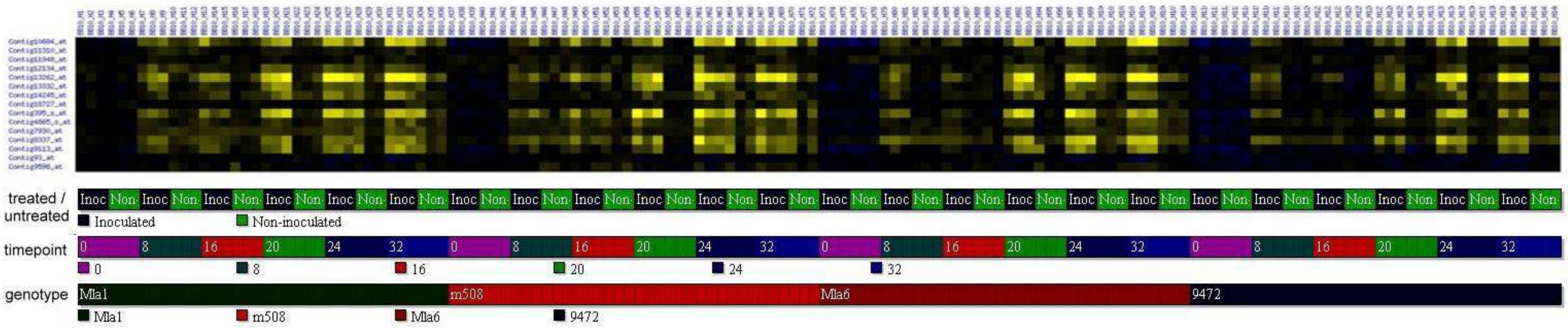

FigureS1: PLEXdb analysis of important genes used in this work.
Summary of the expression pattern of COG complex subunits, potential COG3 interaction partners and the two ARF GTPases using the PLEXdb experiment BB10 (control: H4, yellow dots indicate upregulation, blue dots indicates downregulation). See TableS5 for IDs.